NASA CR-1481

C. 1

CARBONATION CELL MATERIALS COMPATIBILITY

by N. P. Bannerton, D. L. DeRespiris, and J. W. Vogt

Prepared by
TRW, INC.
Cleveland, Ohio
for Lewis Research Center

NATIONAL AERONAUTICS AND SPACE ADMINISTRATION • WASHINGTON, D. C. • DECEMBER 1969

CARBONATION CELL MATERIALS COMPATIBILITY

By N. P. Bannerton, D. L. DeRespiris, and J. W. Vogt

Distribution of this report is provided in the interest of information exchange. Responsibility for the contents resides in the author or organization that prepared it.

ABSTRACT

A materials test and evaluation program was conducted to investi-
gate the compatibility of selected materials with the alkaline
and acid electrolyte environments of Stages I, II and III of the
TRW Carbonation Cell System.

Stage I and Stage II operate at 175°F with a 30 weight   percent
concentration of potassium carbonate as the electrolyte. The gas
compositions are 0.5 percent carbon dioxide with balance of air
for Stage I and 57 percent carbon dioxide with balance of oxygen
for Stage II. Stage III operates at 195°F with a 38 weight
percent concentration of sulfuric acid as the electrolyte. The
gas composition of Stage III is 79 percent carbon dioxide with
balance of oxygen.

Metallic materials and gasket materials were evaluated for com-
patability with the operating environments of the three stages.
Matrix materials were evaluated for the acid electrolyte environ-
ment of Stage III.

FOREWORD

The research described herein, which was conducted by the Mechanical Products Division of TRW Inc., was performed under NASA Contract NAS 3-10930. The work was done under the technical management of Mr. Meyer Unger, Direct Energy Conversion Division, NASA-Lewis Research Center. The report was originally issued as TRW Report ER-7131-10, May 1968.

TABLE OF CONTENTS

TABLE OF CONTENTS (Continued)

ILLUSTRATIONS

ILLUSTRATIONS (Continued)

ILLUSTRATIONS (Continued)

ILLUSTRATIONS (Continued)

LIST OF TABLES

CARBONATION CELL MATERIALS COMPATIBILITY

by N. P. Bannerton, D. L. DeRespiris, and J. W. Vogt

SUMMARY

The objective of Contract NAS 3-10930 was to select metallic, gasket and acid electrolyte matrix materials compatible with the environmental exposures in the TRW Carbonation Cell System.

The program consisted of a literature survey, a preliminary screening test and environmental testing of selected samples to be used as (1) metallic materials (electrode substrates, cell structural components) for the alkaline (K_2CO_3) and acid (H_2SO_4) stages, (2) electrolyte matrix materials for the acid stage only, and (3) gasket materials for the alkaline and acid stages.

Metallic Materials

The metallic materials review and screening consisted of a survey of metallic elements in the Periodic Table and estimation of their suitability from a corrosion standpoint using Pourbaix diagrams. A preliminary selection of candidate materials resulted from this review. These materials were then electrochemically screened using a potentiostatic technique for determining corrosion of the metallic materials. The final list of metallic materials for the chemical immersion tests was then made based on the results of the potentiostatic screening tests. The selected materials were as follows:

Stage I   (K_2CO_3)   Platinum, Zirconium

Stage II   (K_2CO_3)   Platinum, Zirconium, Titanium

Stage III (H_2SO_4)   Tantalum

Material samples were then subjected to chemical immersion tests under the following environmental exposures:

Stage	Temperature (°F)	Electrolyte Type	Concentration	Gas Composition
I	175	K_2CO_3	30 wt %	0.5% CO_2 Bal. Air
II	175	K_2CO_3	30 wt %	57% CO_2 Bal. O_2
III	195	H_2SO_4	38 wt %	79% CO_2 Bal. O_2

The gas compositions were specified only for the metallic materials chemical immersion tests.

The material samples were subjected to metallurgical examinations after immersion periods of 200, 400, 600 and 1000 hours to determine any chemical or physical changes. X-ray diffraction, emission spectroscopy and electron microprobe tests and metallographic examinations showed no evidence of metallurgical changes and only minute evidence of build-up of corrosion layers. This was evidenced by the appearance of thin films in the 1000 hour test samples. The film thicknesses were estimated in the region of one micron based on the electron microprobe tests.

The conclusion drawn for the metallic materials test is that all materials selected for the immersion tests were satisfactory for the conditions specified.

Acid Matrix Materials

The acid matrix materials evaluation was initiated with a review of trade journals and manufacturers literature. The materials considered included filters, battery electrode separators and porous mats. A large number of the materials reviewed were found unsuitable for use with sulfuric acid because of some of the following characteristics: non-compatibility with sulfuric acid; low softening temperature; hydrophobicity and low bubble pressure.

Two materials were selected to undergo the corrosion immersion tests, i.e., Refrasil (a silica mat) and TA-1 (a microporous teflon). The environmental test conditions above were used for the chemical immersion tests. The materials were also evaluated for bubble pressure and electrolytic resistance.

Refrasil was considered the better material for use as the electrolyte matrix for the acid stage primarily because of the hydrophobic properties of the TA-1 mat. Refrasil was found virtually inert in sulfuric acid. Initially the bubble pressure of Refrasil (2.9 in. Hg) was significantly lower than the TA-1 mat (13.8 in. Hg), however, the value for Refrasil increased by approximately 26% over the 1000 hour test period while the TA-1 mat value decreased by approximately 24%. The electrolytic resistance data obtained were regarded as not truly representative or meaningful because of the broad range of values recorded. This was attributed to the wide variations in density of the Refrasil and to the non-uniform dewetting of the TA-1 mat.

Gasket Materials Evaluation

An extensive review for gasket materials was conducted and included a review of manufacturers data and recommendations. From the list of candidate materials, three were selected for the actual chemical immersion testing, i.e., Ethylene Propylene and Kel-F for the alkaline stages and Viton and Kel-F for the acid

2

stage. The selection was based on the potential abilities of these materials to withstand physical and chemical degradation and to maintain their sealing properties for periods in excess of 1000 hours.

Samples of each material were tested for periods of 200, 500 and 1000 hours in the electrolytes as listed above. The test program provided for measuring changes in physical properties including weight, thickness, compressibility and permeability to nitrogen.

The weight changes observed for all samples in both the alkaline and acid electrolytes were almost negligible - less than one percent. Kel-F displayed almost identical decrease in compressibility for the same test duration for both electrolytes. Ethylene Propylene in the alkaline electrolyte showed a slight gain in compressibility of approximately 1.5 percent while Viton in the acid electrolyte showed a decrease in compressibility of about 4.0 percent. Permeability values, however, in most cases were more widespread. In the alkaline electrolyte, Ethylene Propylene exhibited the greatest change (12×10^2 percent) with Kel-F showing a decrease of approximately 30 percent for the 1000 hour test period. In the acid electrolyte, both Kel-F and Viton exhibited a cyclic pattern for the 200, 500 and 1000 hour samples. The 500 hour samples showed an increase over that at the 200 hour test and both materials then decreased to approximately zero permeability after the 1000 hour test period.

Because of the high increase in permeability of Ethylene Propylene after 1000 hour test, Kel-F is considered the better choice for the alkaline electrolyte. Kel-F and Viton were both favorable performers in the acid electrolyte. A selection based chiefly on the results obtained would favor Viton for the acid electrolyte because of the small change in compressibility.

1.0 INTRODUCTION

The feasibility of the three-stage electrochemical carbon dioxide concentrator called a Carbonation Cell System, was demonstrated under Contract No. NAS 3-7638 by TRW Mechanical Products Division (formerly TRW Equipment Laboratories Division). Single cells of the three-stage Carbonation Cell System were tested under the program and materials degradation problems became evident with long term tests. Corrosion of metallic components and degradation of the acid stage matrix were the limiting factors to the life tests conducted during the program. The initial test data obtained showed that the Carbonation Cell System has excellent potential with the satisfactory solution of the materials problems.

The objective of this contract was to provide the necessary screening and test programs to generate data for the subsequent selection of materials compatible with the environmental exposure conditions existing in the different stages of the Carbonation Cell System.

Samples of three types of materials, viz. metallic, matrix and gasket were tested under this program to evaluate compatibility with the environmental exposure conditions found in the electro-chemical cells of the TRW Carbonation Cell System. The Carbonation Cell System which concentrates carbon dioxide from air uses both alkaline and acid electrolytes for the carbon dioxide concentration process. The alkaline electrolyte cells primarily allow the concentration of CO_2 and O_2 from air and the acid electrolyte cells in the last stage permit the selective separation of O_2 from the concentrated CO_2 gas mixture. The composition of the gas stream at the cathode outlet of the acid stage is essentially pure CO_2.

The test program consisted of examination of samples of the various materials in the "as received" condition and then exposing the samples to the environmental conditions for varying test periods up to 1000 hours. The object was to identify the onset of physical and/or chemical changes in the different materials and, through periodic examinations to determine rates of change for properties such as: corrosion film formation, weight, resistance, permeability, compressibility, etc.

The metallic materials which were selected for evaluation in the three stages were as follows. Platinum and Zirconium were tested at the alkaline Stage I exposure conditions and Platinum, Zirconium and Titanium were tested at the alkaline Stage II exposure conditions. Tantalum was the only material selected for evaluation in the exposure conditions of Stage III, the acid stage. From the tests conducted, Platinum and Tantalum were found to be chemically most suitable for the alkaline and acid stages, respectively.

Evaluation of matrix materials was confined to the acid stage only under this program since the alkaline matrix (Johns Mansville Fuel Cell Asbestos) performed satisfactorily in the previous program. Refrasil silica fiber gave the best results in the acid stage environment.

Testing conducted on samples of Kel F, Ethylene Propylene and Viton showed Kel F and Viton as the most suitable gasket materials for the alkaline and acid stages, respectively.

2.0 PROGRAM PLAN AND TASK DESCRIPTIONS

The materials compatibility program consisted of a literature survey followed by a materials corrosion test phase for each of the major cell components being evaluated. The literature surveys and materials' physical properties examinations were performed in order to select candidate materials for the test programs. Following the sample selection, a limited life-test program was conducted to evaluate the ability of the selected materials to withstand the environmental exposure conditions within the system (see Table 1).

The work under the contract was divided into three program tasks as follows:

(1)   Metallic materials

(2)   Acid matrix materials, and

(3)   Gasket materials.

The above division corresponds with the major cell components found in the Carbonation Cell System.

2.1   Task Description

2.1.1   Task 1 - Metallic Materials Evaluation

Evaluation of the metallic materials required under this task consisted of two parts: 1) a material literature review and 2) a test program.

The material literature review was undertaken to make preliminary screening and selection of materials for the major metallic cell components of each stage including the electrode substrates and cell structural components. Selection of candidate materials was to be based primarily on the following characteristics - ability to withstand electrolyte corrosion, mechanical strength, ease of fabrication, electrical conductivity and applicability to a flight-weight system.

The test program for the metallic materials consisted of two parts, viz: 1) Electrochemical Corrosion Tests and 2) Chemical Immersion Tests.

The electrochemical corrosion tests were conducted to screen potential materials and to provide data for the selection of samples for the chemical immersion tests. Following the literature review, further materials screening tests were made using a "Potentiostatic Technique" for predetermination of corrosion characteristics of metals and alloys. This test consisted of running a constant potential scan of both the anodic and cathodic polarization for the test specimen at the required environmental exposures. The corrosion current obtained over the

TABLE 1

EXPOSURE TEST CONDITIONS
FOR
THE CARBONATION CELL SYSTEM

Exposure Condition (Stage)	Temperature (°F)	Electrolyte		Gas(1) Composition
		Type	Concentration	
I	175	K_2CO_3	30 wt %	0.5% CO_2 Bal Air
II	175	K_2CO_3	30 wt %	57% CO_2 Bal O_2
III	195	H_2SO_4	38 wt %	79% CO_2 Bal O_2

(1) For chemical immersion test only.

observed potential region was recorded. The resulting current-potential curve gear can be interpreted to delineate regions of active, passive and transpassive behavior. In order to evaluate the effects that O_2 and CO_2 have on the corrosion current for each material, the potentiostatic screening test was repeated, first with pure O_2 and then with pure CO_2 bubbled over the surface of the test specimen. Details and results of this testing are presented in Section 3.1.2.

The chemical immersion tests were conducted using sample materials of approximate thickness equal to that required for the application in the system. Test samples were immersed for certain test periods up to 1000 hours in electrolytes at specified temperatures and concentrations. During this period mixtures of O_2 and CO_2 gases were bubbled over the surface of the test specimens. Saturation of the electrolyte with respect to the gas and a constant electrolyte composition maintained within ± 1 percent, were required throughout the 1000 hour test.

Specific samples were withdrawn from the test beakers at intervals of 200, 400, 600 and 1000 hours and were examined for evidence of corrosion. The corrosion evaluation techniques used were as follows:

a. Photographs

b. Weight changes

c. Metallographic examination

d. Film corrosion layer examination

   1. X-ray diffraction

   2. Microprobe study of metallographic specimen

e. Electrical conductivity change

f. Chemical analyses of material and electrolyte.

Detailed description of these tests and interpretation of the results are presented in Section 3.1.4.

2.1.2   Task II - Acid Matrix Evaluation

The acid matrix materials evaluation task required under this program consisted of 1) a material screening and evaluation and 2) an immersion test program for selected candidate materials.

The material screening and evaluation phase required was primarily a literature review including consultation with manufacturers for the selection of sample materials based on their potential ability to withstand physical and chemical degradation under the operating conditions specified for the acid stage.

Materials initially selected as candidates were tested for the following physical properties:

   1. Void volume.

   2. Bubble pressure of material saturated with electrolyte under the temperature-concentration combination required for the acid stage.

   3. Cell resistance under conditions similar to (2).

Based on the results of the initial screening tests and the preliminary physical properties testing, two candidate materials were selected to undergo the chemical immersion testing in sulfuric acid. After elapsed times of 200, 400, 600 and 1000 hour periods, specific samples were removed for examination and evaluation with respect to the following where applicable:

   1. Weight

   2. Electrical conductivity (sample saturated with electrolyte)

   3. Gas permeability (bubble pressure)

   4. Void volume

5. Linear dimensions

6. Analyses of electrolyte for matrix constituents

The results of this evaluation program are presented in Section 3.2.

2.1.3   Task III - Gasket Materials Evaluation

The gasket materials evaluation program also consisted of two parts: 1) a materials screening phase with preliminary physical properties measurement and 2) a chemical immersion test phase.

A literature survey was first conducted under the screening program to select suitable candidate materials for both the alkaline and acid stages. Material selection was based primarily on the potential ability to withstand physical and chemical degradation, and to maintain sealing properties for periods up to 10,000 hours. Review of the following properties was required in the evaluation of the gasket materials:

1. Composition

2. Gas permeability

3. Compressibility

The chemical immersion tests consisted of immersing sample materials in electrolytes at the specified temperatures and concentrations. The materials were subjected to chemical immersion tests similar to those conducted for the matrix materials. Again, following test periods of 200, 500 and 1000 hours one sample of each material was removed and evaluated for the following properties were applicable.

1. Weight

2. Linear dimensions

3. Permeability

4. Compressibility

These tests and resulting data are described and discussed in Section 3.3.

9

3.0 MATERIALS EVALUATION AND TEST

3.1 Metallic Materials

3.1.1 Material Screening

The use of a metallic material in the Carbonation Cell System will, in general, be dictated by the following characteristics:

1. Corrosion resistance under the operating conditions of temperature, electrode potential and the nature and concentration of both the liquid and gas phase constituents.

2. Resistivity.

3. Mechanical strength.

4. Availability and ease of fabrication.

5. General applicability to a flight weight system.

Primary consideration was given to characteristic (1) above because the remaining considerations are somewhat flexible and subject to design. With the exception of the electrode potentials* all individual cell operating conditions are defined by the Final Report of NASA Contract NAS 3-7638, i.e., cell temperature, electrolyte concentration and gas composition.

Since corrosion resistance is primarily a function of a metal's electrochemical potential and solution pH, these data were first defined for the individual cells of the Carbonation Cell System and the method employed is described in the following section. Prior to this work no such data were known to exist.

3.1.1.1 Estimation of Metallic Operating Domain (Potential-pH)

The operational domains of Stages I, II, and III were estimated from relative systems data with the use of basic electrochemical principles. Essentially a two point half-cell polarization curve was constructed for the Pt Black/O_2/OH$^-$ couple of each stage, the two current density coordinate points being zero and 75 amps per square foot (ASF).

A simplifying assumption necessary to the derivation was that the kinetics of the oxygen reduction and oxygen evolution processes were independent of the nature of the solution anion. The necessity for the above assumption was dictated by the lack of reliable and/or absence of Pt Black/O_2/K_2CO_3 system data in the literature.

---

*It is assumed that the selected cell design will result in electrical contact of the electrode with the cell metallic components. Thus, the metallic components will assume the same potential as the working electrodes.

10

The following is a general description of steps involved in the estimation of the half cell potential domain. Specific derivations are presented in Appendix 1.

1) The calculated half cell oxygen potential is determined for the pH* values of the individual stages for the system Pt Black/O_2/OH^-.

2) The potential difference between the calculated O_2 potential and actual measured potential for an analogous O_2 system, e.g., Pt Black/O_2/30% KOH is then determined. This potential is a measure of the deviation from the calculated cell potential.

3) The potential difference found in step 2) is then algebraically added to the calculated half cell value in step 1) for each stage. This sum is the corrected Pt Black/O_2 open circuit potential for Stages I, II and III which approximates the measured O_2 potential at the indicated pH.

4) From the referenced system data, the potential at 75 ASF for oxygen reduction and evolution processes is determined for the system Pt Black/O_2/30% KOH.

5) The actual measured Pt Black/O_2 open circuit potential is then algebraically added to the potential referenced in step 4). This sum is the polarization from the measured open circuit potential for the O_2 reduction and evolution processes for the analogous system, Pt Black/O_2/30% KOH.

6) Now, the values determined in step 5) are algebraically added to the corrected Pt Black/O_2 open circuit potentials determined in step 3). The values obtained are the potentials for the oxygen evolution and reduction processes at 75 ASF for Stages I, II and III. These values contain activation polarization losses only.

7) For the alkaline stages (I and II) an additional correction must be applied to include possible concentration polarization losses at the anode, the oxygen evolving electrode.

A summary of the estimated pH - Potential Domains for the three stages is shown below. (Refer to Appendix I for detailed derivations.)

---

*Estimates of pH for the stages are given in Appendix 2.

Estimated pH - Potential Domains

Stage	pH Anode	Cathode	Maximum Potential (75 ASF) Anode	Cathode
I	8.7	10	1.363	0.289
II	8.3	8.4	1.473	0.333
III*	<0	<0	1.825	0.75

The validity of the pH-Potential Domains shown are subject to the assumptions made in the derivation of the pH = $F[PCO_2]$ function. It must also be noted that the calculated pH is that of the bulk electrolyte and does not predict the solution pH in the immediate vicinity of the electrode. The concentration gradient of OH^- ions (pH) that is obtained during current flow will result in a higher concentration of OH^- ions at the cathode. The equilibrium concentration of OH^- ions will in part be determined by the concentration of carbon dioxide in the electrolyte as discussed in Appendix II; see $[CO_2]* = k\ PCO_2$, etc. The value of k, the solubility coefficient, used in the derivation is for the carbon dioxide-water system. The actual solubility coefficient k for a strong electrolyte such as 30% K_2CO_3 may well be several orders of magnitude lower than the value assumed. This would result in a more alkaline (higher pH) solution than the one estimated.

The calculated pH using the analysis described in Appendix II is one pH unit lower than the measured value. This difference is most probably due to the use of concentration coefficients instead of activity coefficients in the expressions for K_1 and K_2. All of the above considerations would indicate a higher pH range than the ones calculated. Since, in general, metals tend to corrode at the extremes of the pH spectrum it would be more in keeping with the intent of this study to extend the estimated pH range into the more alkaline regions.

Revised pH Potential Domains

Stage	pH Anode	Cathode	Maximum Potential (75 ASF) Anode	Cathode
I	12.0	13.0	1.11	-0.027
II	9.0	10.5	1.29	0.148
III	<0	<0	1.825	0.75

---

*60 ASF

*[ ] = concentration of substance in Moles/Liter.

3.1.1.2   Philosophy of Screening Methods

The approach adopted for the selection of candidate metallic materials for electrochemical screening was essentially a process of elimination. The universe selected for the possible candidate materials was the periodic table of elements - Figure 1. All those elements satisfying the application of a three-fold set of criteria were subjected to electrochemical analysis. Pertinent materials' information abstracted from the literature was used to verify, enlarge or delete from the body of candidate elemental materials selected by the above mentioned methods.

The three sets of selection criteria used are as follows:

    I.   The candidate elemental material should be: 1) a solid with reasonably high conductivity and have chemical stability in the intended aqueous solution; 2) commercially available.

    II.   For the application: 1) the projected operating domain (potential/pH) of the metal should not lie within the corrosion region of the Pourbaix diagram for the intended metal.

    III.   The chosen material should: 1) have a general applicability to operation in both anodic and cathodic mode for the specific stage in question, 2) be easily fabricated, 3) be non-toxic, 4) offer an advantage such as lower weight, higher thermal conductivity or lower cost in the case where there is a choice between two similar materials, 5) have a general applicability to use in a flight weight system.

It should be noted that large numbers of candidate materials may exist in classes of materials such as compounds, alloys and intermetallics. The appearance of any of this classification of materials in the final recommended set of candidate materials is only by virtue of having been specifically referenced in the experimental corrosion literature or fuel cell literature.

3.1.1.2.1 Periodic Table

The application of criteria I to the elements appearing in Figure 1, the Periodic Table of Elements, results in the rejection of the following elements.

Group 1-A

The alkali metals exert extremely low saturation potentials.

These metals are very unstable in the presence of aqueous solutions of any pH. Because the oxides are very soluble they cannot produce any passivation and the metals decompose aqueous solutions very vigorously with the evolution of hydrogen. These metals also have low melting points.

GROUP / PERIOD	Ia	IIa	IIIa	IVa	Va	VIa	VIIa	VIII			Ib	IIb	IIIb	IVb	Vb	VIb	VIIb	0
1	1 H																1 H	2 He
2	3 Li	4 Be											5 B	6 C	7 N	8 O	9 F	10 Ne
3	11 Na	12 Mg											13 Al	14 Si	15 P	16 S	17 Cl	18 A
4	19 K	20 Ca	21 Sc	22 Ti	23 V	24 Cr	25 Mn	26 Fe	27 Co	28 Ni	29 Cu	30 Zn	31 Ga	32 Ge	33 As	34 Se	35 Br	36 Kr
5	37 Rb	38 Sr	39 Y	40 Zr	41 Nb	42 Mo	43 Tc	44 Ru	45 Rh	46 Pd	47 Ag	48 Cd	49 In	50 Sn	51 Sb	52 Te	53 I	54 Xe
6	55 Cs	56 Ba	57 La	72 Hf	73 Ta	74 W	75 Re	76 Os	77 Lr	78 Pt	79 Au	80 Hg	81 Tl	82 Pb	83 Bi	84 Po	85 At	86 Rn
7	87 Fr	88 Ra	89 Ac															

LANTHANIDE SERIES 4f	58 Ce	59 Pr	60 Nd	61	62 Sm	63 Eu	64 Gd	65 Tb	66 Dy	67 Ho	68 Er	69 Tm	70 Yb	71 Lu

ACTINIDE SERIES 5f	90 Th	91 Pa	92 U	93 Np	94 Pu	95 Am	96 Cm	97 Bk	98 Cf					

FIGURE 1 PERIODIC TABLE OF ELEMENTS

Group 2-A

The alkaline earth metals, including magnesium and beryllium, also exert extremely low solution potential. They are extremely base metals and powerful reducing agents. They have a large affinity to react with water which they theoretically decompose with the evolution of hydrogen, the exception being beryllium which passivates in neutral to moderately alkaline solutions.

Group 3-A

Scandium and yttrium are extremely base metals and powerful reducing agents having a great affinity to react with water which they decompose with the evolution of hydrogen. In the presence of acid and neutral solutions the liberation of hydrogen is accompanied by the dissolution of scandium and yttrium to form ions of the metal. In the presence of alkaline solutions the evolution of hydrogen takes place concurrently with the formation of scandium hydroxide and yttrium hydroxide.

Remaining Groups

The lanthanide series of elements and the actinide series of elements together with Group 0 and Group 7B elements are all eliminated for the obvious reason of not satisfying either one or all of the first criteria. All the elements from Groups 2B through 6B except zinc, lead, tin, and carbon are eliminated for similar reasons.

With the exceptions noted above, the remaining twenty-eight (28) elements appearing in Groups 4-A through 1-B (see Figure 2) are now subjected to the second selection criteria as discussed in the following section.
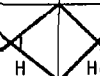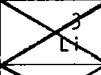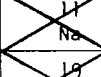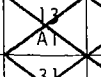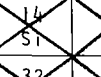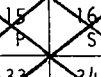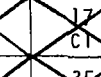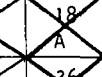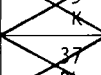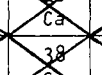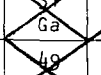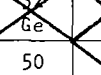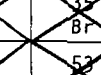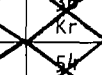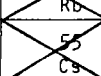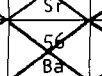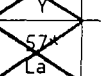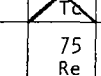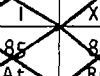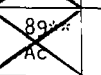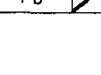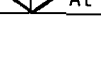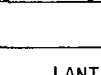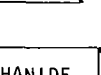
3.1.1.2.2 Pourbaix Diagrams* (15, 16, 18, 65, 66)
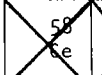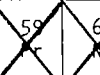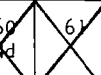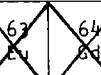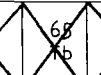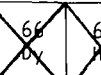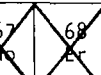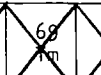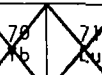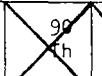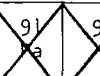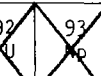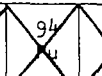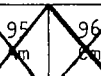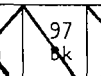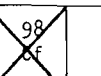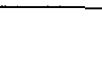
Description

Pourbaix diagrams may be defined as electrochemical equilibrium diagrams useful for obtaining as complete and overall a view as possible of the interface reactions thermodynamically possible in a particular set of conditions. Such diagrams indicate as a function of the metal electrode potentials and of the solution pH, the thermodynamic limits of the stability of the metal in relation to its ions, to the ions of water and to the reaction products of these ions. The limitations in the application of Pourbaix diagrams to real systems may be briefly summarized as follows. Real corrosion situations often involve significant

---

*A detailed explanation of construction method and data interpretation is presented in Appendix III.

GROUP PERIOD	Ia	IIa	IIIa	IVa	Va	VIa	VIIa	VIII			Ib	IIb	IIIb	IVb	Vb	VIb	VIIb	0
1	1 H																1 H	2 He
2	3 Li	4 Be											5 B	6 C	7 N	8 O	9 F	10 Ne
3	11 Na	12 Mg											13 Al	14 Si	15 P	16 S	17 Cl	18 A
4	19 K	20 Ca	21 Sc	22 Ti	23 V	24 Cr	25 Mn	26 Fe	27 Co	28 Ni	29 Cu	30 Zn	31 Ga	32 Ge	33 As	34 Se	35 Br	36 Kr
5	37 Rb	38 Sr	39 Y	40 Zr	41 Nb	42 Mo	43 Tc	44 Ru	45 Rh	46 Pd	47 Ag	48 Cd	49 In	50 Sn	51 Sb	52 Te	53 I	54 Xe
6	55 Cs	56 Ba	57* La	72 Hf	73 Ta	74 W	75 Re	76 Os	77 Ir	78 Pt	79 Au	80 Hg	81 Tl	82 Pb	83 Bi	84 Po	85 At	86 Rn
7	87 Fr	88 Ra	89** Ac															

LANTHANIDE SERIES 4f	58 Ce	59 Pr	60 Nd	61	62 Sm	63 Eu	64 Gd	65 Tb	66 Dy	67 Ho	68 Er	69 Tm	70 Yb	71 Lu

ACTINIDE SERIES 5f	90 Th	91 Pa	92 U	93 Np	94 Pu	95 Am	96 Cm	97 Bk	98 Cf

Note: ⊠ Indicates Rejection of Element

FIGURE 2 ELEMENTS REJECTED BY CRITERIA I

departures from equilibrium. The diagram refers to the pure metal, not alloys, and to pure water, free of substances capable of either forming soluble complexes or insoluble compounds. The pH value indicated in the diagram is that of the solution in direct contact with the metal and is not necessarily that of the solution as a whole. Information on the rate of corrosion is not given directly by the diagram.

Application to Materials Selection

The application of the second criteria to the remaining twenty-eight (28) elements in Paragraph 3.1.1.2.1 above was accomplished as follows. Refer to Figure 2. The revised estimated operating domains for Stages I, II and III, Paragraph 3.1.1.1, were plotted on Pourbaix diagrams for the elements in question. These domains defined for Stages I, II and III are the projected maximum operating conditions to be expected, and the common areas of stability and/or corrosion were noted. An element was rejected for either anodic or cathodic use if its estimated projected operating domain was coincident with any part of a Pourbaix corrosion domain. In the case of minor coincidence the element was not rejected. As a result, 19 of the 28 elements were judged to be acceptable. (Note: Not all of the accepted elements are applicable to all three stages.) Shown in Figures 3 through 8 are reproductions of 17 Pourbaix Diagrams for materials judged acceptable. The two elements not shown are carbon and cadmium which were rejected for reasons discussed in Section 3.1.1.2.3. Examples of whole or partial coincidences of a corrosion domain with the operating domain are as follows: silver - Stages I, II; tin - Stage I; gold - Stages I, II and III anodic only; zirconium-Stage III; lead - Stage I; copper - Stage I; tungsten - Stages I and II; iridium - Stages I and II anodic only. An element was not rejected if: (1) its anodic or cathodic domain were separately coincident with the corrosion domain, or (2), it did not have immunity or passivation characteristics for all three stages.

3.1.1.2.3 Literature - Corrosion, Electrochemical Technology

The purpose of the survey was two-fold: 1) to discover applicable commercially available materials such as alloys and compounds which are suitable for the Carbonation Cell System, and 2) to substantiate or reject the candidate elemental materials selected according to the method outlined in Section 3.1.1.2. A total of 80 selected papers, contract reports, articles and notes were reviewed. The main sources of the literature used in the survey were the basic Corrosion Journals, the Electrochemical Journals, and Government Contract Reports.

In general, it was found that for the alkaline Stages I and II no analogous systems were directly identified in the literature. The closest approximations to the systems in terms of the nature of the electrolyte were aqueous systems involving concentrated potassium hydroxide or dilute solutions of sodium carbonate or

POURBAIX DIAGRAMS
SHOWING
THEORETICAL DOMAINS OF CORROSION, IMMUNITY & PASSIVATION

Passivation by film of Fe₂O₃

Passivation by films of Fe₂O₃ and Fe₃O₄

STAGE I ▨

STAGE II ▢
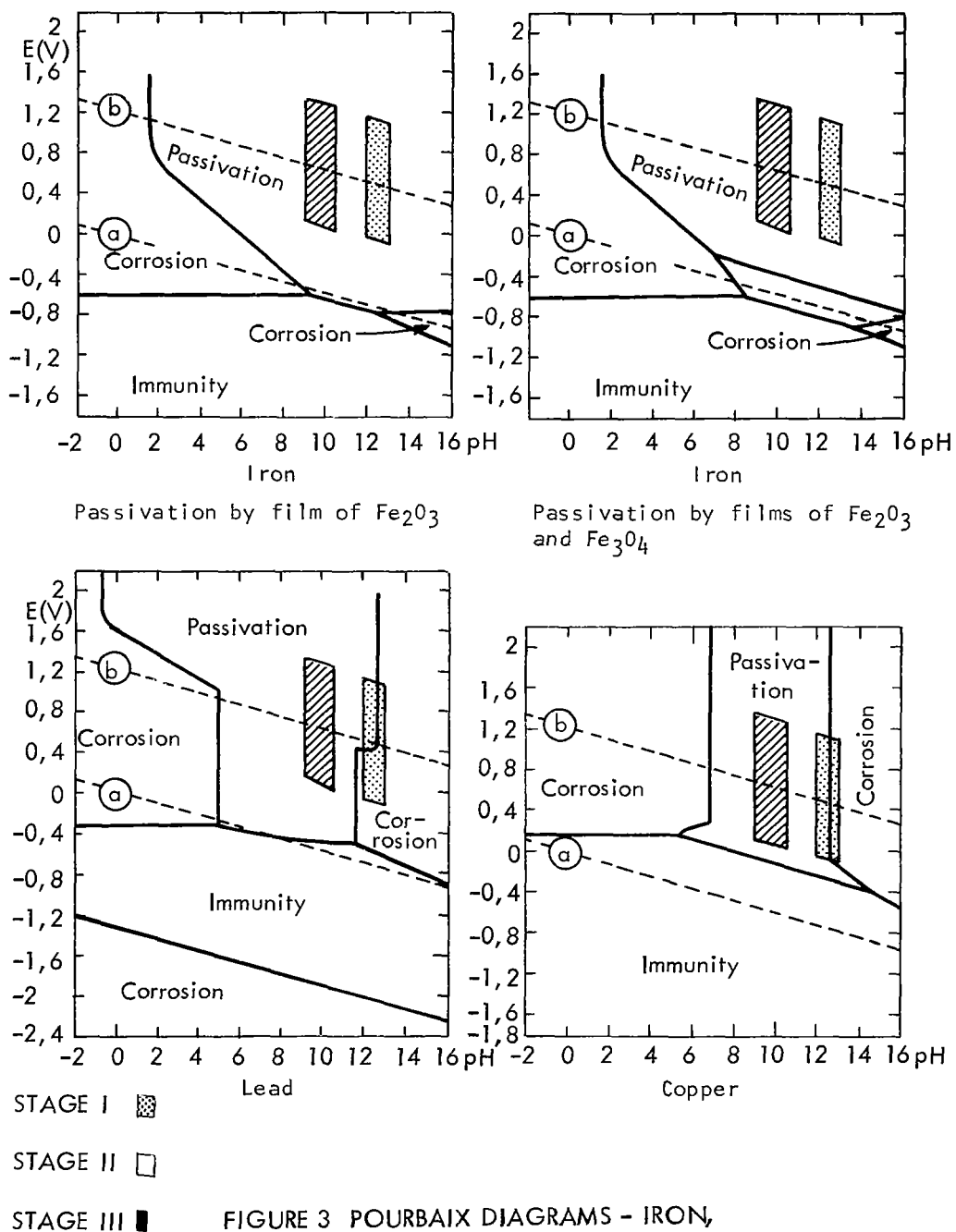
STAGE III ▓   FIGURE 3 POURBAIX DIAGRAMS - IRON,
                          LEAD, COPPER
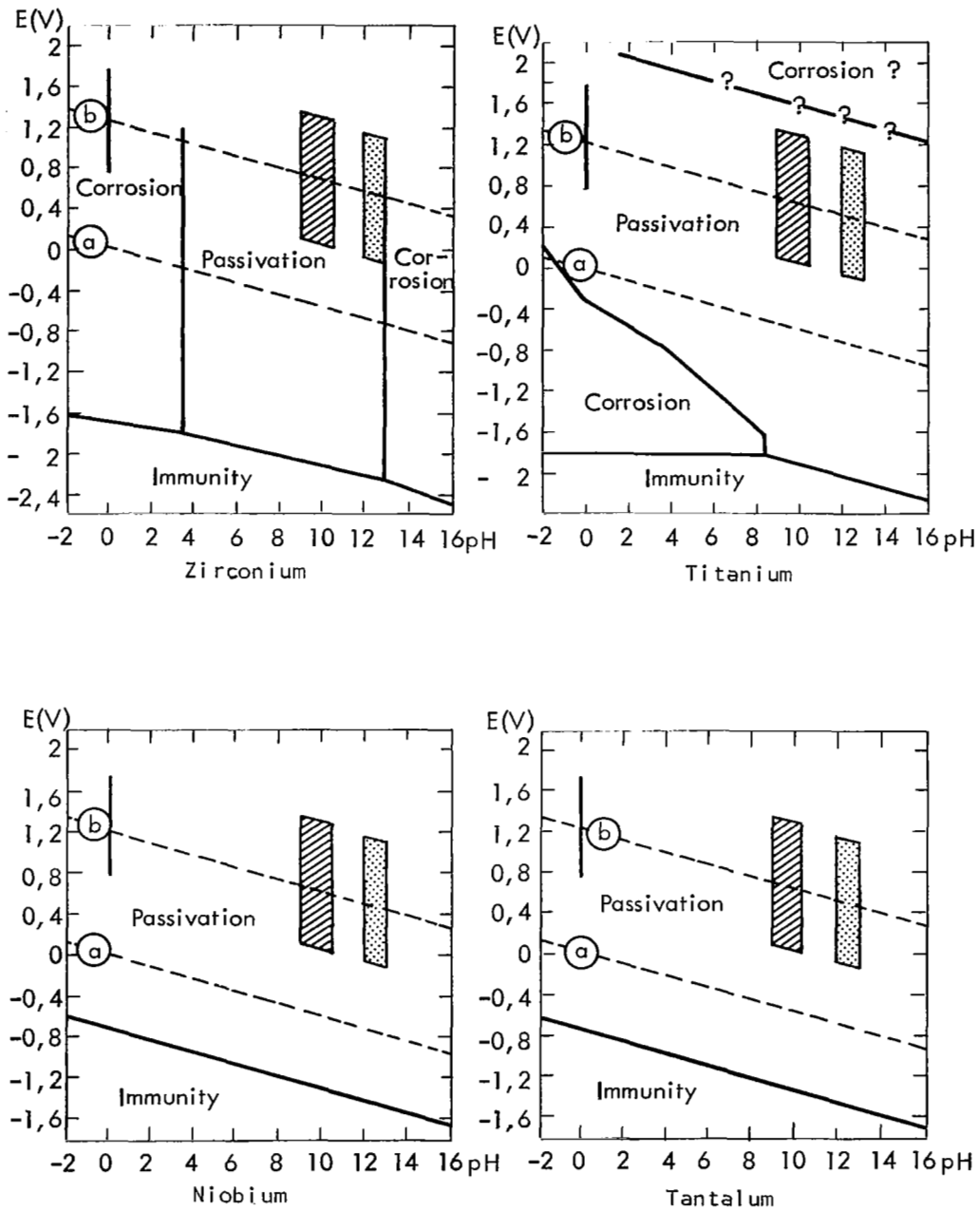
FIGURE 4 POURBAIX DIAGRAMS – ZIRCONIUM, TITANIUM, NIOBIUM, TANTALUM
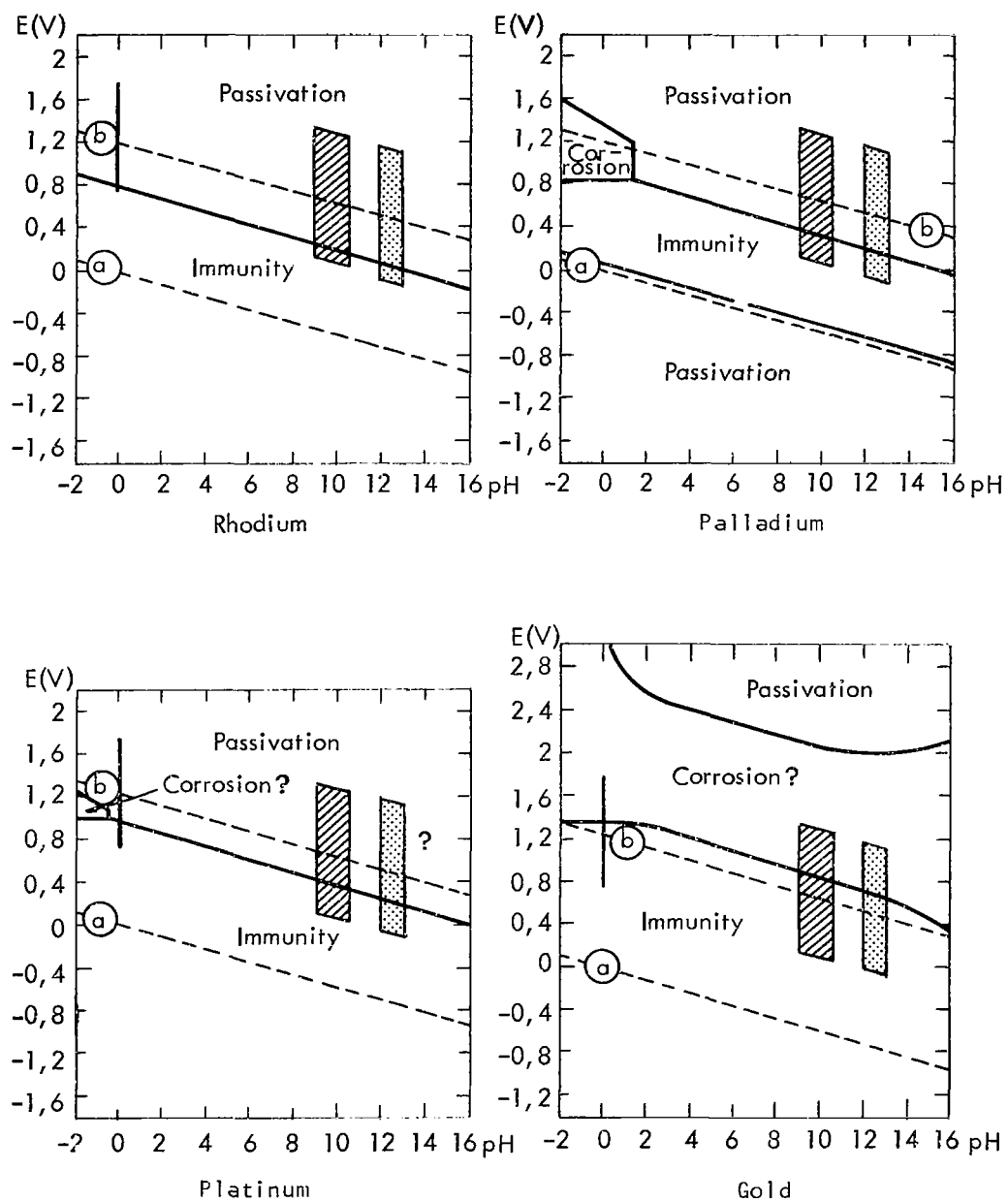
FIGURE 5 POURBAIX DIAGRAMS - RHODIUM, PALLADIUM, PLATINUM,
         GOLD
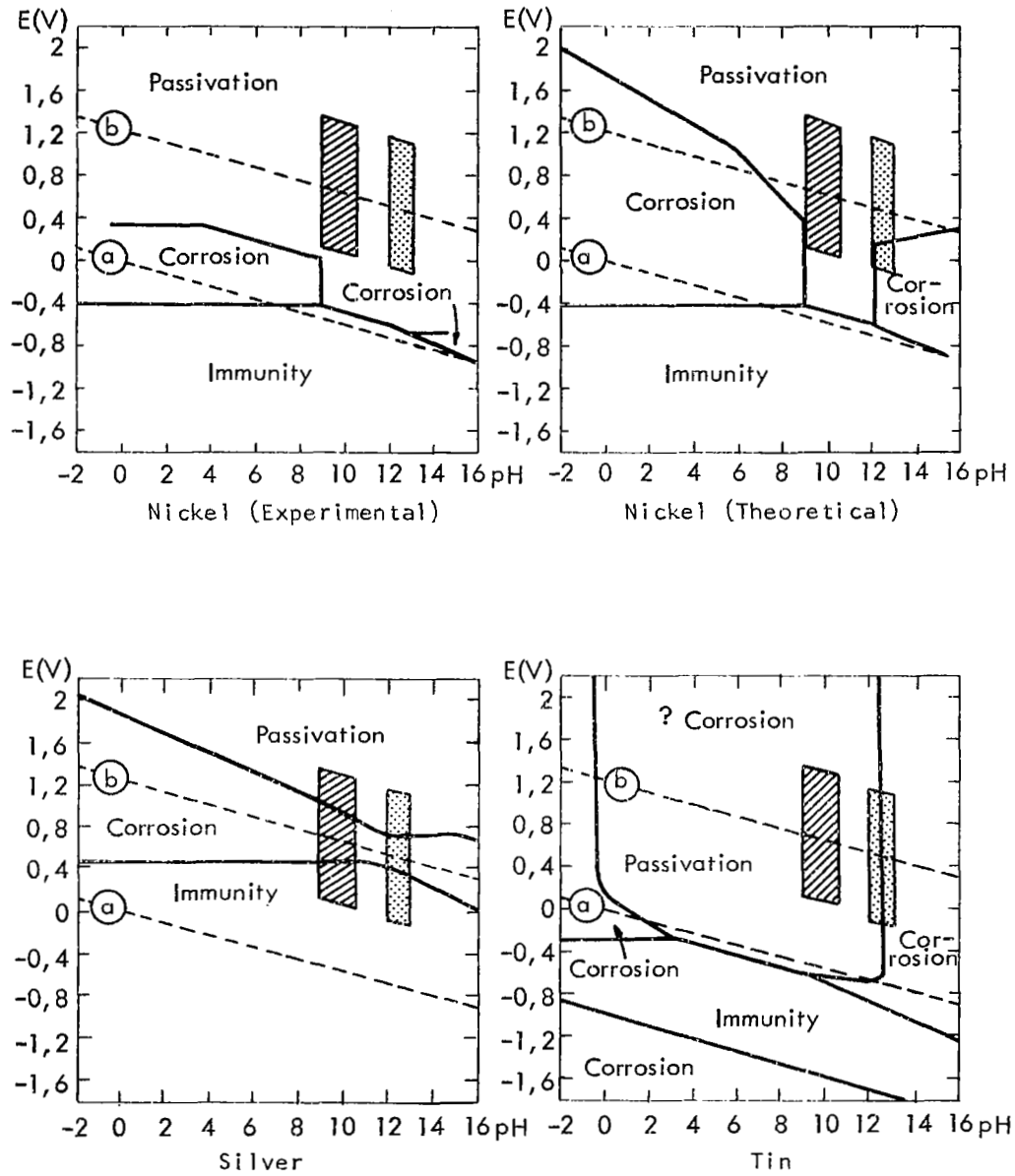
FIGURE 6 POURBAIX DIAGRAMS – NICKEL, SILVER, TIN

POURBAIX DIAGRAMS
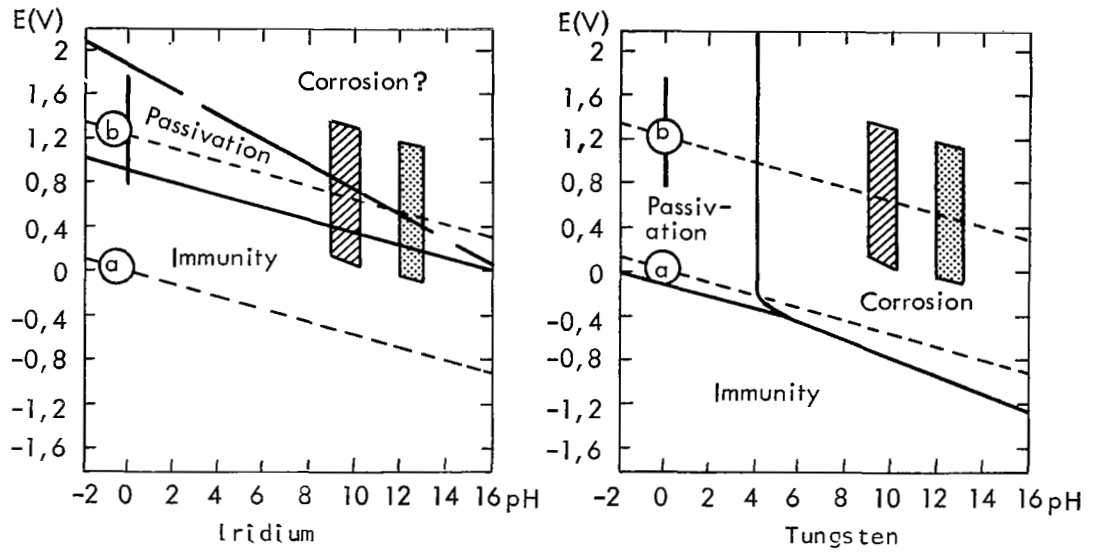
FIGURE 7 POURBAIX DIAGRAMS - IRIDIUM, TUNGSTEN

POURBAIX DIAGRAM
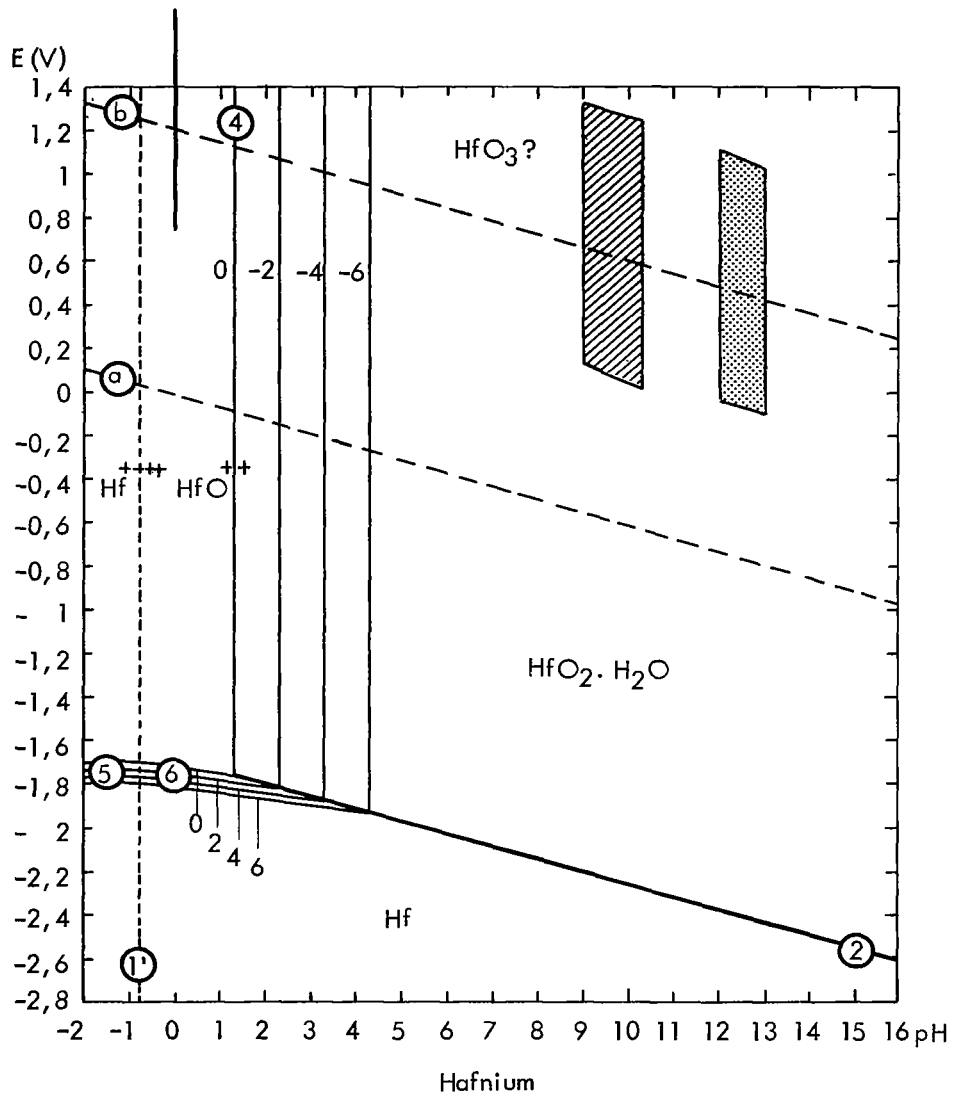
FIGURE 8 POURBAIX DIAGRAM - HAFNIUM

sodium bicarbonate (1, 9, 25). In terms of the metal operating potential range it can be categorically stated as a result of the literature review, that no evaluation was carried out at potentials greater than 1.2 volts with respect to the hydrogen electrode in the same solution (the anodic operating region of Stages I and II). From the standpoint of metals, the bulk of the applied technology literature dealing with metal-acid systems deals with alloy, interstitial or intermetallic type materials, which at present, are not commercially available (2, 5, 19, 20, 28, 29, 30, 31, 32). Classes of materials such as intermetallics and interstitials were also shown to be stable in highly alkaline solutions up to potentials of 1.2 volts (9, 25).

A possible acid candidate material, Nionel 825, (2) was experimentally determined to have a stable region of operation up to potentials of 1.2 volts in 5 normal sulfuric acid at ambient temperature. Above 1.2 volts, the limited data indicated relatively large increases in corrosion rates. The inclusion of this alloy in the final group of candidate materials was dictated by its possible use in the cathodic region of Stage III. The alloy, Monel 400, was included in the list of candidate metallic materials for two reasons. The literature specifically references this alloy as being stable in alkaline solutions of potassium carbonate (68). It is also of interest since the alloy is principally a composite of nickel and copper elemental materials previously recommended by the application of criteria II.

In summary, no specific reference could be found in literature which could negate the elemental material selection which was made for the environments defined in Table 1 by the application of criteria I and II. However, the literature identifies limited areas of non-compatibility of some of the elemental materials referenced in Table 2. For example, the element tantalum is reported to corrode when polarized anodically in alkaline solutions (65). The remaining elements of the Periodic Table after the application of Criteria II are shown in Figure 9 and are next to be analyzed by the application of Criteria III. Also shown in Table 2 are those elements recommended by the application of Criteria I and II specified according to the intended use in either Stage I, II or III.

3.1.1.3 Selection and Recommendations of Candidate Materials for Electrochemical Testing

The final selection of candidate materials for electrochemical testing was made by the application of Criteria III to the materials listed in Table 2, also shown in Figure 10*. The materials which were thus disqualified and the reasons for their elimination are presented in Table 3.

---

*Monel 400 and Nionel 825 not shown.

Note: ⊠ Indicates Rejection of Element

FIGURE 9 ELEMENTS REJECTED BY CRITERIA I & II

Note: ☒ Indicates Rejection of Element

FIGURE 10 ELEMENTS REJECTED BY CRITERIA I, II, III

The contractual requirements for recommendations of candidate materials for electrochemical testing were two-fold. 1) It was required that a minimum of two and a maximum of 4 materials per component be recommended, 2) the components to be considered were the cell end plates (current collectors) and the electrode substrate for the platinum black catalyst. Since the form of the material to be used was not specified, the use of composite structures such as plated materials or clad materials or materials in bulk form could be considered. However, no material could be recommended for use in the plated form due to uncertainties in the thickness of deposit necessary to achieve a non-porous plate. Therefore, the following selections are for the bulk or clad form of the material only. The final selection of candidate materials for the specific stages of operation is shown in Table 4. The translation of a material from the final selection of materials to a specific use, i.e., electrode substrate or end plate is electrochemically arbitrary, since in cell operation the material does not know if it is an end plate or electrode substrate. Therefore, the criteria used in recommending a material for a specific component were first, cost and second the objective of submitting the maximum number of candidate materials for electrochemical testing. The recommended materials for electrochemical testing are presented in Table 4, according to their intended use.

3.1.2   Electrochemical Corrosion Tests

A method employing potentiostatic control of the test specimen was selected for the electrochemical evaluation of candidate materials. The reader is referred to the numerous texts and papers which deal with the theory and application of this method (11, 17, 18, 34, 69, 70). Essentially the method utilizes the potentiostat which forces the electrodes under test to maintain a fixed or a linearly changing voltage as was employed in this evaluation. The net current flow which is necessary to polarize the test electrode is recorded. The resultant voltage-current relationship yields information as to the voltage at which reactions begin and the range of voltage over which these reactions extend. If a single reaction is being considered, qualitative information about the nature of the reaction may be obtained from the voltage characteristic while the rate of the process is directly proportional to the current produced.

Experimental Cell Design. A conventional three-electrode cell design was adopted for the scanning tests. The reference and counter electrodes are isolated from the main cell compartment by sintered glass discs.

Potentiostatic evaluation of the test electrodes was accomplished with the use of a Beckman "Electro-Scan 30" (71). In the potentiostatic mode of operation the range of current sensitivity is from 0.7 micro-ampere to 140 milliamperes and the voltage scan rates from 0.5 to 500 millivolts/min. Figure 11 shows the

TABLE 2

RECOMMENDED MATERIALS BASED ON CRITERIA I & II

Stage I	Stage II	Stage III
Carbon	Carbon	Carbon
Iron	Iron	Nionel (Incoloy) 825
Zirconium	Zirconium	Zirconium
Hafnium	Hafnium	Niobium
Nickel	Nickel	Tantalum
Niobium	Niobium	Rhodium
Gold	Gold	Platinum
Monel 400	Monel 400	Gold
Platinum	Platinum	Titanium
Palladium	Palladium	Tungsten
Rhodium	Rhodium	Iridium
Cadmium	Titanium	Hafnium
Tantalum	Copper	
Cobalt	Tin	
	Tantalum	
	Lead	
	Cobalt	

TABLE 3

MATERIALS REJECTED BASED ON CRITERIA III

Material	Stage	Reason for Rejection
Hafnium	I, II, III	Properties similar to those of zirconium and zirconium is half as dense as hafnium and 1/35 of the cost of hafnium.
Titanium	III	By direction of NASA Project Manager - other references indicate passivity in the operating range of Stage III (64).
Iridium	III	Properties similar to those of platinum. The cost of iridium is almost twice as high as platinum.
Tantalum	I, II	Evidence of corrosion at anodic potentials in alkaline solution (65). As a result would not be generally applicable to both anodic and cathodic mode of operation.
Niobium	I, II	Similar to tantalum.
Gold	I, II, III	Anodic dissolution indicated by Pourbaix diagrams. Partial dissolution in cathodic mode also indicated, therefore not generally applicable.
Palladium	I, II	Chemical properties similar to platinum which will be evaluated.
Rhodium	I, II, III	Cost is high - difficult to obtain - chemical properties similar to platinum.
Tungsten	III	Ease of fabrication criteria not satisfied.
Carbon	I, II, III	Ease of fabrication criteria not satisfied for electrode support. Mechanical strength criteria not satisfied for end plate use.
Cadmium	I	Must be used in plated form due to lack of mechanical strength. Contract not evaluating composite materials.
Cobalt	I, II	Limited applicability cathodic mode.
Lead	II	Difficult to obtain in pure form. Impurity level may well control corrosion behavior.
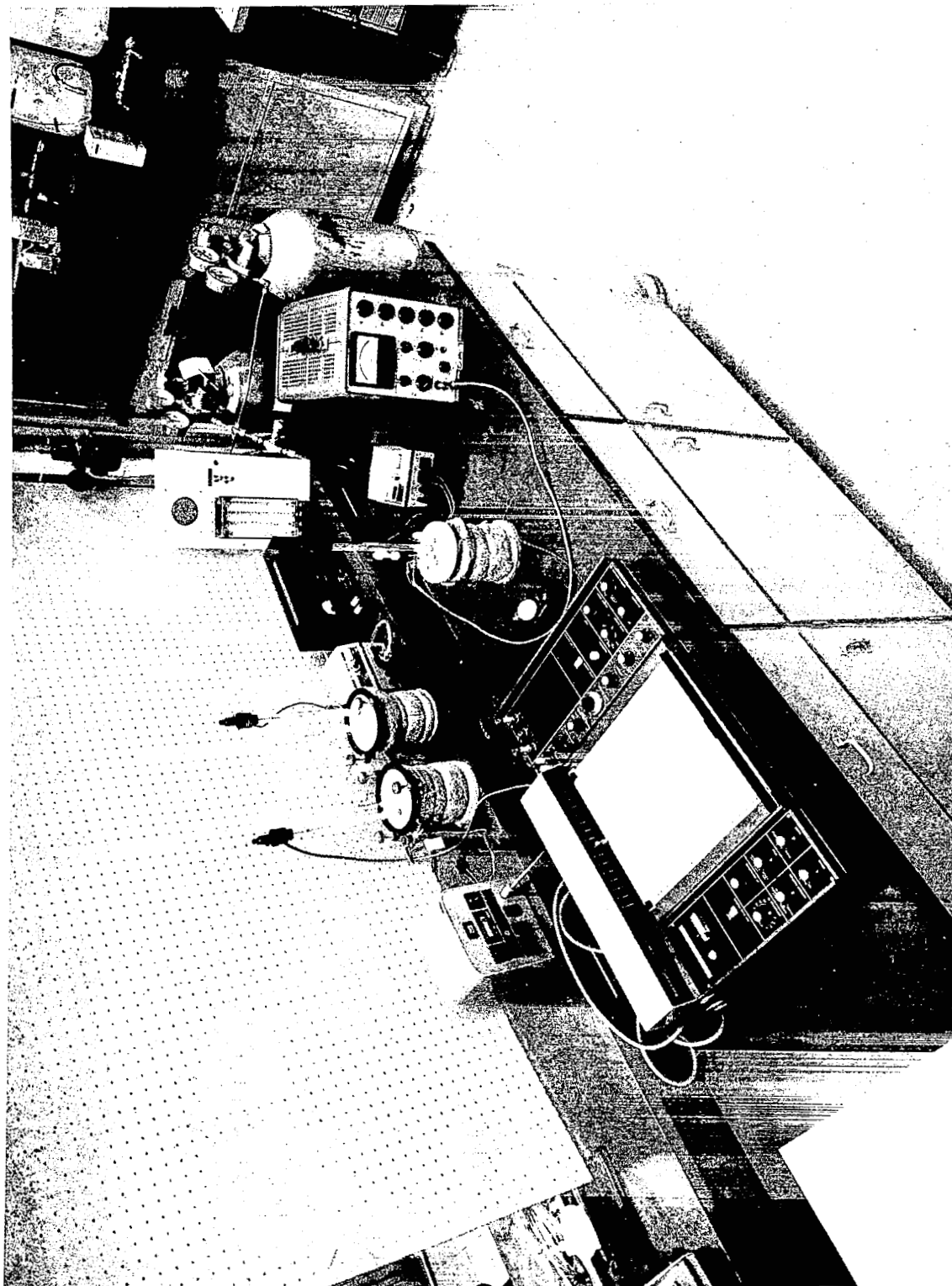
FIGURE 11 POTENTIOSTATIC SCREENING TEST

TABLE 4

FINAL SELECTION OF CANDIDATE
MATERIALS FOR ELECTROCHEMICAL TESTING

Stage I	Stage II	Stage III
Iron	Iron	Nionel (Incoloy) 825
Zirconium	Zirconium	Zirconium
Nickel	Nickel	Niobium
Monel 400	Monel 400	Tantalum
Platinum	Platinum	Platinum
	Titanium	
	Copper	
	Tin	

general arrangement of the test apparatus used for the potentiostatic screening tests. A schematic of the test system is shown in Figure 12.

A 500 cc resin reaction vessel serves as the main cell compartment. A 0.5 inch thick teflon cover, secured to the vessel via a circular clamp, contains entry ports for the various cell components. "O" rings located at an appropriate height around the O.D. of the various cell components serve as a vapor seal, mounting support, and as a simple height adjustment device. Cell heating and temperature control are accomplished by the use of a cylindrical heating mantle, the power input to which is controlled by an immersible glass thermo-regulator which senses the cell electrolyte temperature.

A Dynamic Hydrogen Reference Electrode (Figure 13) proposed by J. Giner (10) was employed to reference the working electrode potential in the acanning tests. The advantages and principles of operation are described in the above reference. The Reference Electrode system consists of two platinized platinum electrodes 1.0 cm x 1.0 cm (Figure 14) welded to a platinum wire, sealed to a glass tube. These electrode tubes are introduced into a larger tube containing a Luggin-Haber capillary tip and a sintered glass diaphgram. The platinized platinum electrodes are secured to the open end of the fritted glass tube by a teflon stopper. A schematic of the Reference Electrode power supply is shown in Figure 15.

The counter electrode assembly (Figure 16) consists of a platinized platinum electrode 1.0 cm x 1.0 cm (Figure 14) welded to a

W.E. – WORKING ELECTRODE ASSEMBLY
R.E. – REFERENCE ELECTRODE ASSEMBLY
C.E. – COUNTER ELECTRODE ASSEMBLY
T.R. – THERMO-REGULATOR
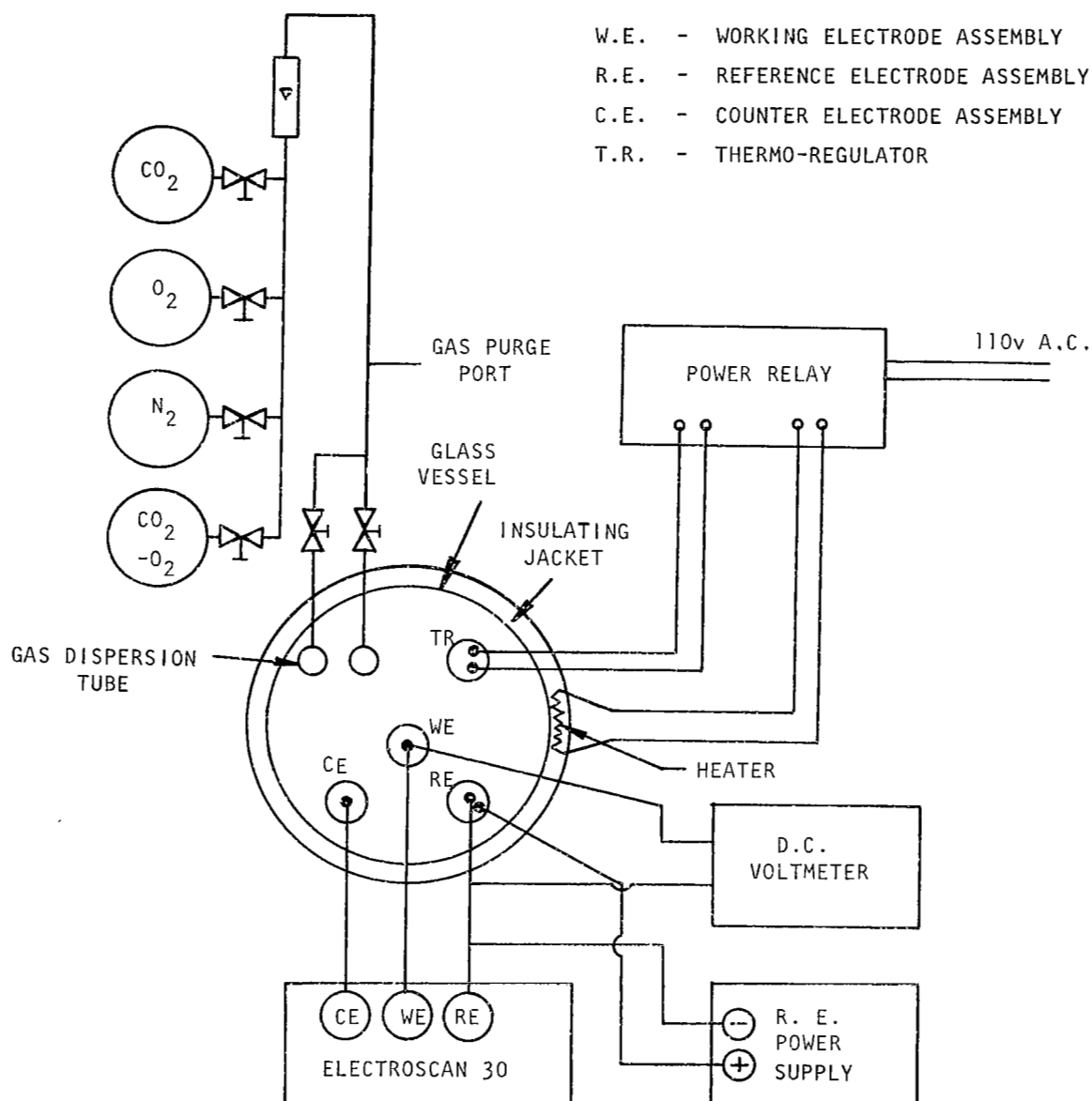
FIGURE 12 POTENTIOSTATIC SCANNING TEST SYSTEM SCHEMATIC

TEFLON STOPPER

GLASS TUBING

5.0"

6-1/2"

PLATINIZED Pt ELECTRODE
ASSEMBLY

SINTERED GLASS DISC

LUGGIN-HABER
CAPILLARY

1/2"

1/16" O.D., 0.04" I.D.
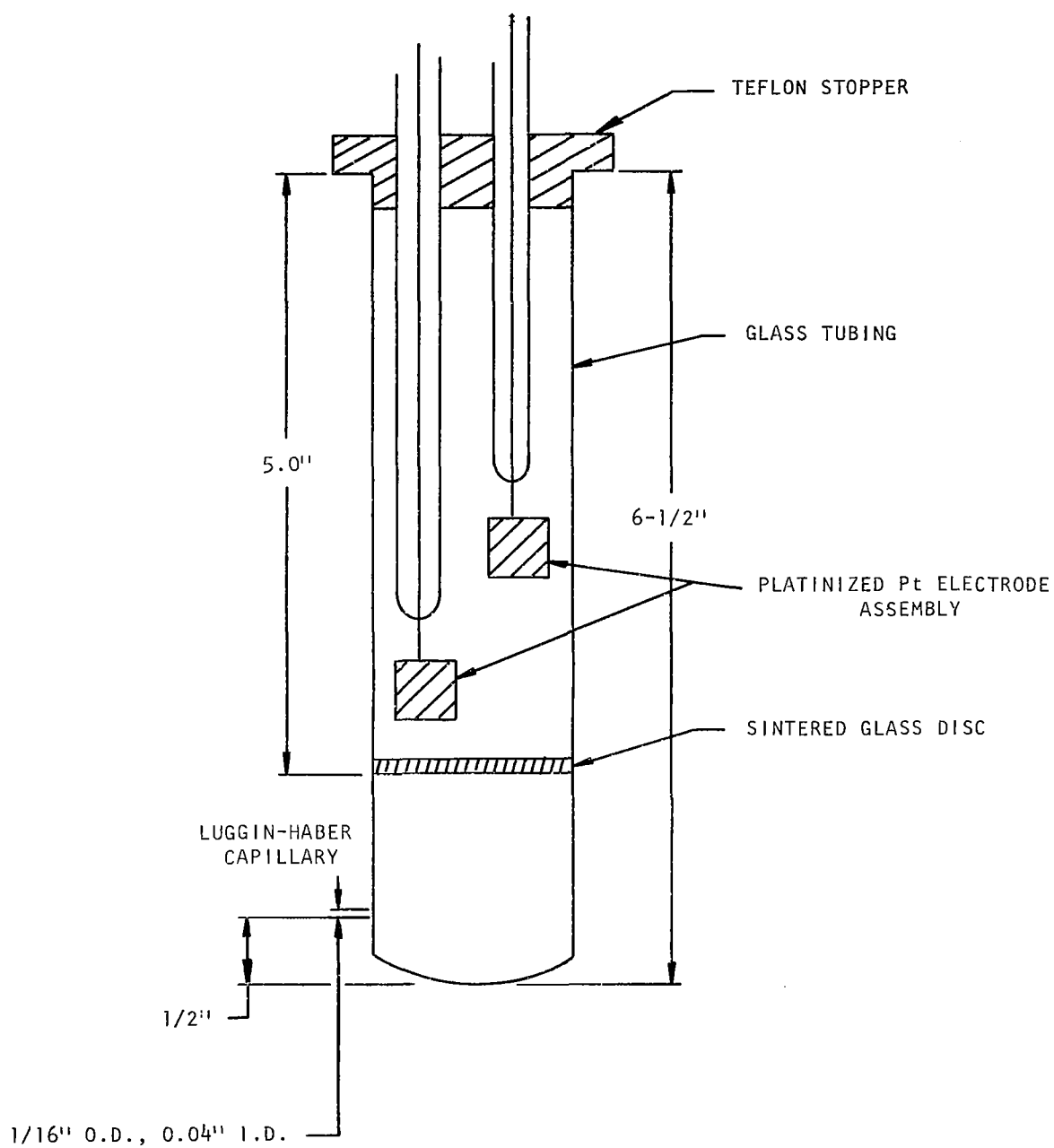
FIGURE 13 DYNAMIC HYDROGEN ELECTRODE - REFERENCE ELECTRODE ASSEMBLY

33

0.030" DIA. COPPER WIRE

PYREX TUBING - 1/4" O.D. - 3/64" WALL THICKNESS

Pt-Cu WELD

GLASS - Pt SEAL

PLATINIZED Pt SCREEN ELECTRODE (1.0 cm x 1.0 cm)
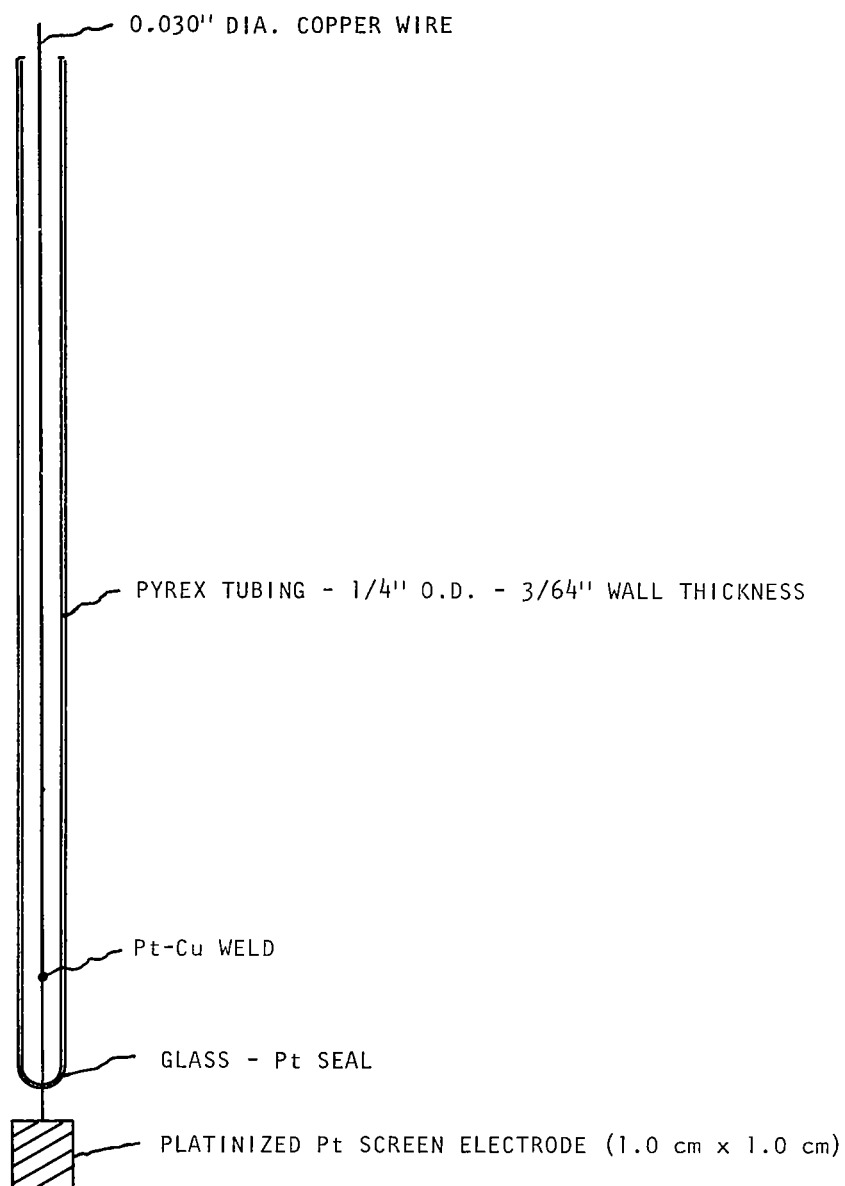
FIGURE 14 PLATINIZED PLATINUM ELECTRODE ASSEMBLY
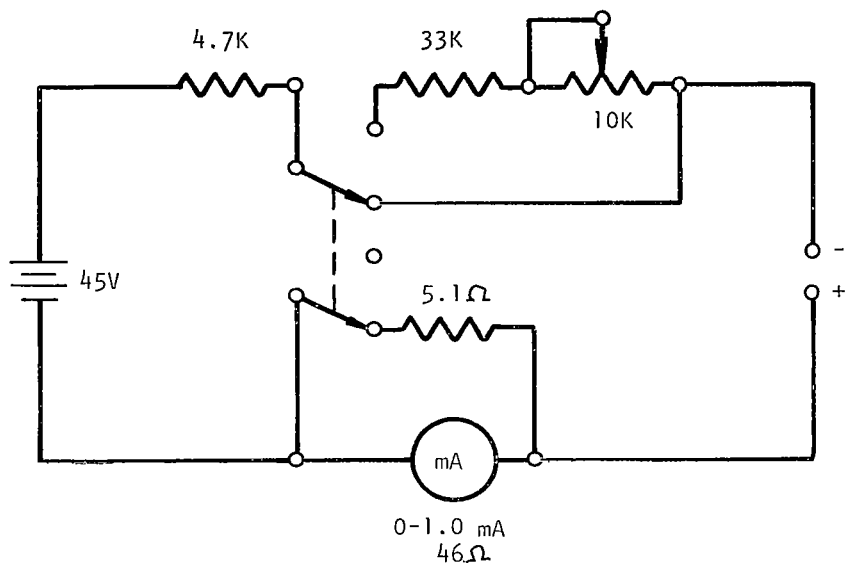
FIGURE 15 REFERENCE ELECTRODE CONSTANT CURRENT POWER SUPPLY

TEFLON STOPPER

GLASS TUBING

6"

PT/ PT ELECTRODE ASSEMBLY

SINTERED GLASS DISC
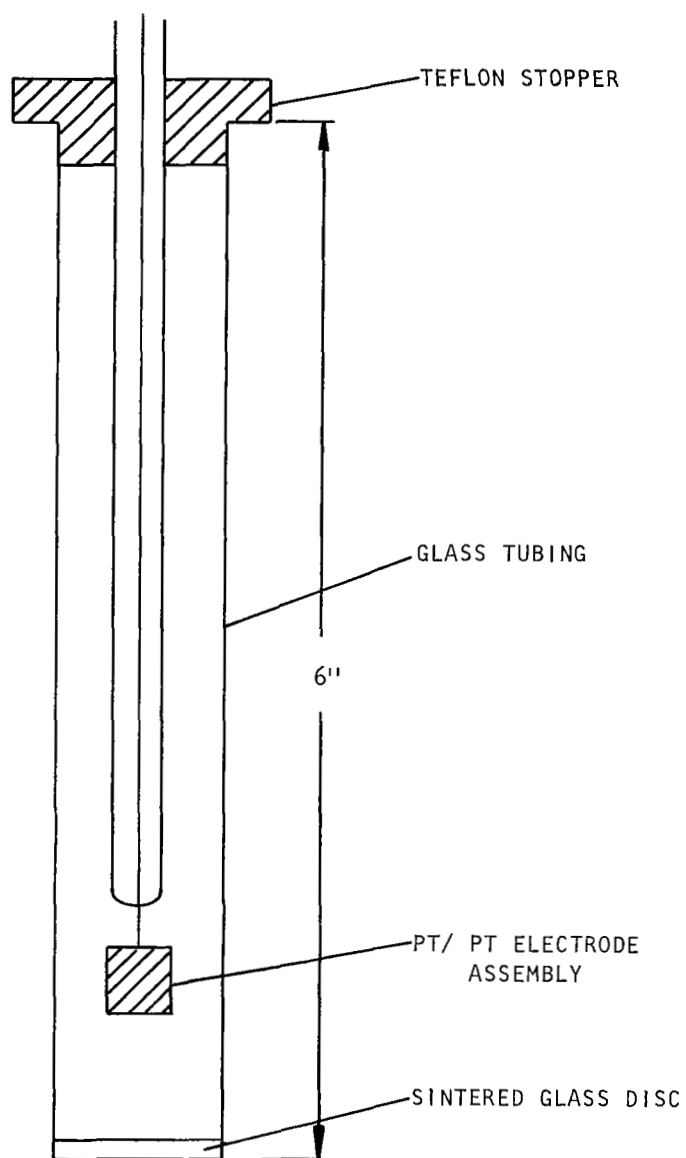
FIGURE 16 COUNTER ELECTRODE ASSEMBLY

platinum wire, sealed to a glass tube. The electrode-tube is introduced into a larger glass tube containing a glass frit at the bottom. The electrode is secured to the open end of the fritted glass tube by a teflon stopper.

The work of Greene et, al (12) has shown the necessity for avoiding crevices at the electrode-sealant interface. Thus, the working electrode or test electrode assembly (Figure 17) is essentially the one proposed by Stern-Makrides (13). The use of this type of electrode mounting allows only teflon, glass and the test specimen to contact the solution. The test electrode is a cylinder, 0.5 cm outside diameter x 0.75 cm long (10, 13, 71).

Reference Electrode Calibration

The reference electrode employed in this study, namely the Dynamic Hydrogen Electrode (D.H.E.), is a platinized platinum electrode cathodically polarized at a very low current density (1 milliampere per square centimeter). If this electrode were immersed in a solution normal in hydrogen ions at 25°C its potential would differ only slightly from that of the standard hydrogen electrode. However, this electrode operates in the same solution and at the same temperature as the test specimen electrode. It is necessary to calibrate this electrode potential with respect to some objective reference. Thus, the dynamic hydrogen electrode was calibrated with respect to a saturated calomel electrode at the temperature and solution concentration that exists for the test evaluation. Furthermore, since the potential of the saturated calomel electrode is known with respect to the standard hydrogen electrode for a range of temperatures, (72) the potential of the dynamic hydrogen electrode can easily be referred to that of the standard hydrogen electrode. The calibration was accomplished by immersing a saturated calomel electrode in the same solution at the same temperature as the dynamic hydrogen electrode. The appropriate gas was bubbled through the solution for a period of at least 12 hours. At equilibrium, the potential difference was noted and the potential of the dynamic hydrogen electrode with respect to that of the saturated calomel electrode at the same solution temperature was converted to that of the standard hydrogen electrode (S.H.E.) at 25°C.

Shown below is the measured potential of the dynamic hydrogen electrode (at the indicated temperature and solution) with respect to the standard hydrogen electrode at 25°C for the range of test conditions to be encountered. It should be noted that for both solutions the presence of oxygen did not depolarize the dynamic hydrogen electrode. Periodic calibration checks were carried out on equilibrated test solutions and in all cases the measured potential was within ± 10 millivolts as those indicated in the list below.

Solution	Equilibrating Gas	Temperature (°C)	Potential of the DHE with Respect to the SHE
30% K_2CO_3	100% CO_2	80	-0.582
30% K_2CO_3	10% CO_2 90% Oxygen	80	-0.690
30% K_2CO_3	100% Nitrogen or Oxygen	80	-0.795
10 Normal H_2SO_4	100% Nitrogen	90	+0.097
10 Normal H_2SO_4	100% Nitrogen or Air	22	+0.066

Test Conditions

The recommended materials (See Table 4) were potentiostatically evaluated over a range of conditions which included those outlined in Table 6. The only departures from the projected operating conditions of the various stages in the potentiostatic evaluation were the following:

1. The Stage I materials were evaluated at 80°C--the same temperature as projected operating temperature of Stage II. This decision was made so that the number of evaluations would be reduced to a minimum.

2. The Stage I and II materials were evaluated in a solution of 30% weight potassium carbonate. (Projected solution concentration of Stage I - 28%, of Stage II- 31% potassium carbonate).

Neither of these changes in operating conditions would theoretically lessen the tendency of a material to corrode; in fact, the elevation in temperature would increase the corrosion if the tendency existed. It can be seen from Table 1 that the Stage I cell operates over a projected range of gas composition from 0.5% carbon dioxide, balance air, to 57% carbon dioxide, balance oxygen, and the Stage II cell from a 57% CO_2, balance oxygen, to 79% CO_2, balance oxygen. The Stage III gas composition, having no interaction with the electrolyte may be considered invarient. Since the alkaline stages (I and II) solution pH and anion composition (carbonate or bicarbonate ion) are dependent upon the carbon dioxide pressure in equilibrium with the solution, the potentiostatic evaluation should, strictly speaking, be carried out with the gas mixtures mentioned above. However, it should be noted that the same results would be accomplished by performing the evaluation with gas compositions ranging from 0 to 100% carbon dioxide (balance oxygen). Thus, three gas compositions corresponding to maximum carbonate ion concentration (maximum

1. GLASS TUBE - KIMBLE "KIMAX" KG-33 GLASS
   9MM O.D. X 2MM WALL X 12" LG.

2. METAL ROD - STAINLESS STL ROD - 1/8" DIA. X 12-1/2" LG.

3. TEFLON WASHER - 7/16" OR 1/2" DIA. X 3/4" LG ROD

4. TEST ELECTRODE - 0.5 CM DIA X 0.75 CM LG.

5. TEFLON RING - 3/8" O.D. X 1/8" I.D. X 1/16" TO 1/8" THICK

RETAINING NUT #4-4ONC
AND #4 FLAT WASHER

11"

0.75 cm

1/4"

0.50 CM DIA

#2-56NC THD

1/2"

3"
4

7/8"

12"

#4-4ONC THD

FIGURE 17 WORKING ELECTRODE ASSEMBLY

pH), equal carbonate and bicarbonate ion concentration and maximum bicarbonate ion concentration (minimum pH) were chosen, namely: 100% nitrogen, 10% carbon dioxide 90% oxygen, and 100% carbon dioxide. In addition a fourth gas, 100% oxygen, was employed to discern any contribution of this oxidizing species apart from the effect of carbon dioxide. The potential range over which the materials are to be evaluated have been estimated and are listed in page 13. The estimated voltage range of Stages I and II overlap. In order to simplify the acquisition of data, a common range of potentials was selected for both Stages I and II materials. A summary of the test conditions for the potentiostatic evaluation of Stages I, II and III candidate materials is shown in Table 6.

Several other pertinent operating conditions are discussed below.

Solution Agitation

No forced convection of the solution by mechanical means was employed during the scans (except those caused by thermal convection). Although this hydrodynamic situation is not directly amenable to analysis it was chosen so as to approximate the actual conditions under which the cell operates.

Scan Rate

The slowest scan rate consistent with the potential range of interest was chosen in order to approach steady-state conditions of electrode operation. It has been demonstrated that the reproducibility of curves obtained from specimens in solution was very good in the case of slow scans but inferior in the more rapid scans (14).

Test Procedure

Figure 18 shows the assembly of the conventional three electrode cell. The following is the test procedure observed for the potentiostatic evaluation of recommended materials.

1. The material was machined from the highest purity commercially available rod or bar stock into a cylinder* 0.5 centimeter in diameter x 0.75 centimeter in length. Table 5 summarizes the vendor-supplied certificates of chemical analysis for all the materials evaluated.

2. The test electrode was washed in a train of organic solvents terminating in a distilled water rinse.

3. Test specimen was then mounted on the Stern-Makrides electrode holder and placed in a polyethylene bag until used.

---

*The exception for the above mentioned geometry was platinum which was evaluated in the form of a 0.03-inch diameter wire sealed in glass.
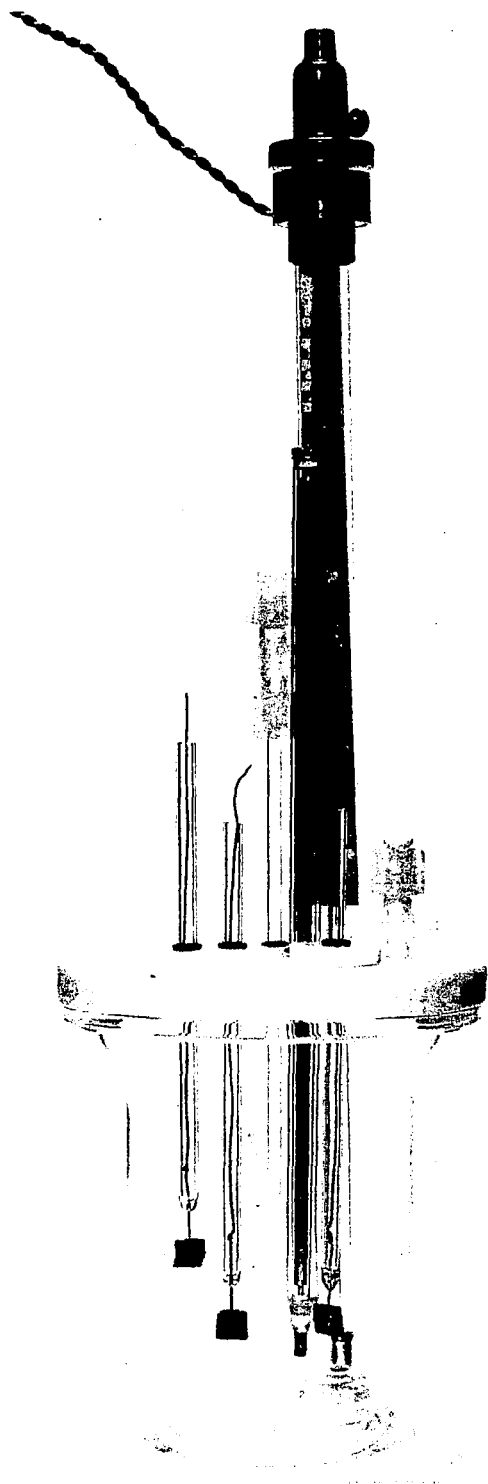
FIGURE 18 CONVENTIONAL THREE ELECTRODE CELL

TABLE 5 METALLIC MATERIALS
TYPICAL CHEMICAL ANALYSES

Material	Vendor	Form	C	O	N	Fe	W	Mo	Nb	Ta	H	Zr	Ti	Ni	Si
Tantalum (Beam Melt)	Fansteel	Rod	10	10	10	50	100	50	200	BAL	95				
Niobium (Beam Melt)	Fansteel	Rod	30	50	27	50	20	20	BAL	790	4.9	100	40	20	50
Iron (Wrought)	A.M. Byers	Bar	.033			BAL								.016	.135
Titanium (50-A)	Titanium Metals Corp.	Rod	.023		.012	.12					.006		BAL		
Nickel (270)	Int.Nickel Co. Huntington Alloy Division	Rod	.01			.0014							<.001	BAL	.0009
Monel (400)	Int.Nickel Co. Huntington Alloy Division	Rod	.18			.65								66.25	.10
Nionel (825)	Int.Nickel Co.	Rod	.02			30.54	3.04						0.96	43.06	.29
Zirconium (G2)	Amax Specialty Metals	Rod	90		17	800	<20	<20				BAL	<20	<20	55
Copper	Chase Brass & Copper	Rod													
Tin (121)	Fisher Scientific	Bar													
Platinum	Goldsmith Chemical & Metal Co.	Wire													

42

Mn	Cu	Al	Sn	Cr	V	Co	B	Cd	Hf	P	Pt	S	FeSiO$_3$	Analysis Report in
														PPM
20	40	20	10	20	20	10	1	5	100					PPM
.076				.004						.108		.007	2.1	%
														%
<.001	<.001			.0002								.001		%
.92	31.89											.009		%
.67	1.78	0.10		19.51								.007		%
<20	<20	25		170	<20	<10	<0.2		110					PPM
	99.9													%
	.1		99.97											%
											99.9			%

43

4. The appropriate test solution previously equilibrated with the test gas was further sparged for 30 minutes at 100 cc's per minute, while being brought to the test temperature.

5. The test specimen was then immersed in the solution.

    The gas purge stopped and the solution head space blanketed with test gas.

6. The open circuit potential of the test specimen was noted for a period of five minutes.

7. The potentiostatic scan cycle of the test specimen was made from the cathodic to the anodic potential of the desired range. The reverse scan completed the cycle. This cycle was repeated a second time.

8. The test electrode was then placed at open circuit at the completion of the second cycle.

9. If a significant current was observed during the scan the test specimen was removed from solution and the specimen was either abraded or chemically etched. If no significant current was observed the test electrode was rinsed in distilled water and placed in a polyethylene bag until used.

10. Steps 3 to 9 were repeated until all four gas solution tests were completed.

11. For any test specimen which reached the oxygen evolution potential prior to completion of the scan range the evaluation of the possible corrosion of the metal in this region was obtained by maintaining the potential of the test electrode at the most positive potential of the voltage range for a sufficient time to develop a detectable amount of the corrosion product. The solution was then spectrographically analyzed for the metal under tests.

Electrochemical Corrosion Test Results

Prior to discussion of the potentiostatic test results it may be desirable to depict in a general way the expected form of the current voltage curve for the corrosion behavior of a metallic material. Shown in Figure 19 is the anodic polarization behavior of a metal M undergoing the following corrosion reaction. $M \rightarrow M^+ + e$. This curve is obtained by varying the potential of the metal (potentiostatic control) rather than the current. A logarithmic current scale is used since the range of current densities encountered for the active and passive dissolution

TABLE 6

POTENTIOSTATIC TEST CONDITIONS

	Stage I	Stage II	Stage III
Temperature	80°C	80°C	90°C
Electrolyte	30% K_2CO_3	30% K_2CO_3	10 N H_2SO_4
Potential Range*	0.9 $\longrightarrow$ 2.1	0.9 $\longrightarrow$ 2.1	0.75 $\longrightarrow$ 1.75
Gas Compositions	N_2 10% CO_2-90% O_2 100% CO_2 100% O_2	N_2 10% CO_2-90% O_2 100% CO_2 100% O_2	N_2 10% CO_2-90% O_2 100% CO_2 100% O_2

*w.r.t. DHE

rates may differ by several orders of magnitude. At some applied potential (a) the dissolution of the metal begins (corrosion). As the potential is made more anodic, a point (b) is reached which corresponds to the first appearance of the passive state of the metal. The corresponding current density at point (b) is called the Critical Anodic Current Density. The potential corresponding to point (c) is often the minimum potential needed for passivation of the metal. The current density corresponding to line (c-d) is the dissolution rate of the metal in the passive state, while the length of this line indicates the voltage range of passivity. At point (d) called the Transpassive Potential the metal corrosion rate again increases with the evolution of oxygen.

The following discussion of potentiostatic current voltage curves for the recommended materials is divided into two sections: 1) those materials evaluated in the potassium carbonate electrolyte (Stages I and II) and 2), those materials evaluated in the sulfuric acid electrolyte (Stage III).

1. Potassium Carbonate Electrolyte

Iron: Figures 20-23

Iron shows a steadily increasing corrosion from 0.9 volt up to the oxygen evolution potential. This corrosion rate is not significantly different for the nitrogen and oxygen scans; however, at a given potential in the above range there is an

increase in corrosion with increase in carbon dioxide pressure. For example, at 1.3 volts in nitrogen saturated solution, the corrosion rate is 20 microamps while in the carbon dioxide saturated solution the rate is 50 microamps. It should be noted that the oxygen evolution potential also increases in a more anodic direction as the carbon dioxide pressure increases.

Platinum: Figures 24-27

No corrosion was noted for platinum over the potential range 0→1.4 volts. The small peak noted at 0.85 volt is probably due to the formation of some oxide of platinum. The anodic current at constant potential (corresponding to the peak potential) rapidly decreases to zero.

The reduction peak noted at 0.75 volt would correspond to the reduction of the oxide layer formed during the anodic sweep. The increasing current noted at approximately 1.4 volts is due to the evolution of oxygen. The reduction current noted during the oxygen scan is due to the reduction of oxygen at potentials cathodic to 0.95 (during the anodic sweep), and at potentials cathodic to 0.85 volt (during the cathodic sweep). The difference in the oxygen reduction potential is assumed due to the oxide layer formed at the more anodic potentials. It should be noted that the oxygen evolution potential was not noted in the case of the carbon dioxide scans up to potentials as high as 2.0 volts. This apparent increase in the oxygen over-potential is not explainable at this time. The observed current at a constant potential of 0 and 2.0 volts shows an exponential decrease with time to zero current. Since the oxygen evolution potential was reached prior to completion of the scan range the determination of possible platinum corrosion in this region was done by the method outlined in the section Test Procedure. The results of this test indicate an average corrosion of less than 0.5 mil per year at 2.1 volts (see Appendix IV).

Nickel: Figures 28-31

The corrosion of nickel in the oxygen and nitrogen equilibrated solutions appears at a potential of approximately 1.3 volts, at which point further increases in potential results in a large increase in current (approximately 1 - 2 milliamperes at the peak potential of 1.45 volts). At more anodic potentials a slight decrease in corrosion rate takes place prior to the evolution of oxygen. The cathodic scan results in a double peak corresponding to the reduction of the anodically formed nickel oxides. Rather large increases in corrosion rate at potentials cathodic to the first oxidation peak are apparent in the carbon dioxide equilibrated solutions while the current corresponding to the appearance of the first oxidation peak remains approximately the same. A steady-state corrosion rate of 200 microamps at a constant potential of 1.42 volts (corresponding to the first anodic peak) which was observed in nitrogen and carbon is equivalent to a corrosion rate of 66 mils per year.

46

Monel 400:   Figures 32-35

Monel 400 exhibits the same general corrosion behavior as does nickel with the following exceptions. In the nitrogen and oxygen saturated solutions a single peak appears during the cathodic scan. Although the anodic peak appears at approximately the same potential the corresponding current is somewhat lower (as is also the case for the CO_2 equilibrated solution). The steady-state corrosion rate at a constant potential corresponding to the first anodic peak for carbon dioxide equilibrated solutions is an order of magnitude higher than that of the nitrogen saturated solution (at 1.38 volts 60 microamps for nitrogen, 800 microamps for carbon dioxide).

Zirconium: Figures 36-39

Zirconium shows no corrosion between 0.9 volt up to the oxygen evolution potential, and is independent of the nature of the equilibrating gas. A constant potential test of 2.1 volts in nitrogen saturated solution projects a corrosion rate of less than 7 mils per year. (See Appendix IV)

Tin: Figures 40-43

The corrosion rate of tin in nitrogen and oxygen and CO_2 equilibrated solutions is excessive over the range of potentials investigated (0.9 to 2.1 volts). The absence of corrosion in the 10% carbon dioxide equilibrated solution cannot be explained with the limited data at hand.

Copper: Figures 44-45

The corrosion rate of copper in nitrogen saturated solution is a maximum at 0.9 volt with passivation occurring at more anodic potentials. However, the passivation dissolution rate is appreciable and increases up to the oxygen evolution potential. Somewhat reduced rates are noted with the oxygen saturated solution. The corrosion of copper in carbon dioxide saturated solutions at 0.9 volt was greater than 140 milliamperes per square centimeter.

Titanium: Figures 46-49

No evidence of corrosion is noted for titanium over the range of potential 0.9 volt up to the potential of the oxygen evolution. A constant potential test at 2.1 volts in nitrogen saturated solution indicates a corrosion rate of less than 4.5 mil per year.

2. Sulfuric Acid Electrolyte

Platinum: Figures 50-51

No corrosion was noted for platinum over the potential range of zero volts up to the oxygen evolution potential. The small corrosion peak noted at 1.2 volts is most probably due to the formation of an oxide of platinum. When the potential of the electrode was held at a point corresponding to this corrosion peak the current displayed immediately decreased to zero. The reduction peak noted at approximately 0.75 volt is probably the reduction of the oxide formed during the anodic scan. The curve obtained with the oxygen saturated solution is essentially the same as the one obtained with the nitrogen solution with the exception of the oxygen reduction wave noted at 0.85 volt. A constant potential test at 1.75 volts in N_2 saturated solution indicates an average corrosion rate of 2.4 mils per year.

Tantalum: Figures 52-54

No corrosion was evident for tantalum over the potential range examined, 0.75 volt to 1.75 volts, for nitrogen, oxygen or carbon dioxide saturated solutions.

Zirconium: Figures 55-57

Zirconium displays essentially no corrosion up to potentials of 1.25 volts with a moderate increase in corrosion beyond this potential to the maximum observed potential of 1.75 volts. The corrosion at 1.75 volts is approximately 30 microamps. This corresponds to an average corrosion rate of slightly less than 10 mils per year. This corrosion rate is independent of the saturating gas.

Niobium: Figures 58-59

Niobium indicates a corrosion rate in nitrogen saturated solutions of approximately 30 microamps at the maximum observed anodic potential of 1.75 volts. This corrosion rate is equivalent to 6 mils per year. A slightly higher corrosion rate is observed in oxygen saturated solutions and is constant and independent of potential over the range of 0.75 to 1.75 volts.

Nionel (Incoloy) 825: Figures 60-61

This alloy displays no corrosion below potentials of 1.05 volts; however, at a potential slightly positive to 1.1 volts an excessive corrosion rate is noted. This corrosion rate is independent of the saturated gas.
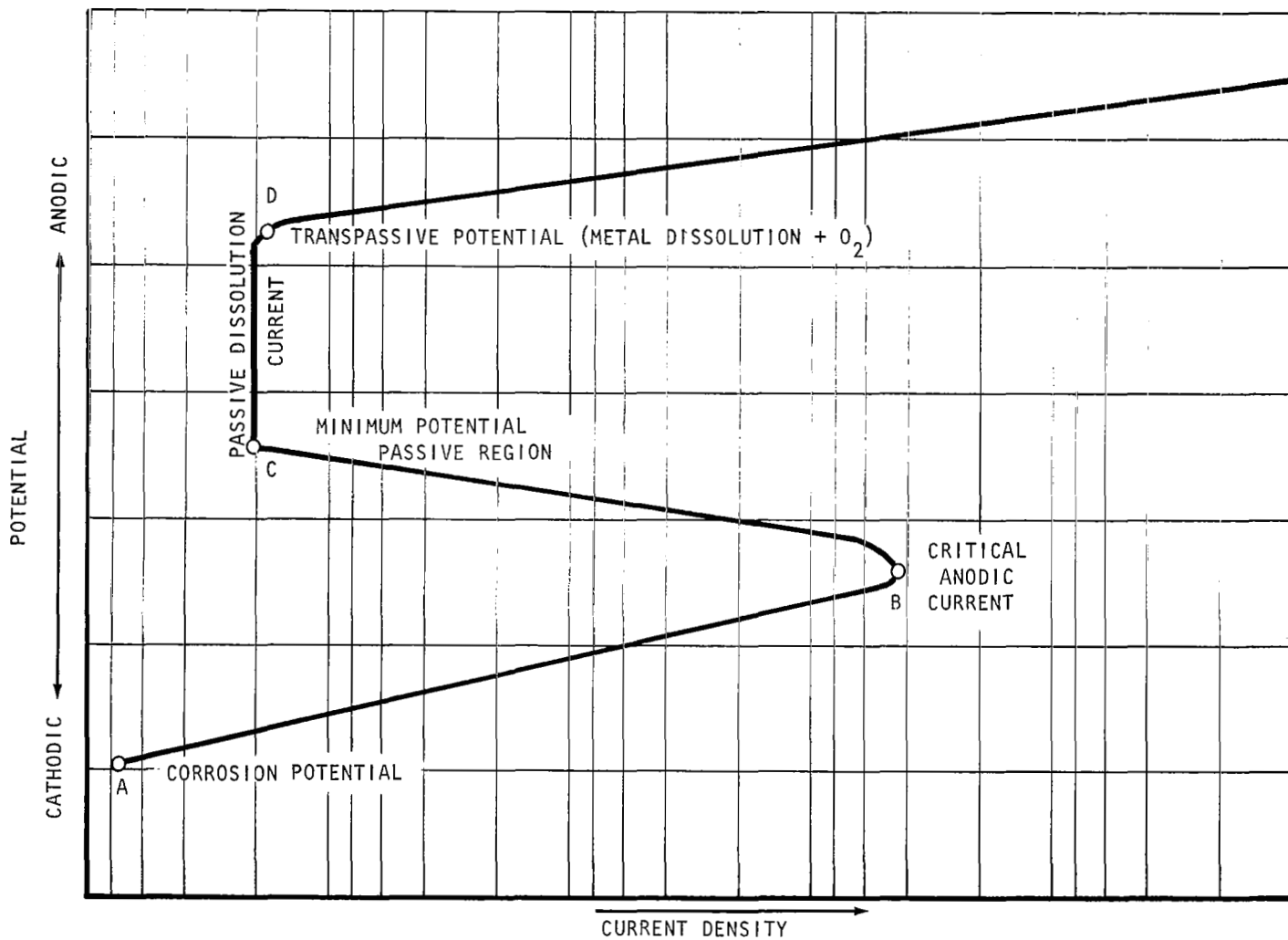
FIGURE 19 IDEALIZED BEHAVIOR OF A CORRODABLE METAL DURING ANODIC POLARIZATION
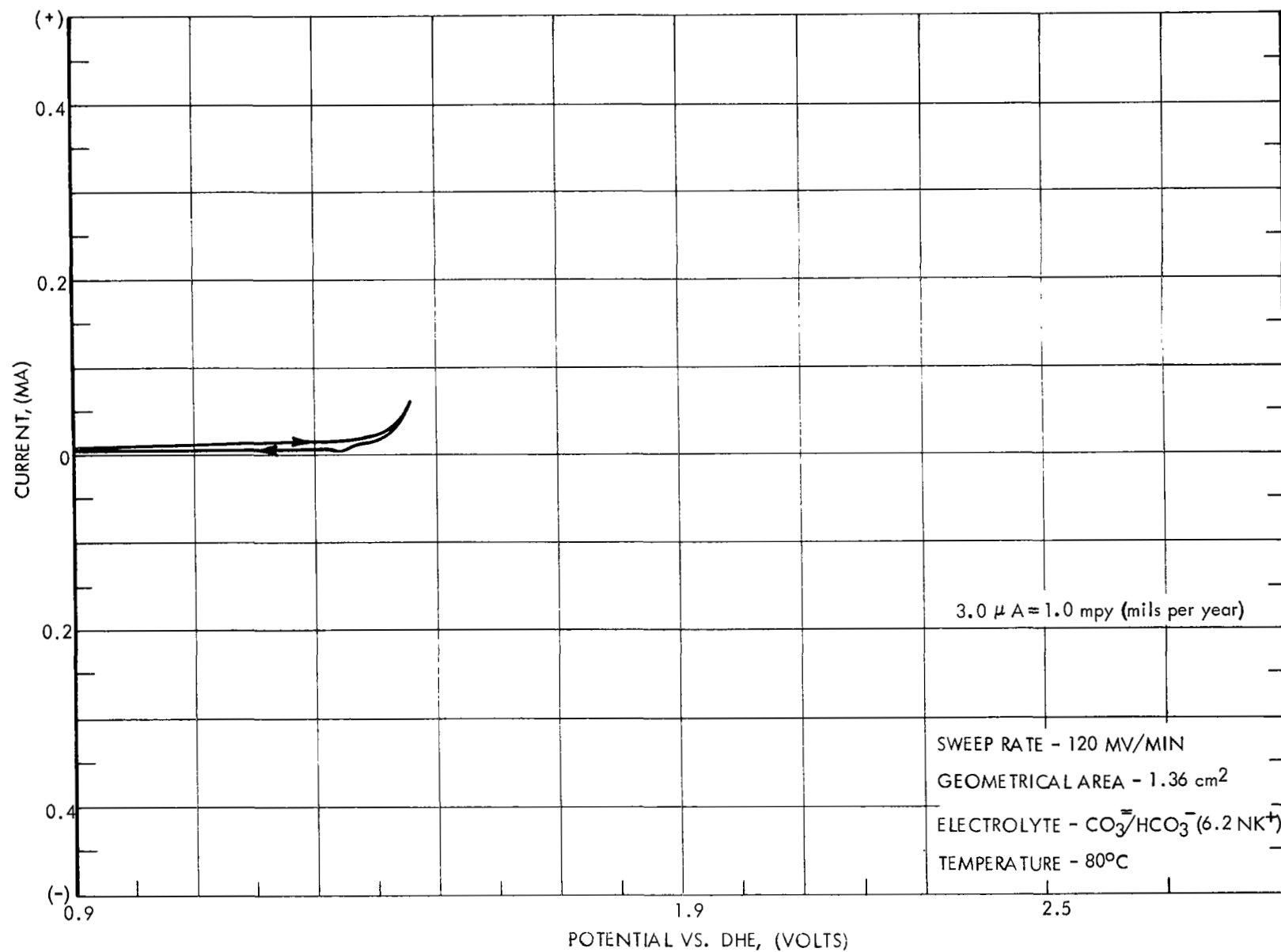
FIGURE 20 POTENTIOSTATIC SCAN FOR IRON/N_2 IN K_2CO_3
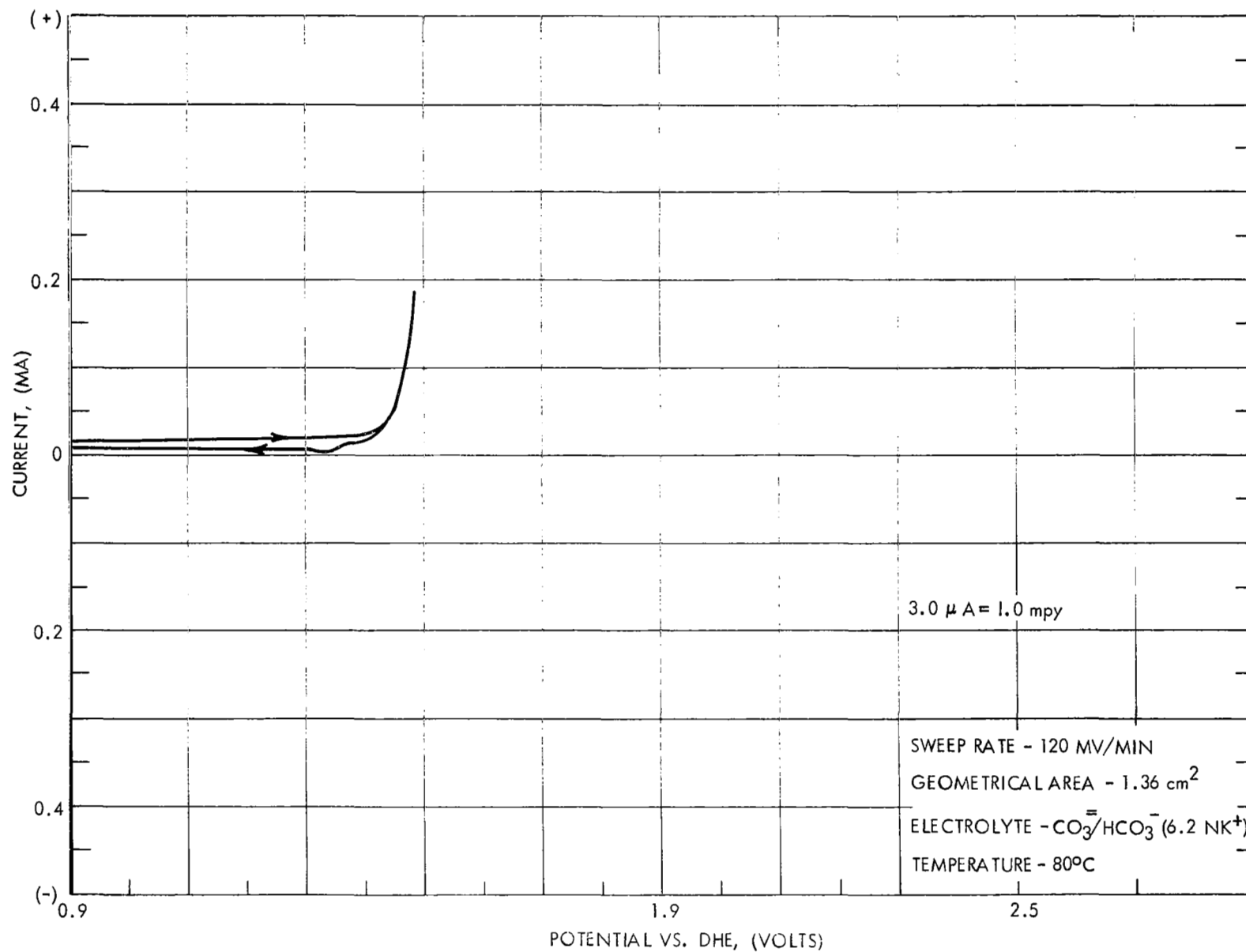
FIGURE 21 POTENTIOSTATIC SCAN FOR IRON/O_2 IN K_2CO_3

The chart shows the following axes and annotations:

CURRENT, (MA) — vertical axis with values (+), 0.4, 0.2, 0, 0.2, 0.4, (−)

POTENTIAL VS. DHE, (VOLTS) — horizontal axis with values 0.9, 1.9, 2.5

3.0 μA = 1.0 mpy

SWEEP RATE − 120 MV/MIN

GEOMETRICAL AREA − 1.36 cm^2

ELECTROLYTE − $CO_3^=$/HCO_3^- (6.2 NK^+)

TEMPERATURE − 80°C
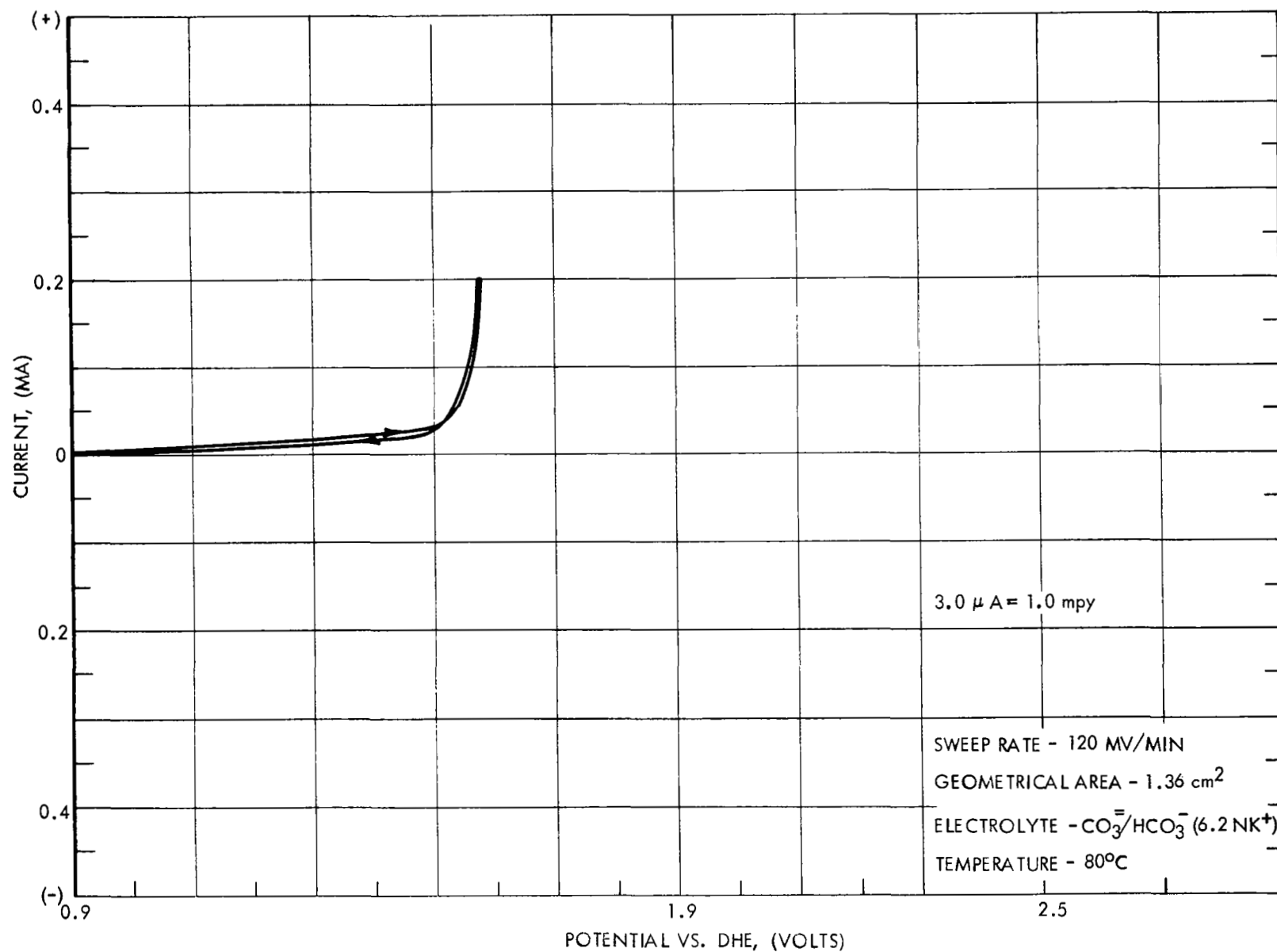
FIGURE 22 POTENTIOSTATIC SCAN FOR IRON/10% CO_2 - 90% O_2 in K_2CO_3
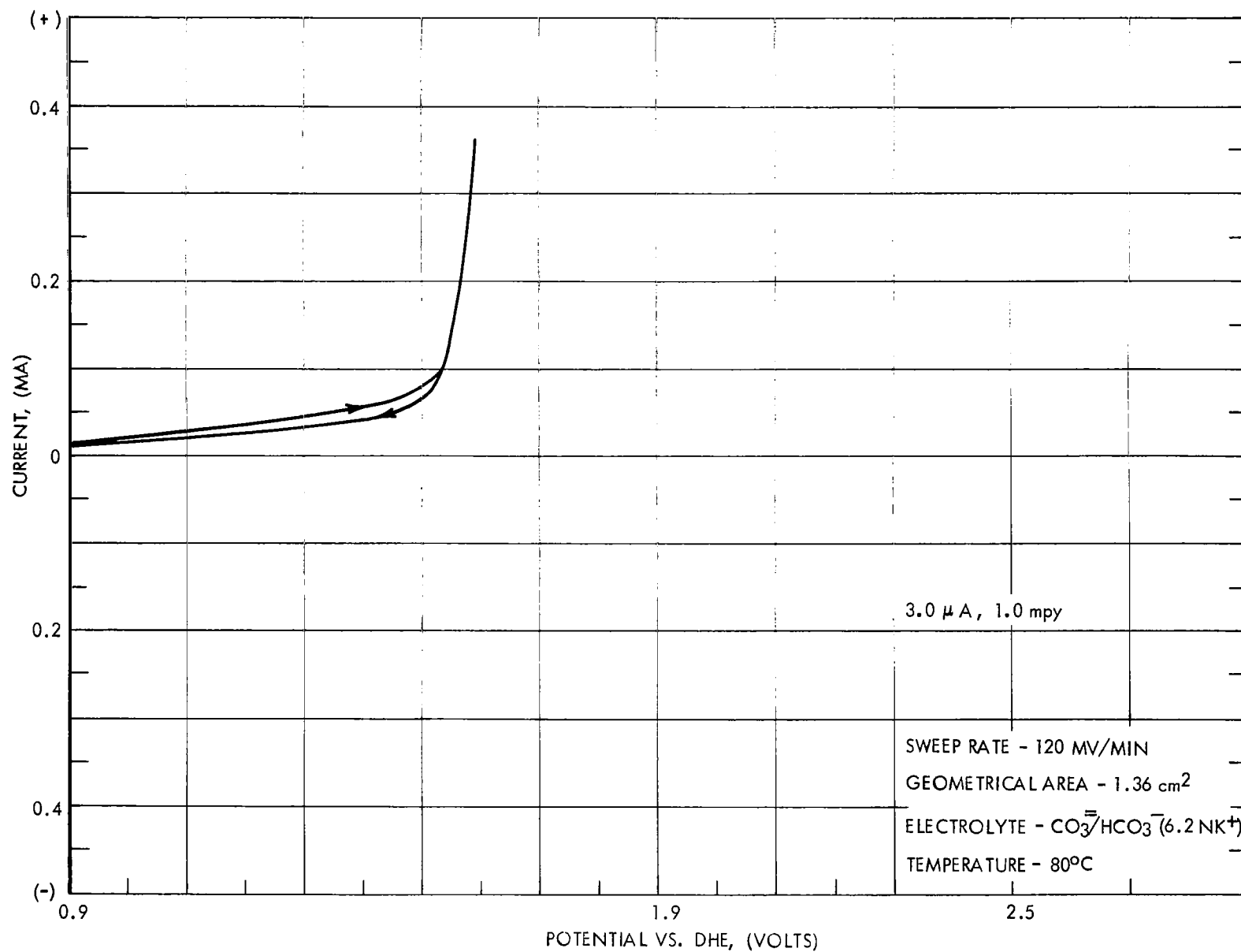
FIGURE 23 POTENTIOSTATIC SCAN FOR IRON/CO$_2$ IN K$_2$CO$_3$

1.2 μ A = 1.0 mpy

SWEEP RATE - 120 MV/MIN

GEOMETRICAL AREA - 0.34 cm^2

ELECTROLYTE - $CO_3^=$/HCO_3^- (6.2 N K$^+$)

TEMPERATURE - 80°C
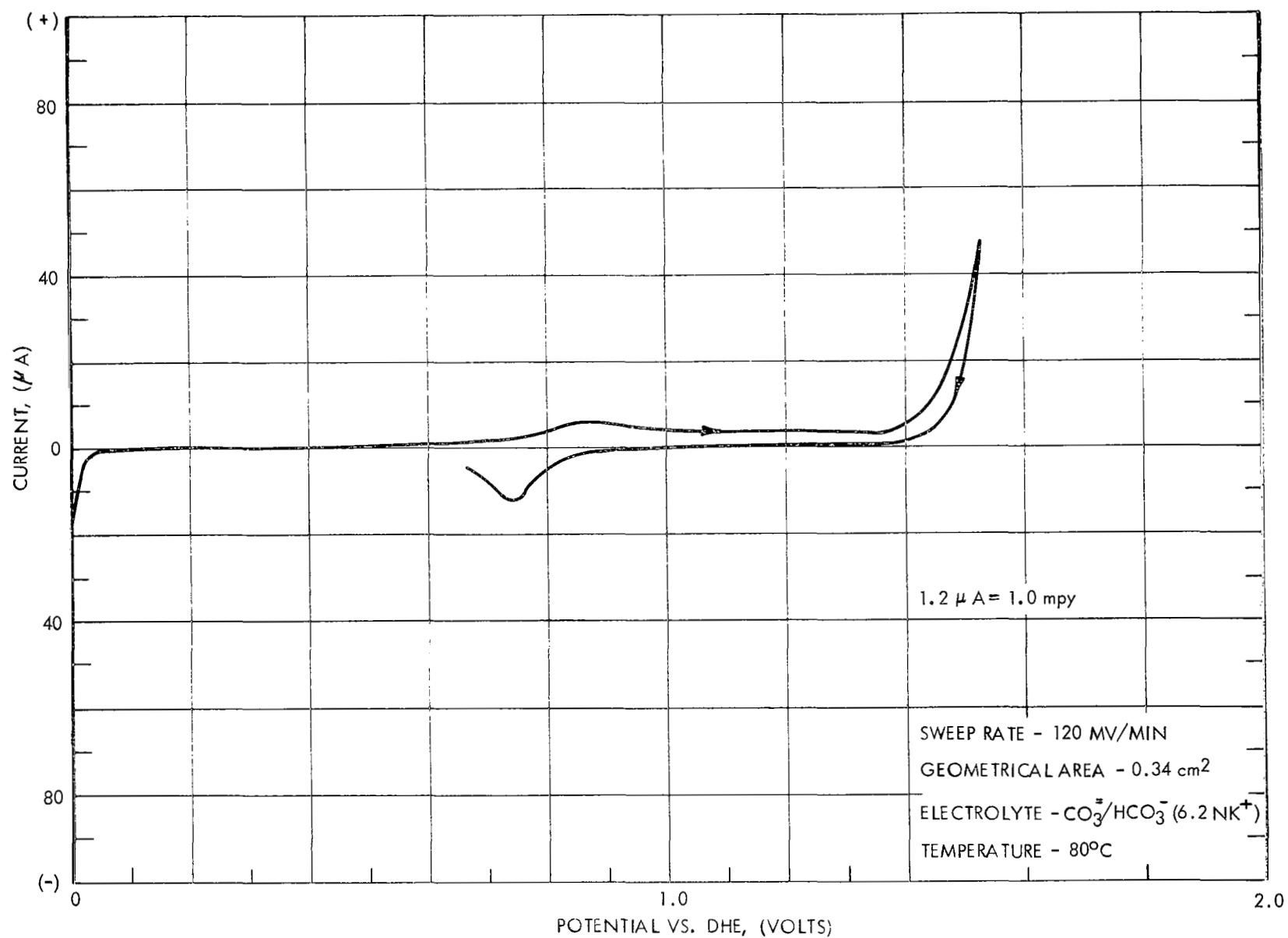
FIGURE 24 POTENTIOSTATIC SCAN FOR PLATINUM/N$_2$ IN K$_2$CO$_3$
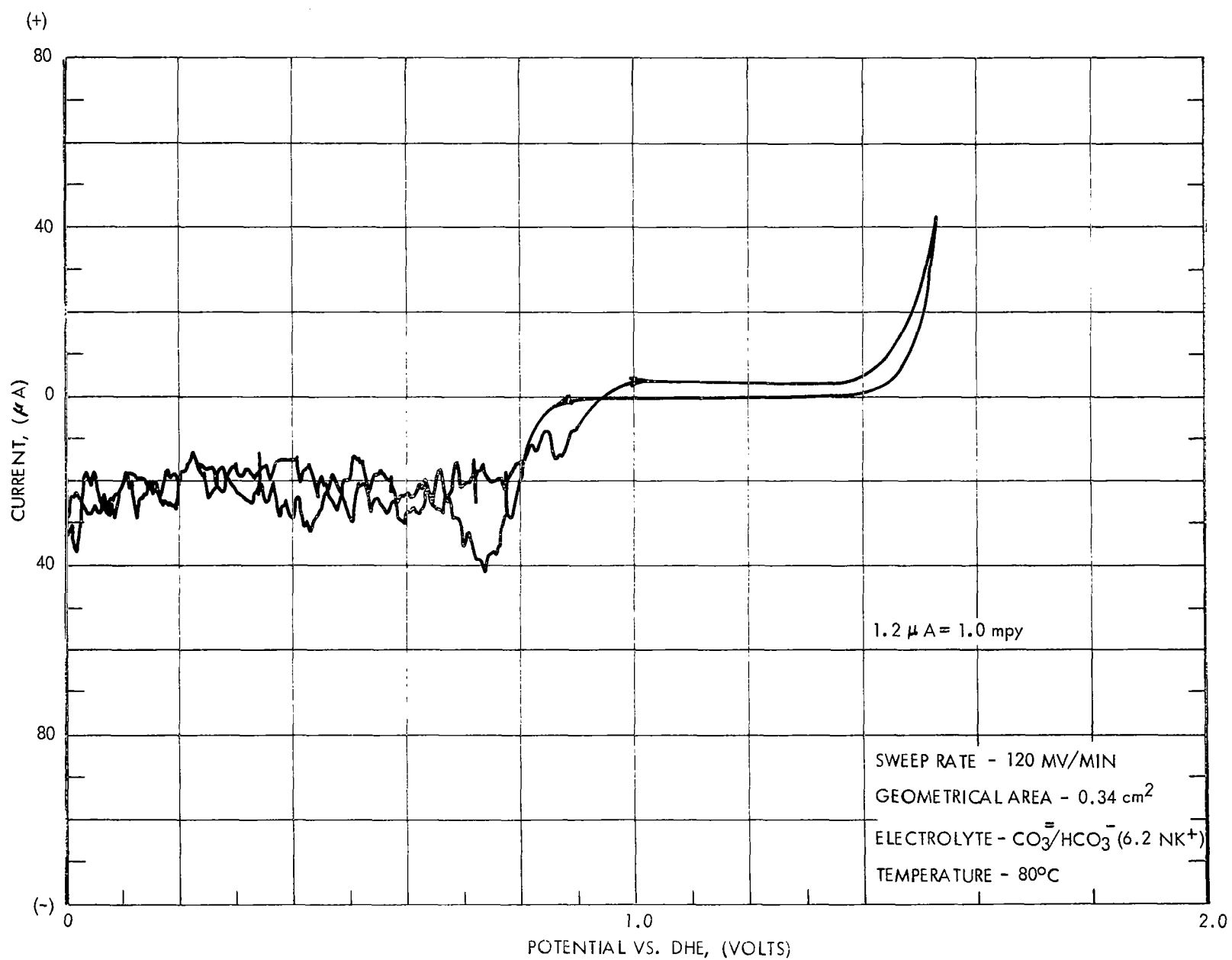
FIGURE 25 POTENTIOSTATIC SCAN FOR PLATINUM/O$_2$ IN K$_2$CO$_3$

Chart annotations:
- (+)
- CURRENT, (μA)
- 80, 40, 0, 40, 80
- POTENTIAL VS. DHE, (VOLTS)
- 0, 1.0, 2.0
- (−)
- 1.2 μA = 1.0 mpy
- SWEEP RATE − 120 MV/MIN
- GEOMETRICAL AREA − 0.34 cm^2
- ELECTROLYTE − CO$_3^=$/HCO$_3^-$ (6.2 NK$^+$)
- TEMPERATURE − 80°C
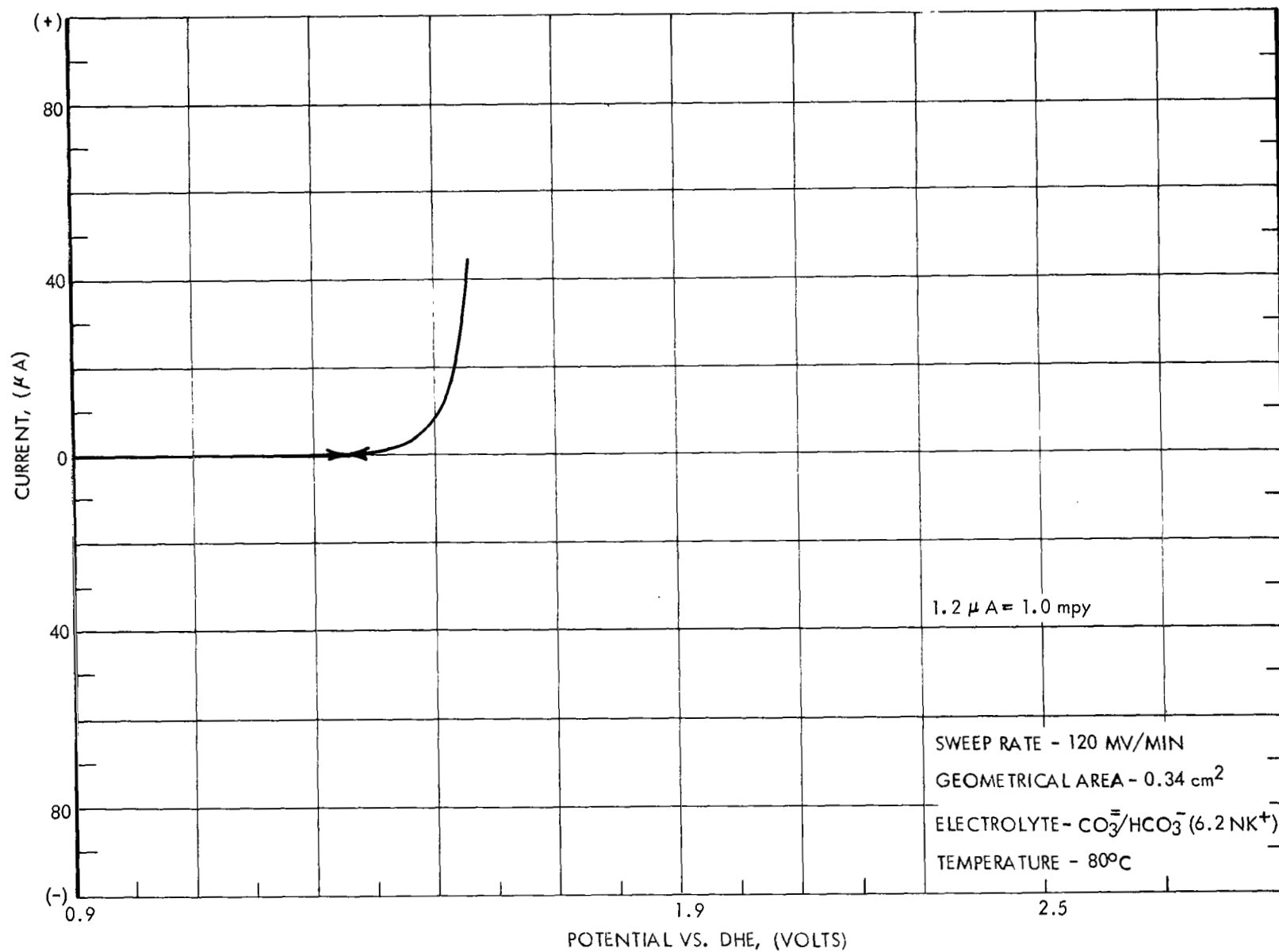
FIGURE 26 POTENTIOSTATIC SCAN FOR PLATINUM/10% CO_2 - 90% O_2 IN K_2CO_3

Chart labels:
- Y-axis: CURRENT, (μA) — values 80, 40, 0, 40, 80 with (+) at top and (-) at bottom
- X-axis: POTENTIAL VS. DHE, (VOLTS) — values 0.9, 1.9, 2.5
- 1.2 μA = 1.0 mpy
- SWEEP RATE - 120 MV/MIN
- GEOMETRICAL AREA - 0.34 cm^2
- ELECTROLYTE - $CO_3^=/HCO_3^-$ (6.2 N K^+)
- TEMPERATURE - 80°C
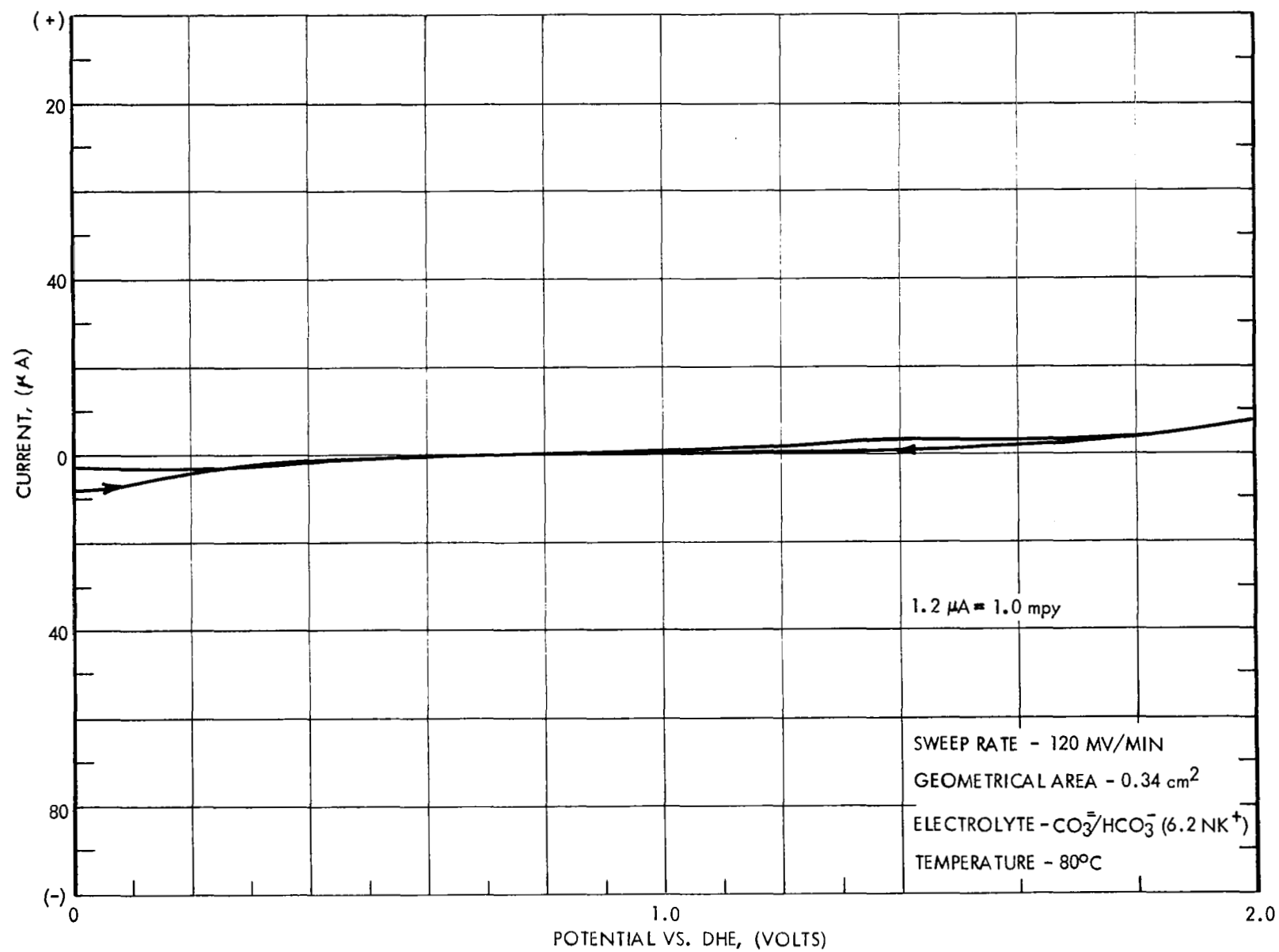
FIGURE 27 POTENTIOSTATIC SCAN FOR PLATINUM/CO_2 IN K_2CO_3
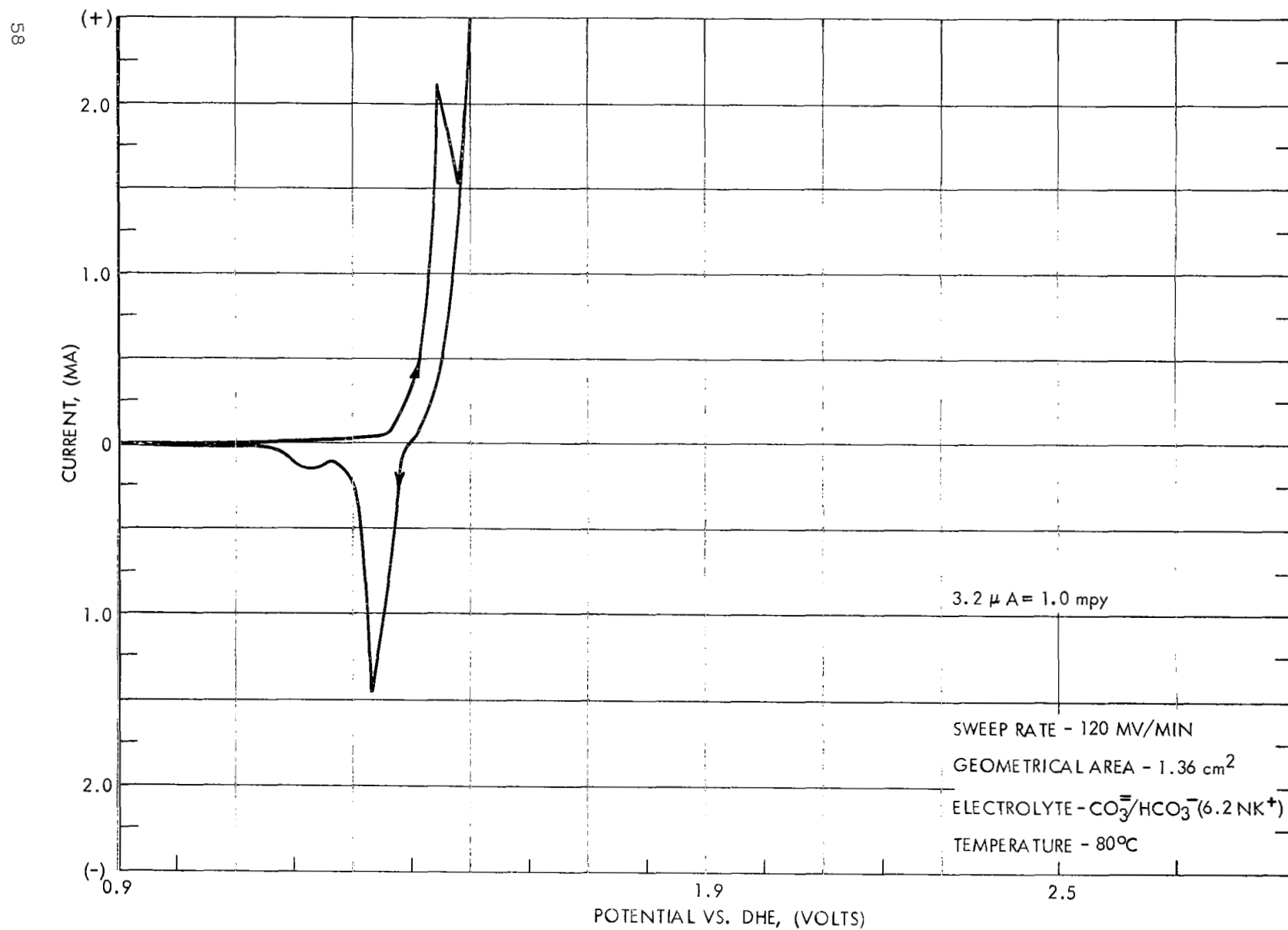
FIGURE 28 POTENTIOSTATIC SCAN FOR NICKEL/N$_2$ IN K$_2$CO$_3$

Chart text:

CURRENT, (MA)

POTENTIAL VS. DHE, (VOLTS)

(+)
2.0
1.0
0
1.0
2.0
(-)

0.9   1.9   2.5

3.2 μ A = 1.0 mpy

SWEEP RATE - 120 MV/MIN

GEOMETRICAL AREA - 1.36 cm^2

ELECTROLYTE - CO$_3^=$/HCO$_3^-$ (6.2 N K$^+$)

TEMPERATURE - 80°C

58
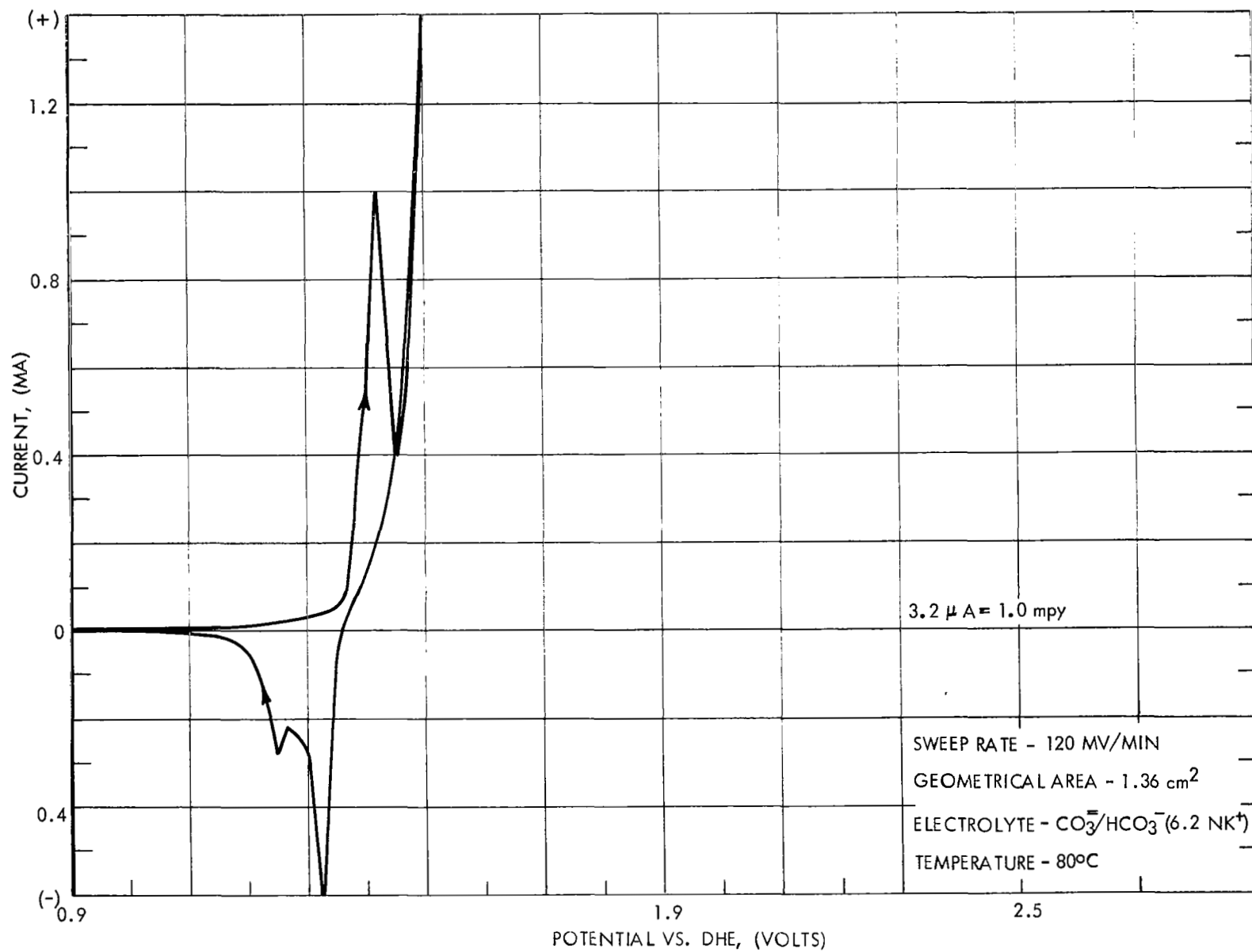
FIGURE 29 POTENTIOSTATIC SCAN FOR NICKEL/O$_2$ IN K$_2$CO$_3$

Chart axes and labels:
- Y-axis: CURRENT, (MA), with values (+) 1.2, 0.8, 0.4, 0, 0.4, (-)
- X-axis: POTENTIAL VS. DHE, (VOLTS), with values 0.9, 1.9, 2.5

3.2 μA = 1.0 mpy

SWEEP RATE - 120 MV/MIN

GEOMETRICAL AREA - 1.36 cm^2

ELECTROLYTE - CO$_3^=$/HCO$_3^-$ (6.2 NK$^+$)

TEMPERATURE - 80°C
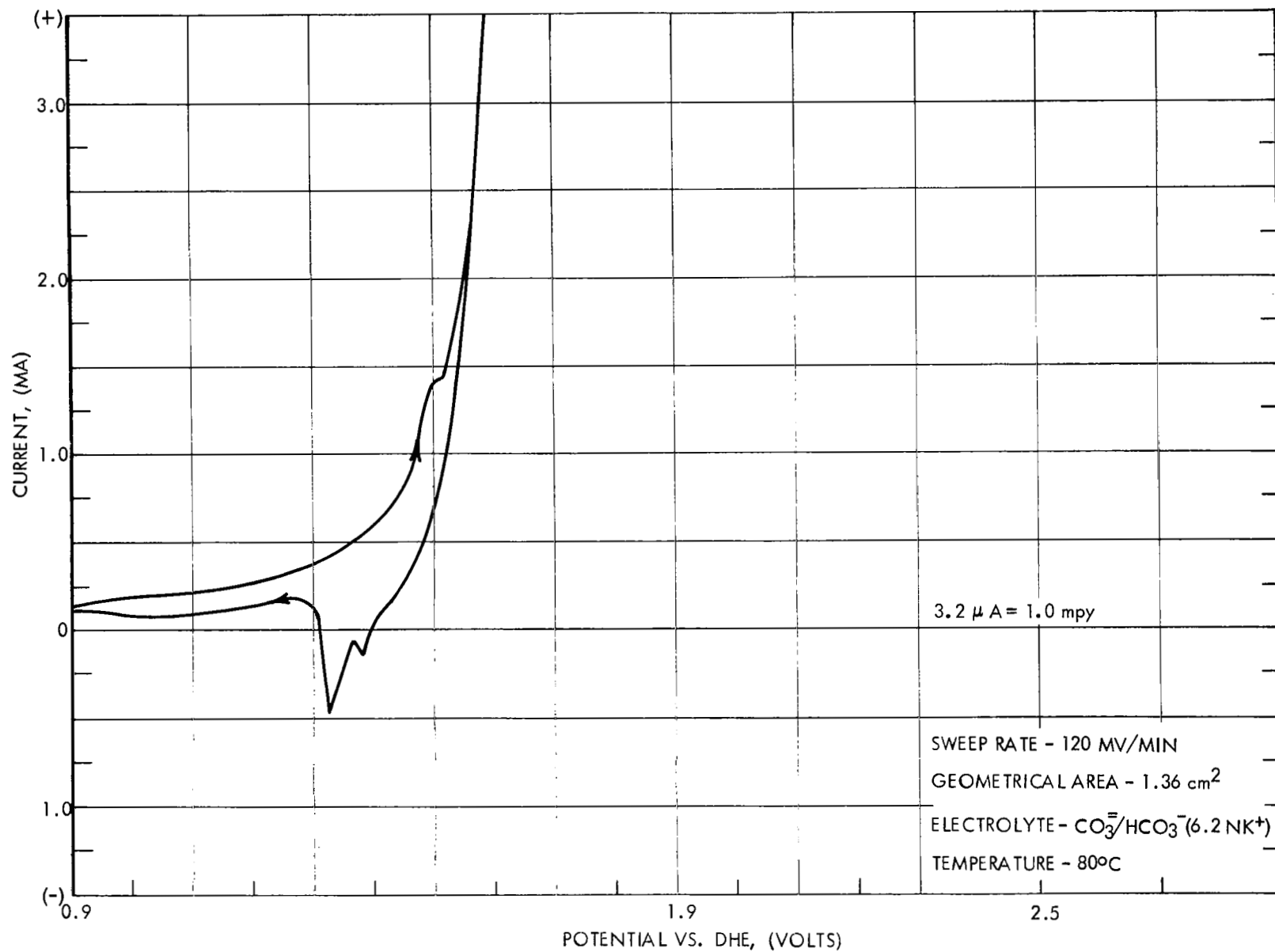
FIGURE 30 POTENTIOSTATIC SCAN FOR NICKEL/10% CO_2 - 90% O_2 IN K_2CO_3
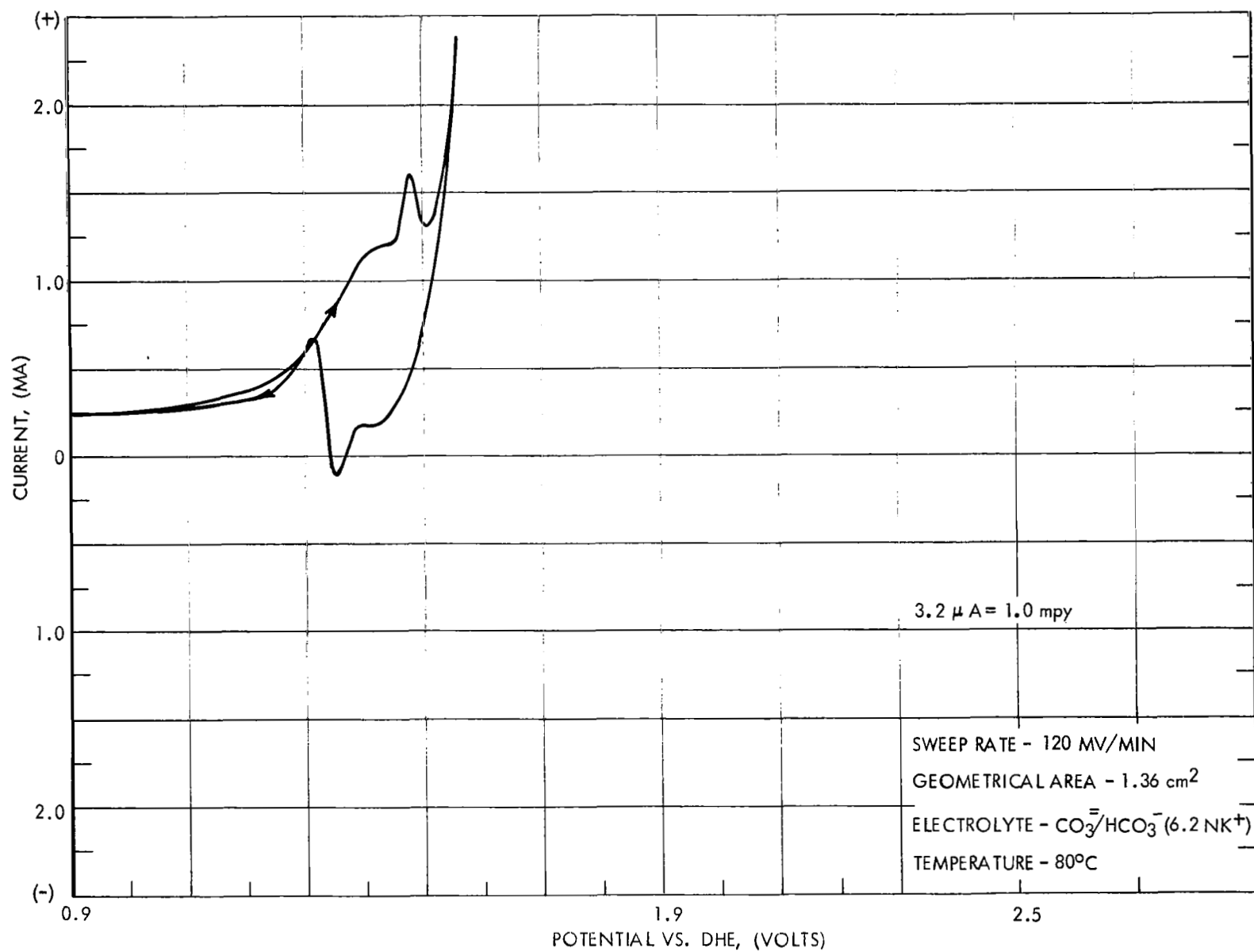
FIGURE 31 POTENTIOSTATIC SCAN FOR NICKEL/CO_2 IN K_2CO_3

Axis labels and annotations within the figure:

CURRENT, (MA)

(+)

2.0

1.0

0

1.0

2.0

(−)

0.9   1.9   2.5

POTENTIAL VS. DHE, (VOLTS)

$3.2\,\mu A = 1.0$ mpy

SWEEP RATE − 120 MV/MIN

GEOMETRICAL AREA − 1.36 cm^2

ELECTROLYTE − $CO_3^=/HCO_3^-$ (6.2 N K$^+$)

TEMPERATURE − 80°C
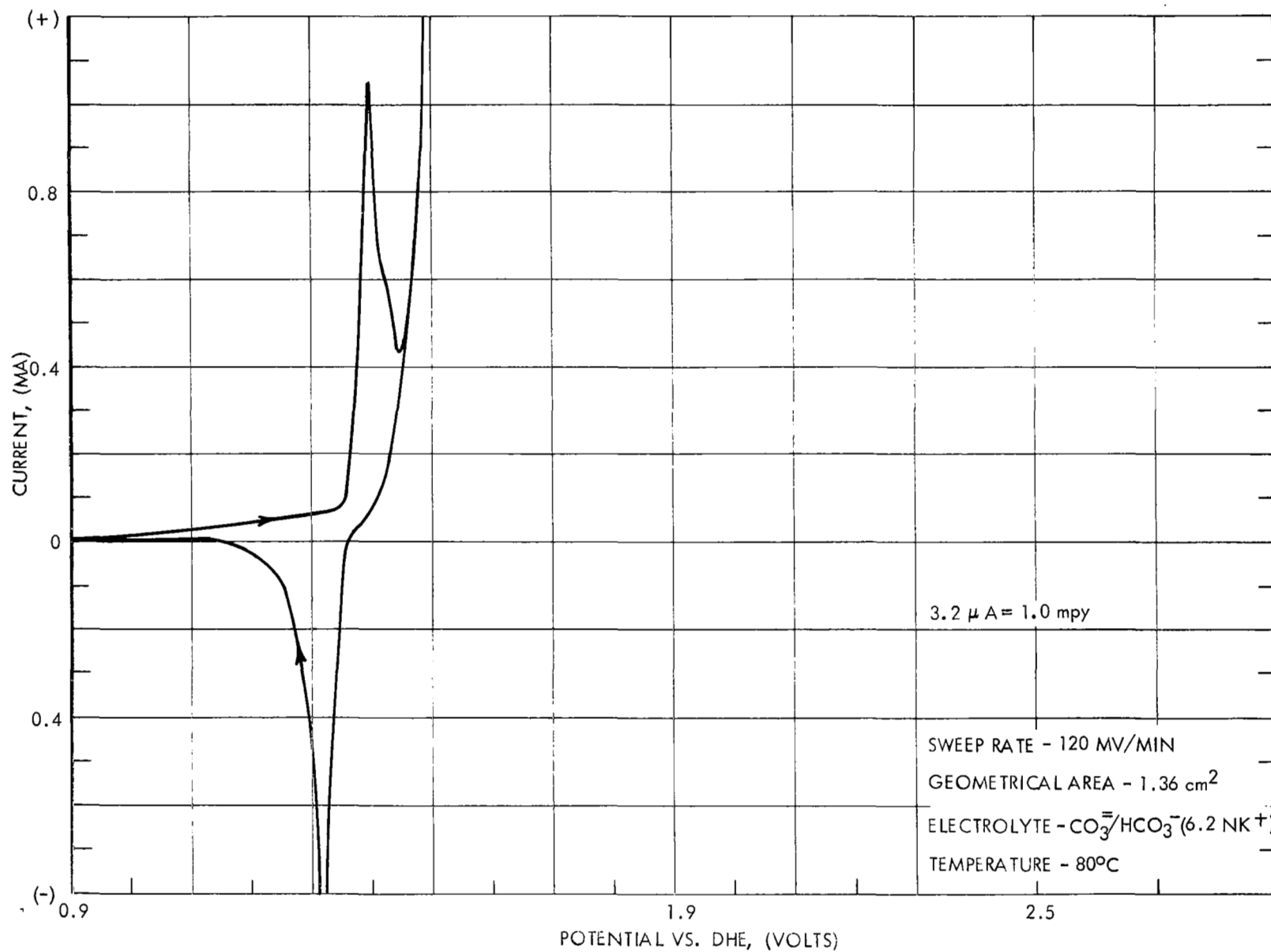
FIGURE 32 POTENTIOSTATIC SCAN FOR MONEL 400/N$_2$ IN K$_2$CO$_3$
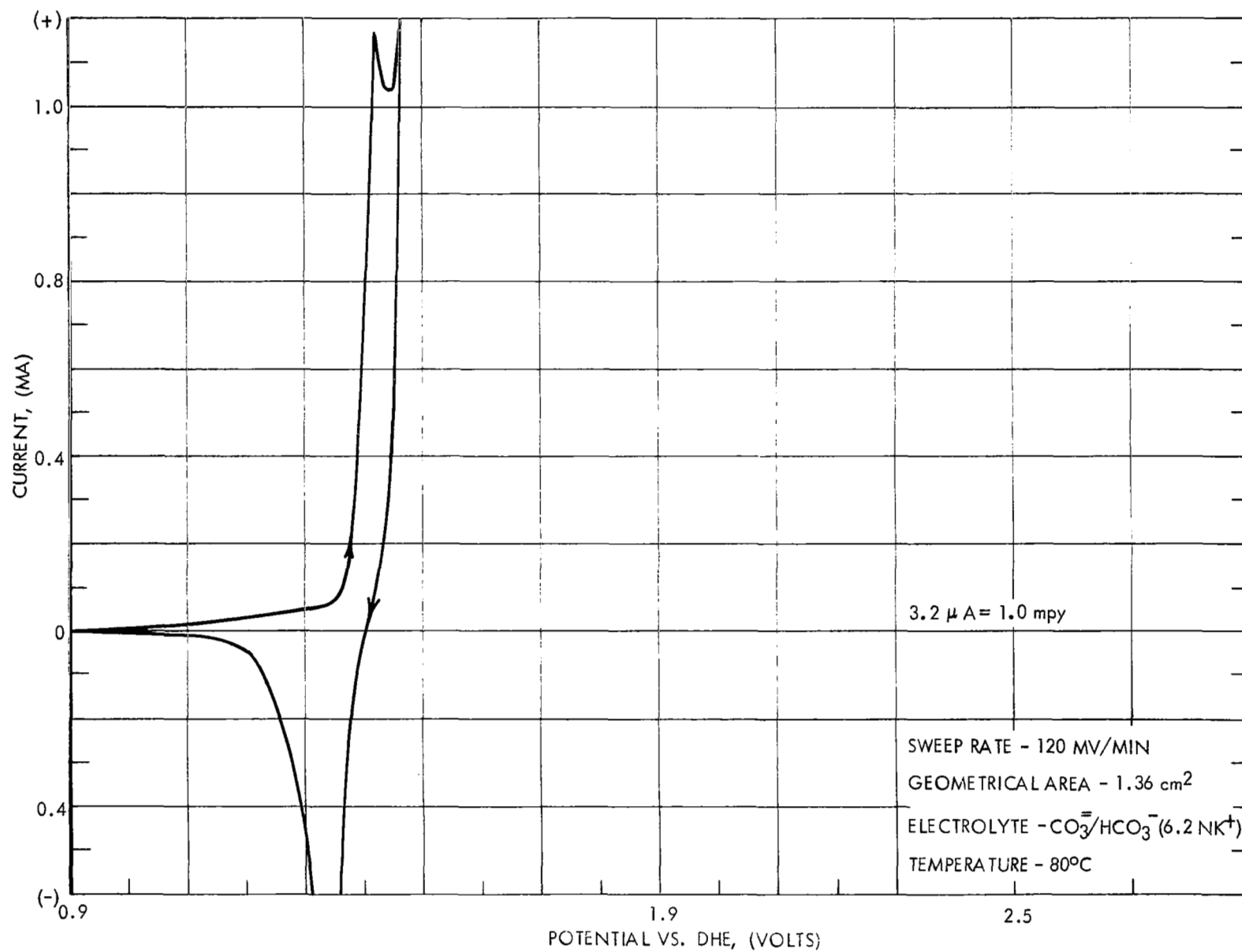
FIGURE 33 POTENTIOSTATIC SCAN FOR MONEL 400/ O$_2$ IN K$_2$CO$_3$
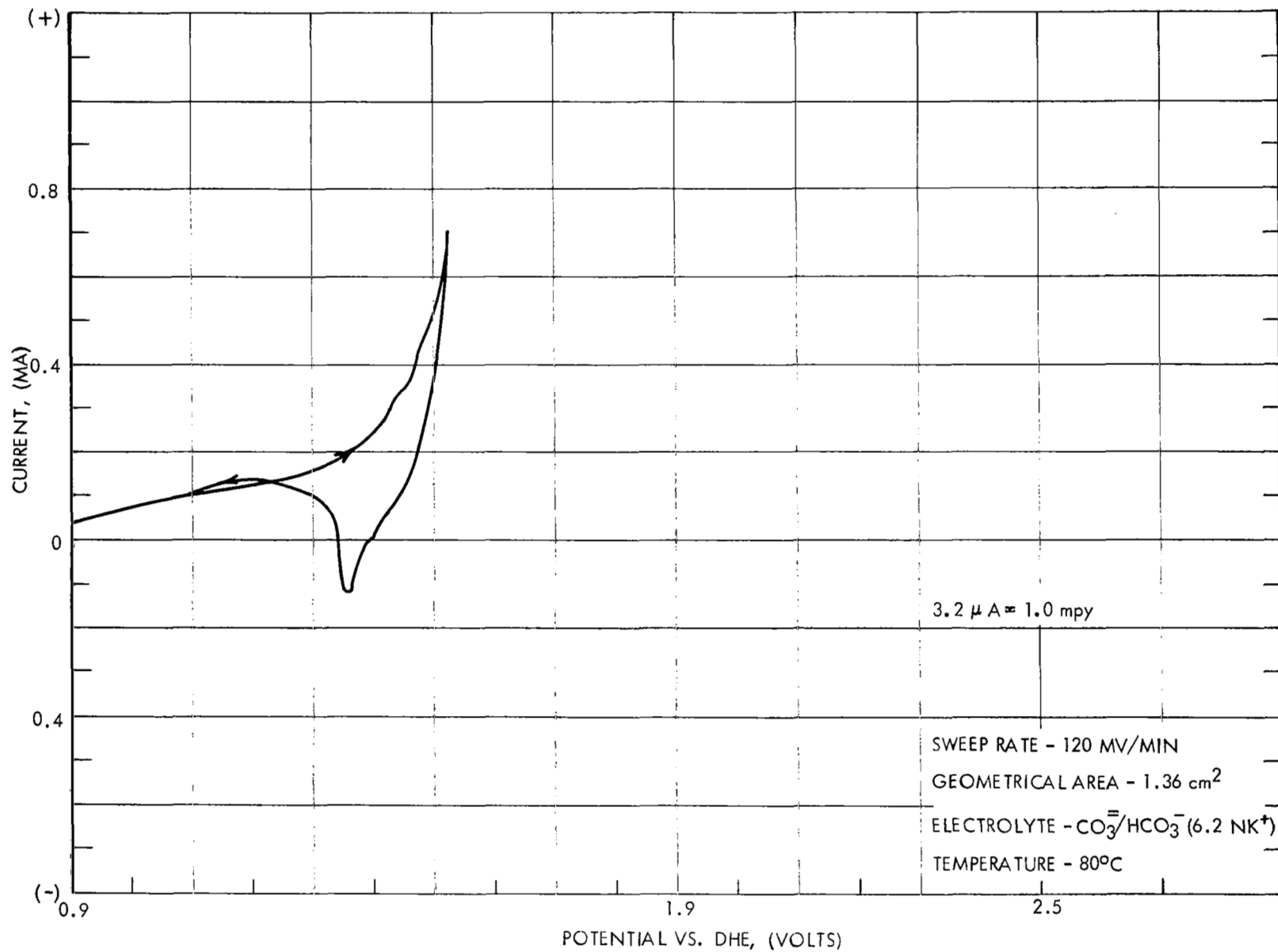
FIGURE 34 POTENTIOSTATIC SCAN FOR MONEL 400/10% CO_2 - 90% O_2 IN K_2CO_3
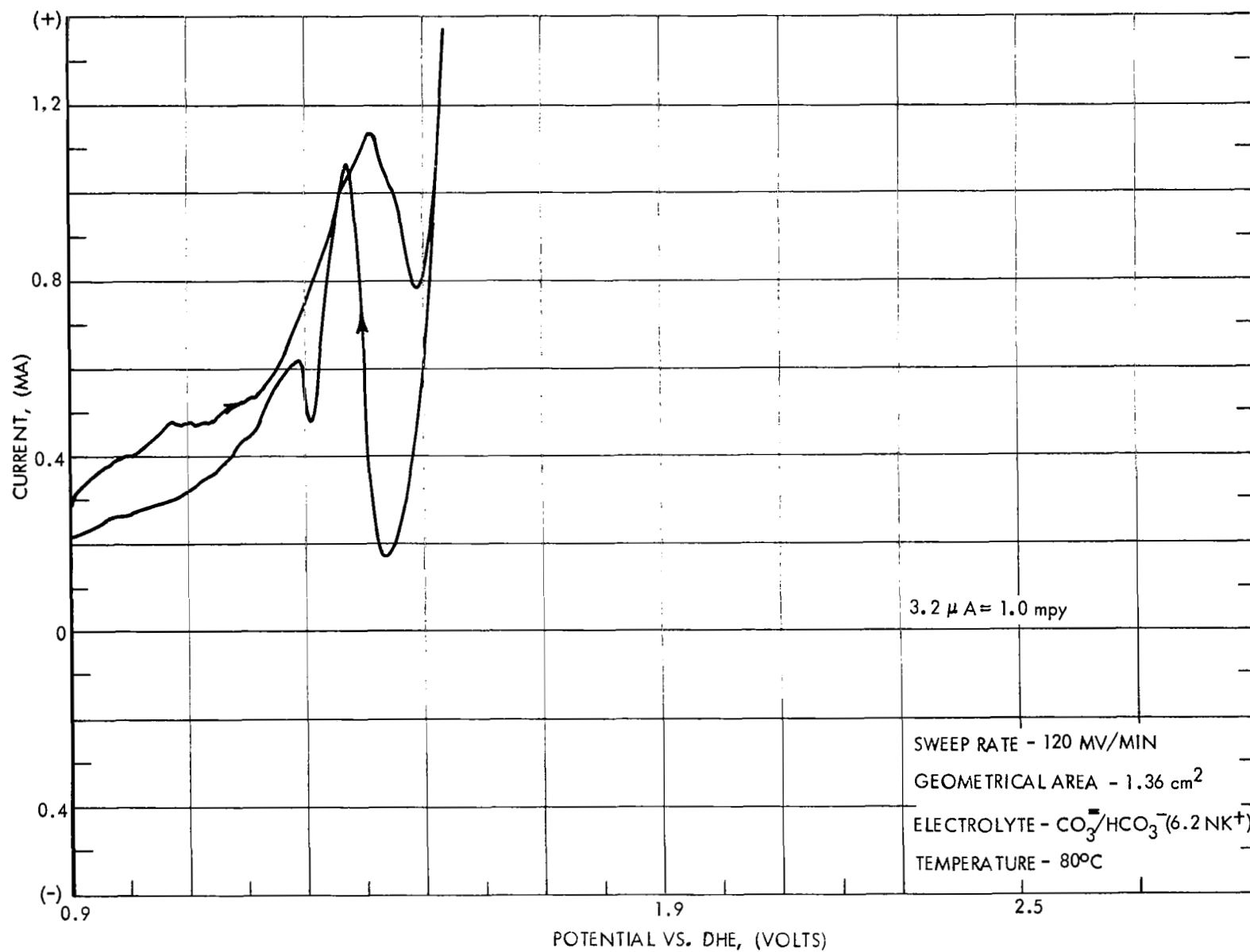
FIGURE 35 POTENTIOSTATIC SCAN FOR MONEL 400/CO_2 IN K_2CO_3

Text within the figure:

3.2 μA $\approx$ 1.0 mpy

SWEEP RATE - 120 MV/MIN

GEOMETRICAL AREA - 1.36 cm^2

ELECTROLYTE - $CO_3^=$/HCO_3^- (6.2 N K^+)

TEMPERATURE - 80°C

CURRENT, (MA)

POTENTIAL VS. DHE, (VOLTS)
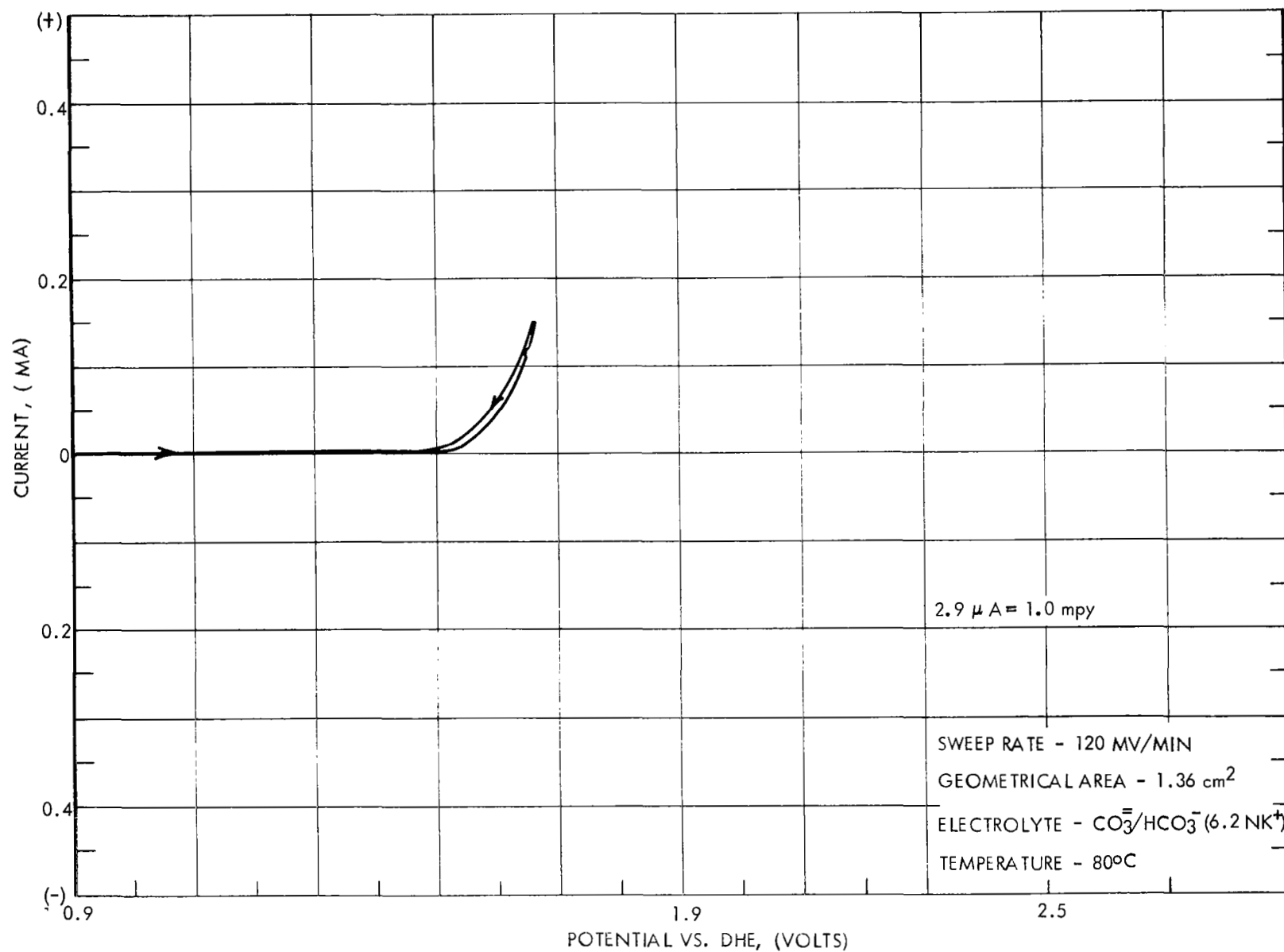
FIGURE 36 POTENTIOSTATIC SCAN FOR ZIRCONIUM/N_2 IN K_2CO_3
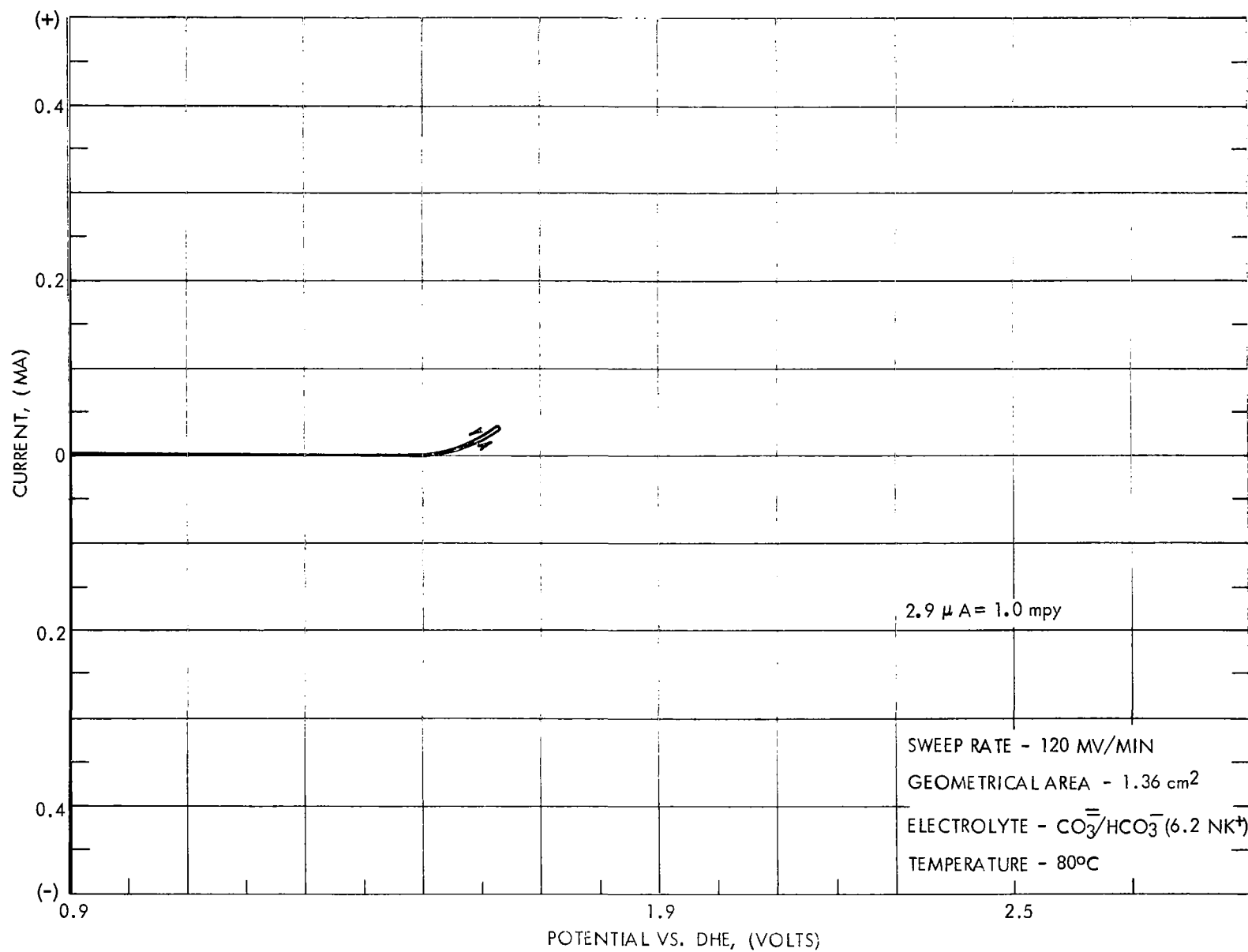
FIGURE 37 POTENTIOSTATIC SCAN FOR ZIRCONIUM/O₂ IN K₂CO₃
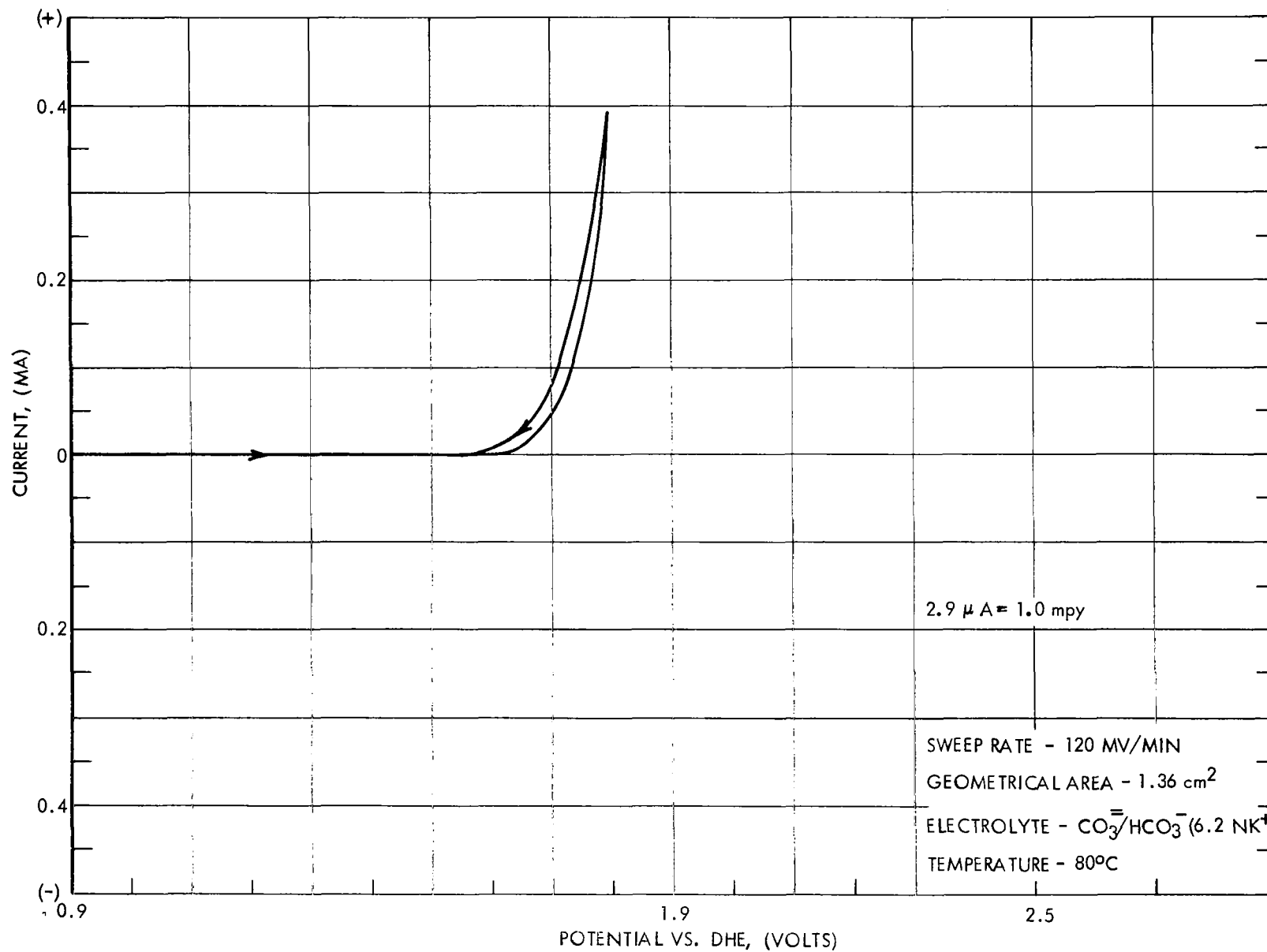
FIGURE 38 POTENTIOSTATIC SCAN FOR ZIRCONIUM/10% CO_2 - 90% O_2 IN K_2CO_3
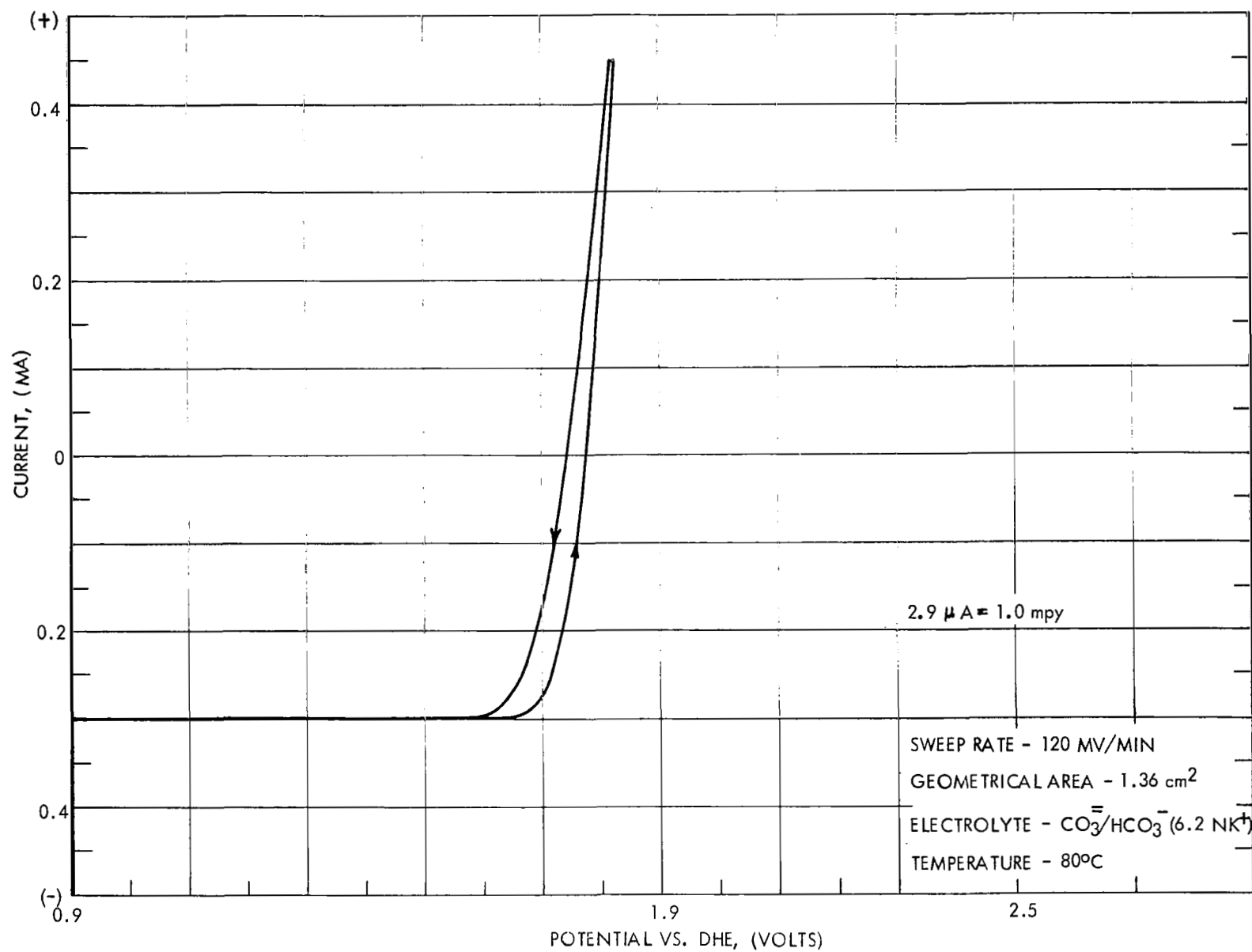
FIGURE 39 POTENTIOSTATIC SCAN FOR ZIRCONIUM/CO$_2$ IN K$_2$CO$_3$
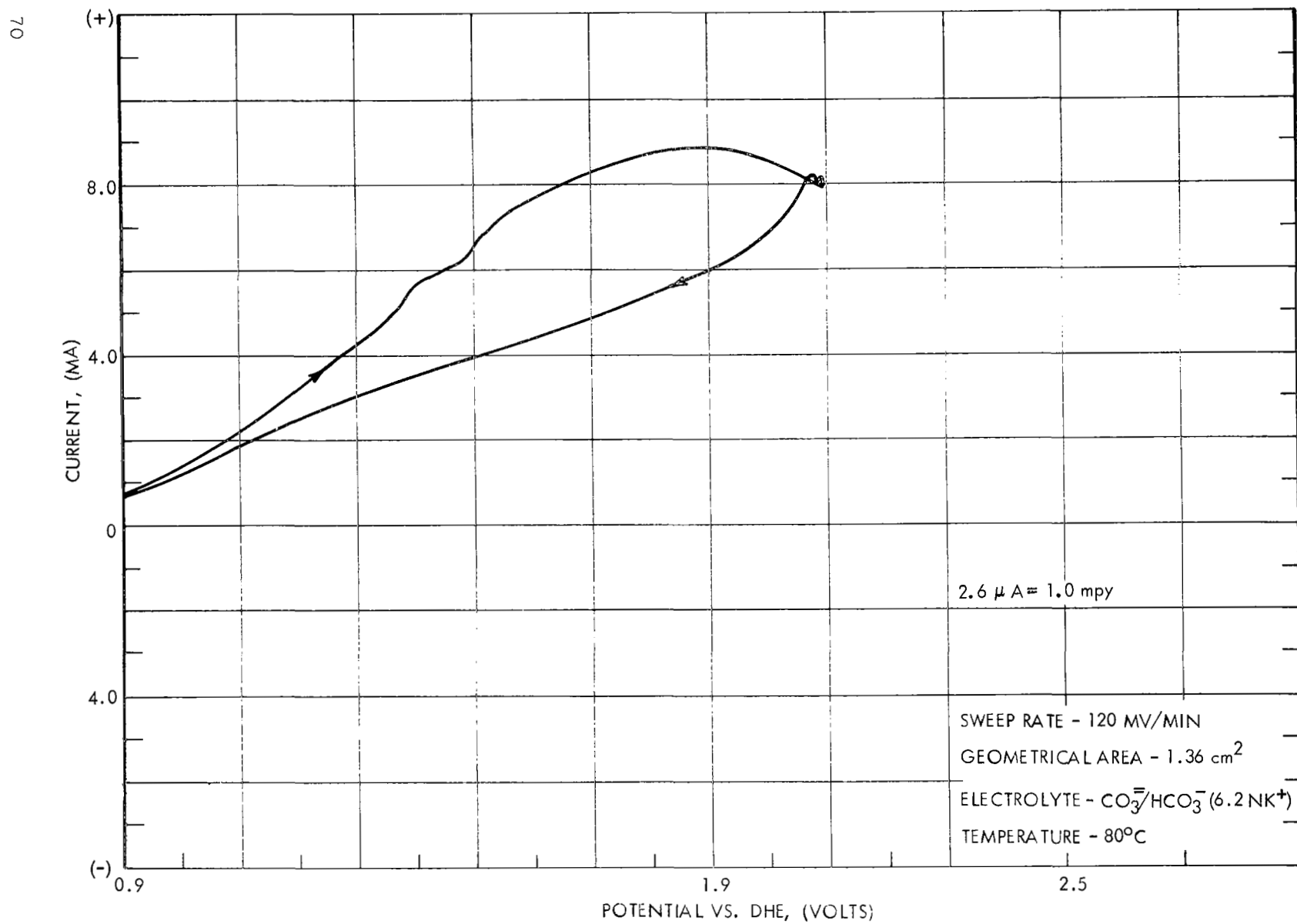
FIGURE 40 POTENTIOSTATIC SCAN FOR TIN/N_2 IN K_2CO_3

Chart annotations:

- y-axis label: CURRENT, (MA)
- y-axis values (top to bottom): (+), 8.0, 4.0, 0, 4.0, 4.0, (−)
- x-axis label: POTENTIAL VS. DHE, (VOLTS)
- x-axis values: 0.9, 1.9, 2.5

2.6 μA = 1.0 mpy

SWEEP RATE − 120 MV/MIN

GEOMETRICAL AREA − 1.36 cm^2

ELECTROLYTE − $CO_3^=$/HCO_3^- (6.2 NK^+)

TEMPERATURE − 80°C
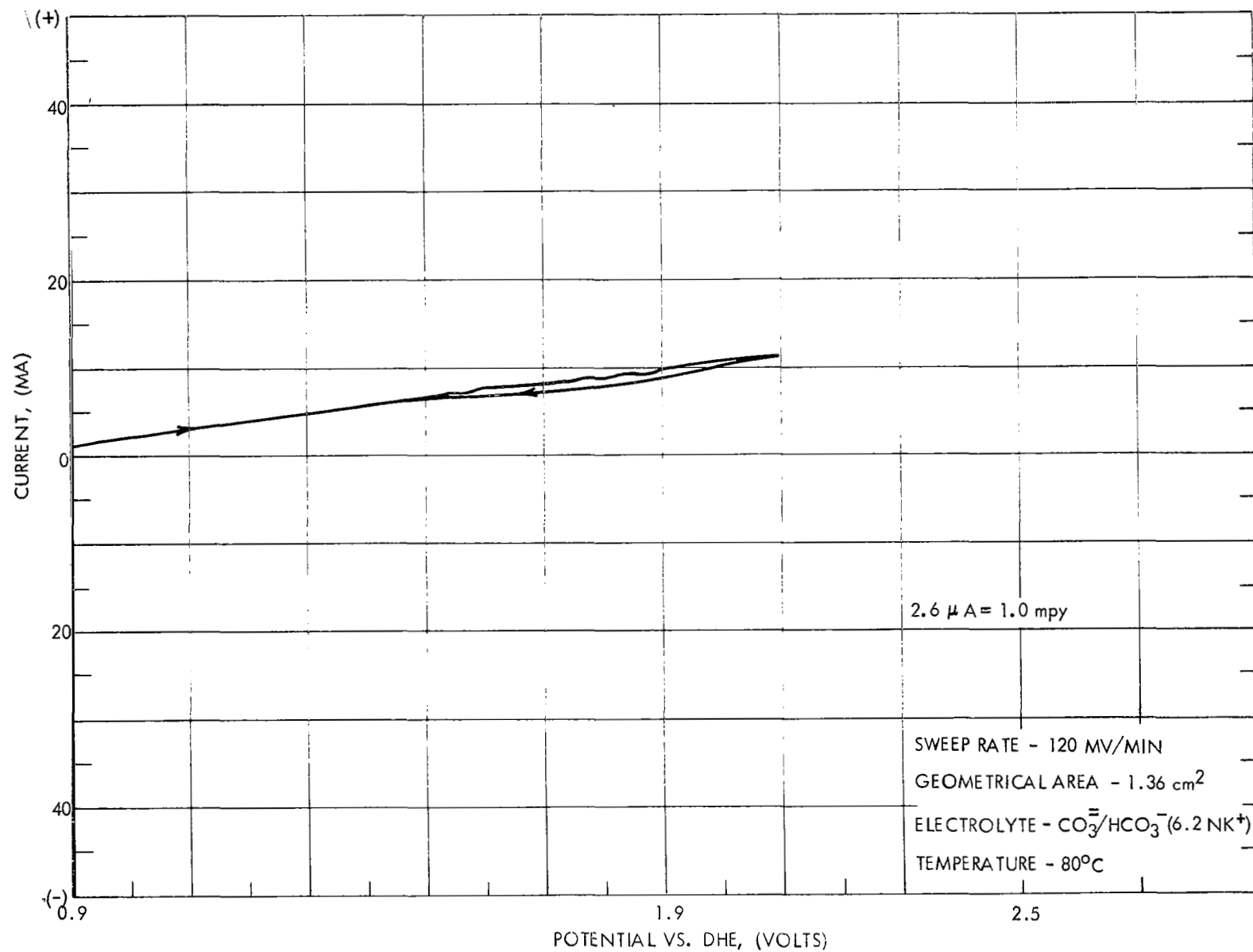
FIGURE 41 POTENTIOSTATIC SCAN FOR TIN/O$_2$ IN K$_2$CO$_3$

Chart annotations:

CURRENT, (MA)

i(+)

40

20

0

20

40

i(-)

2.6 μ A = 1.0 mpy

SWEEP RATE - 120 MV/MIN

GEOMETRICAL AREA - 1.36 cm^2

ELECTROLYTE - CO$_3^=$/HCO$_3^-$ (6.2 N K$^+$)

TEMPERATURE - 80°C

0.9   1.9   2.5

POTENTIAL VS. DHE, (VOLTS)
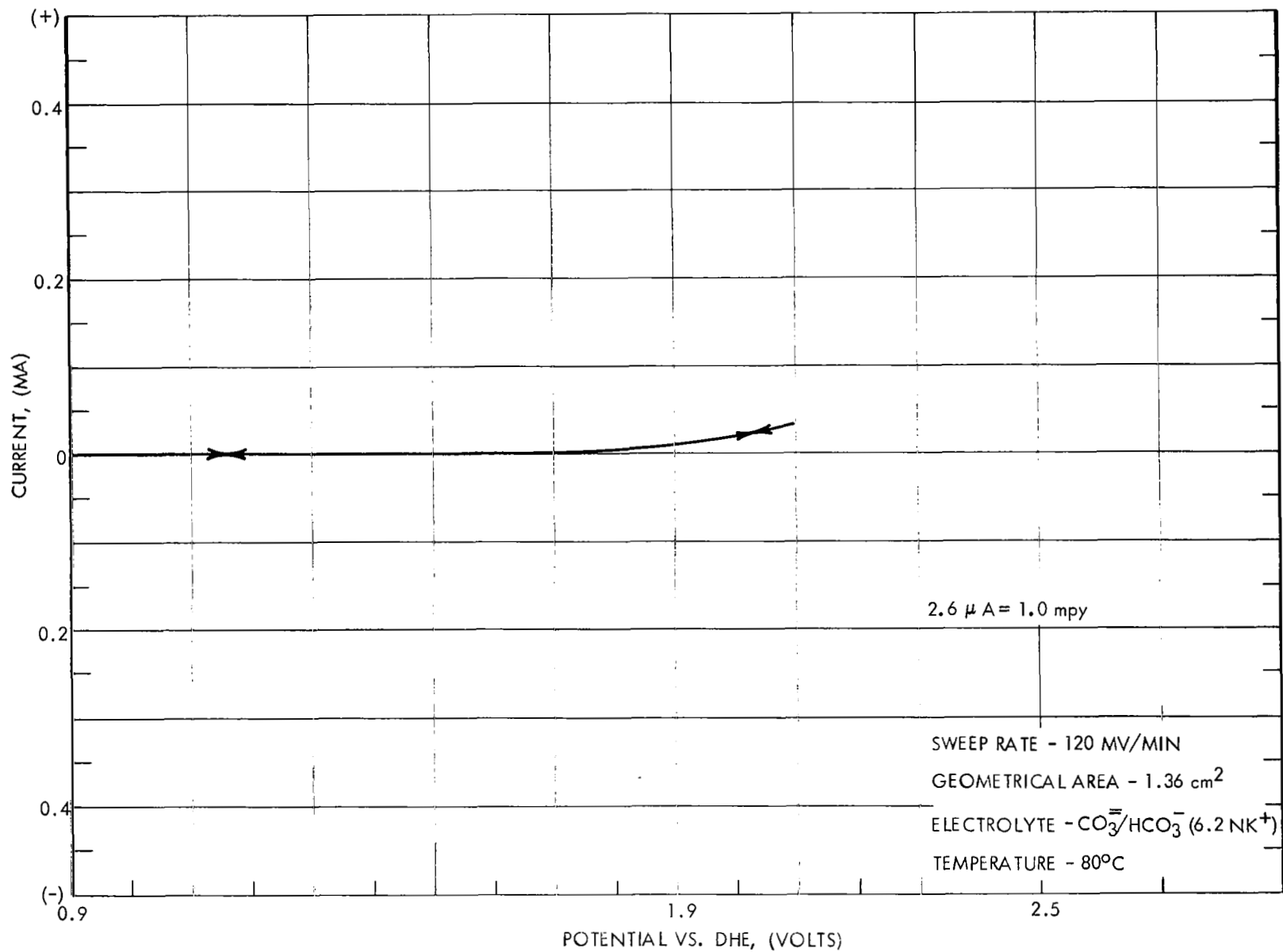
FIGURE 42 POTENTIOSTATIC SCAN FOR TIN/10% CO_2 - 90% O_2 IN K_2CO_3
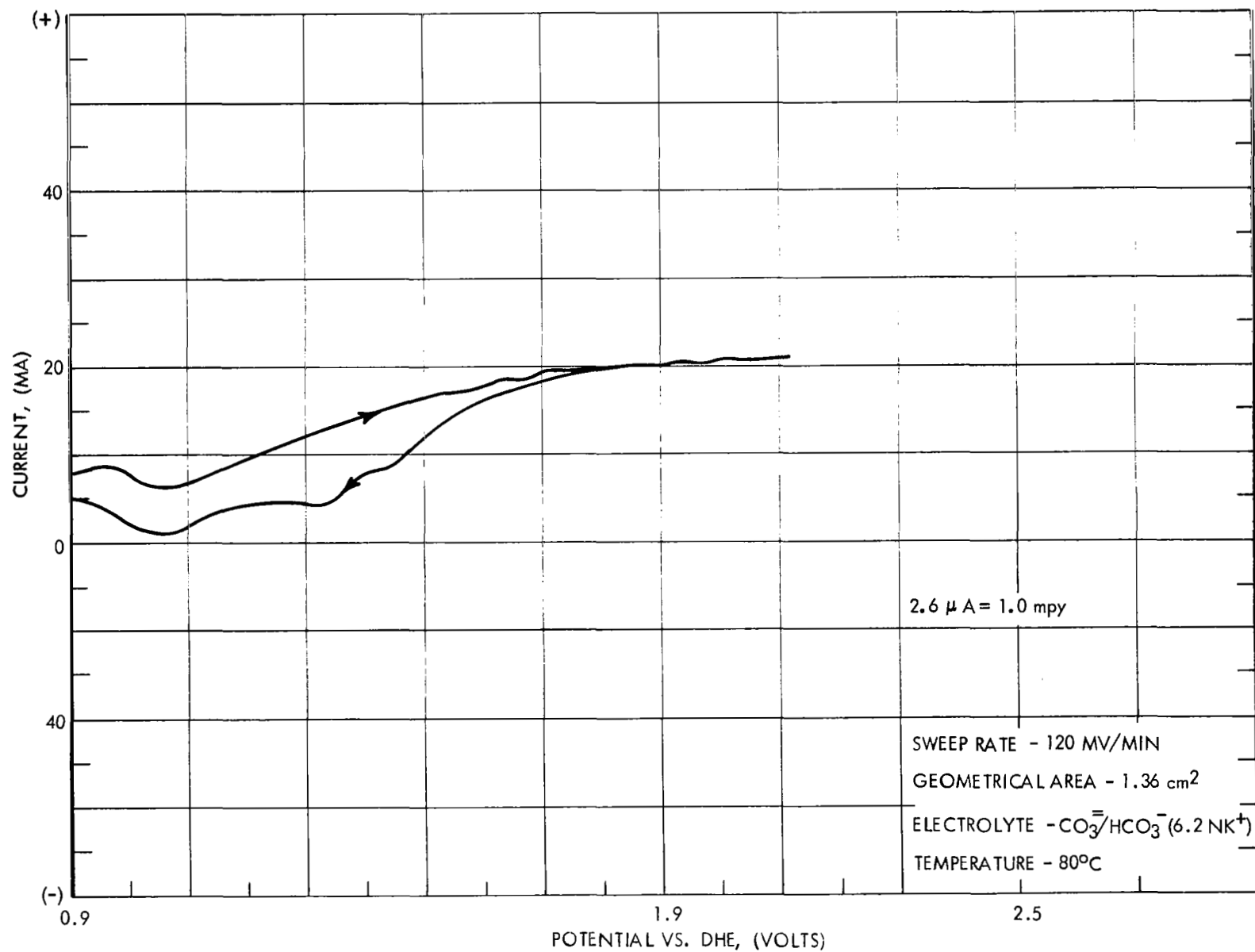
FIGURE 43 POTENTIOSTATIC SCAN FOR TIN/CO_2 IN K_2CO_3
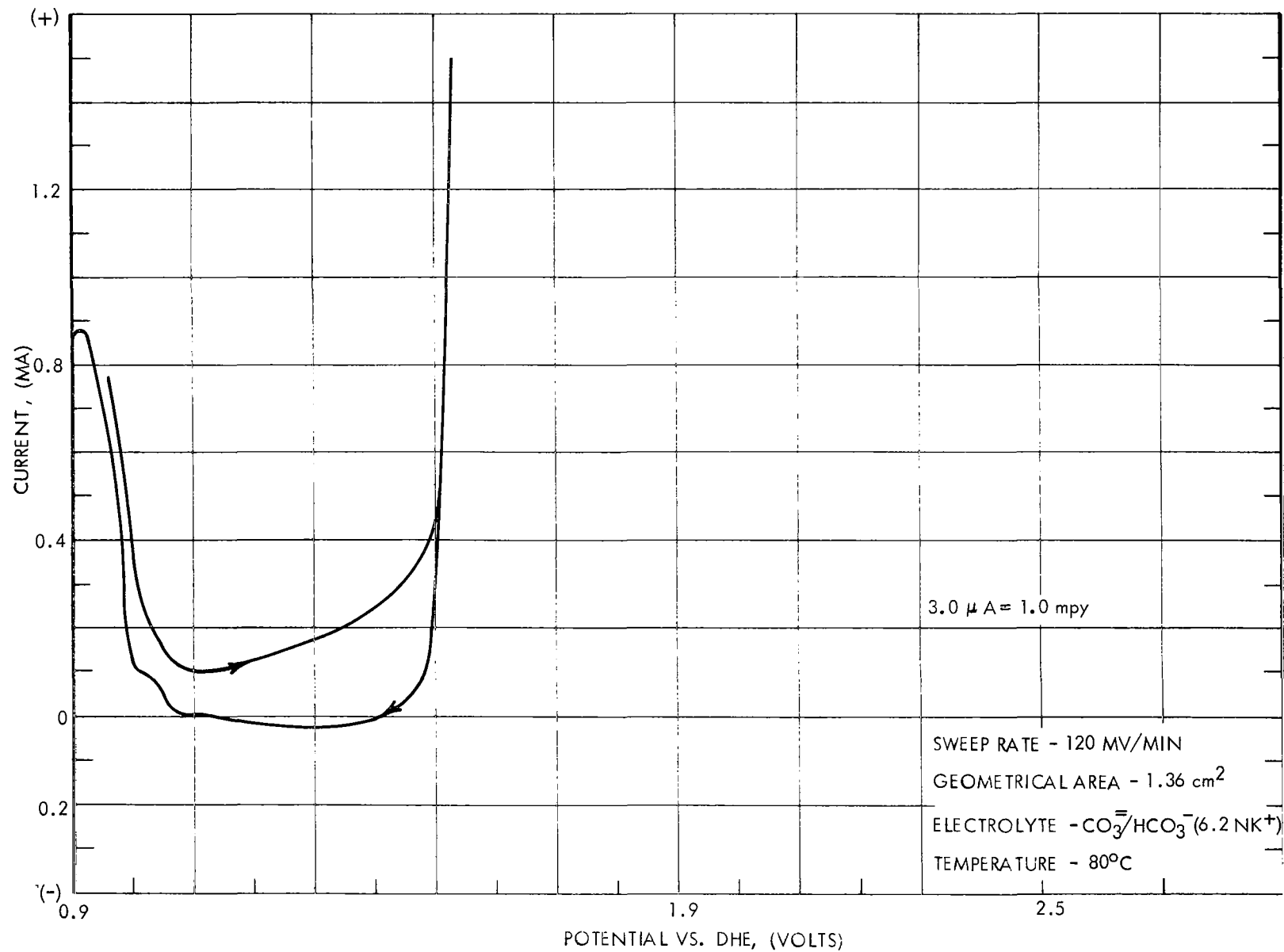
FIGURE 44 POTENTIOSTATIC SCAN FOR COPPER/N_2 IN K_2CO_3

Figure labels and annotations:

(+)

CURRENT, (MA)

1.2

0.8

0.4

0

0.2

(-)

$3.0 \, \mu A = 1.0 \, mpy$

SWEEP RATE - 120 MV/MIN

GEOMETRICAL AREA - 1.36 cm^2

ELECTROLYTE - $CO_3^=/HCO_3^-$ (6.2 N K^+)

TEMPERATURE - 80°C

0.9   1.9   2.5

POTENTIAL VS. DHE, (VOLTS)
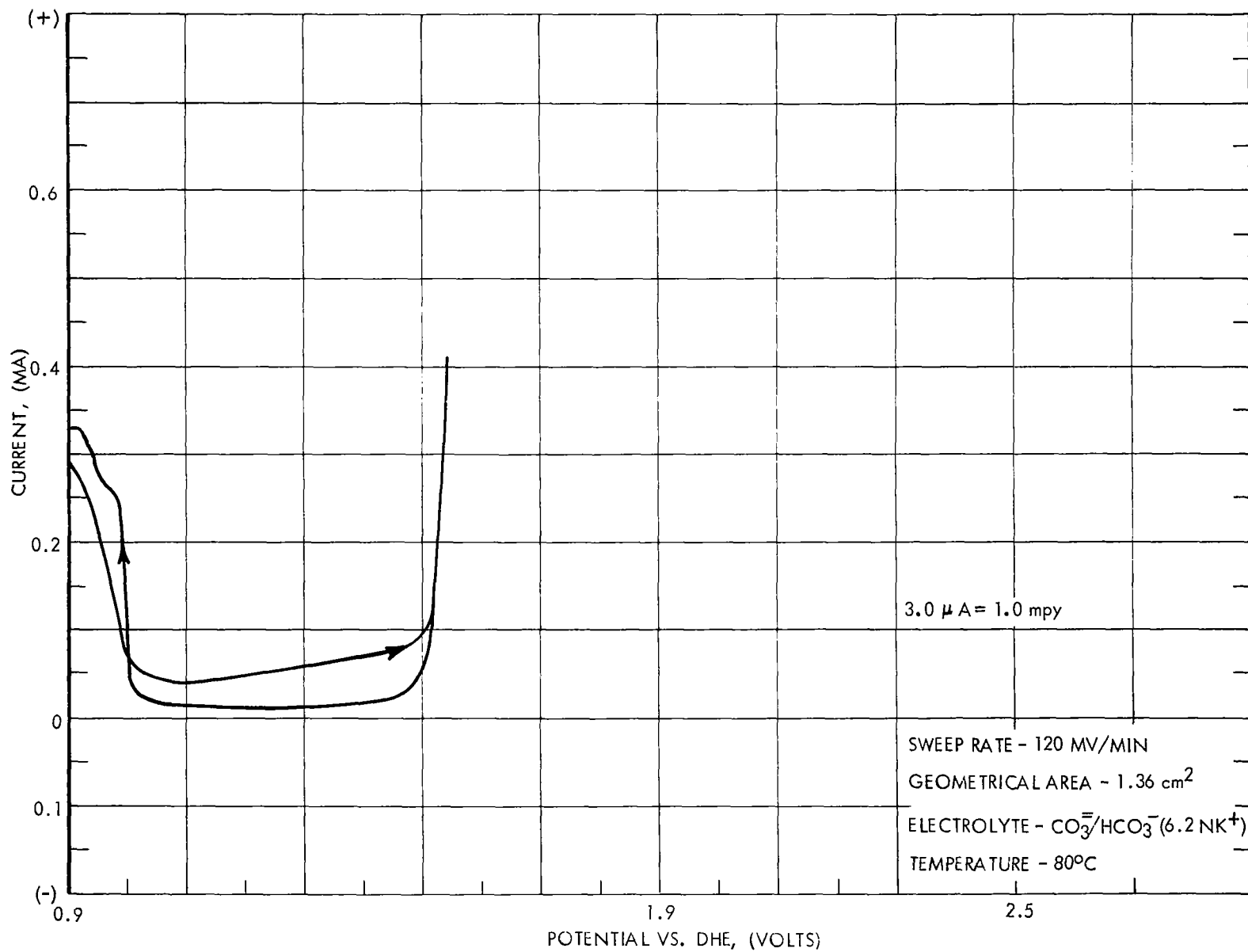
FIGURE 45 POTENTIOSTATIC SCAN FOR COPPER/O$_2$ IN K$_2$CO$_3$

(+)

0.6

0.4

CURRENT, (MA)

0.2

0.2

0

0.1

(−)

0.9   1.9   2.5

POTENTIAL VS. DHE, (VOLTS)

3.0 μA = 1.0 mpy

SWEEP RATE – 120 MV/MIN

GEOMETRICAL AREA – 1.36 cm^2

ELECTROLYTE – CO$_3^=$/HCO$_3^-$ (6.2 NK$^+$)

TEMPERATURE – 80°C
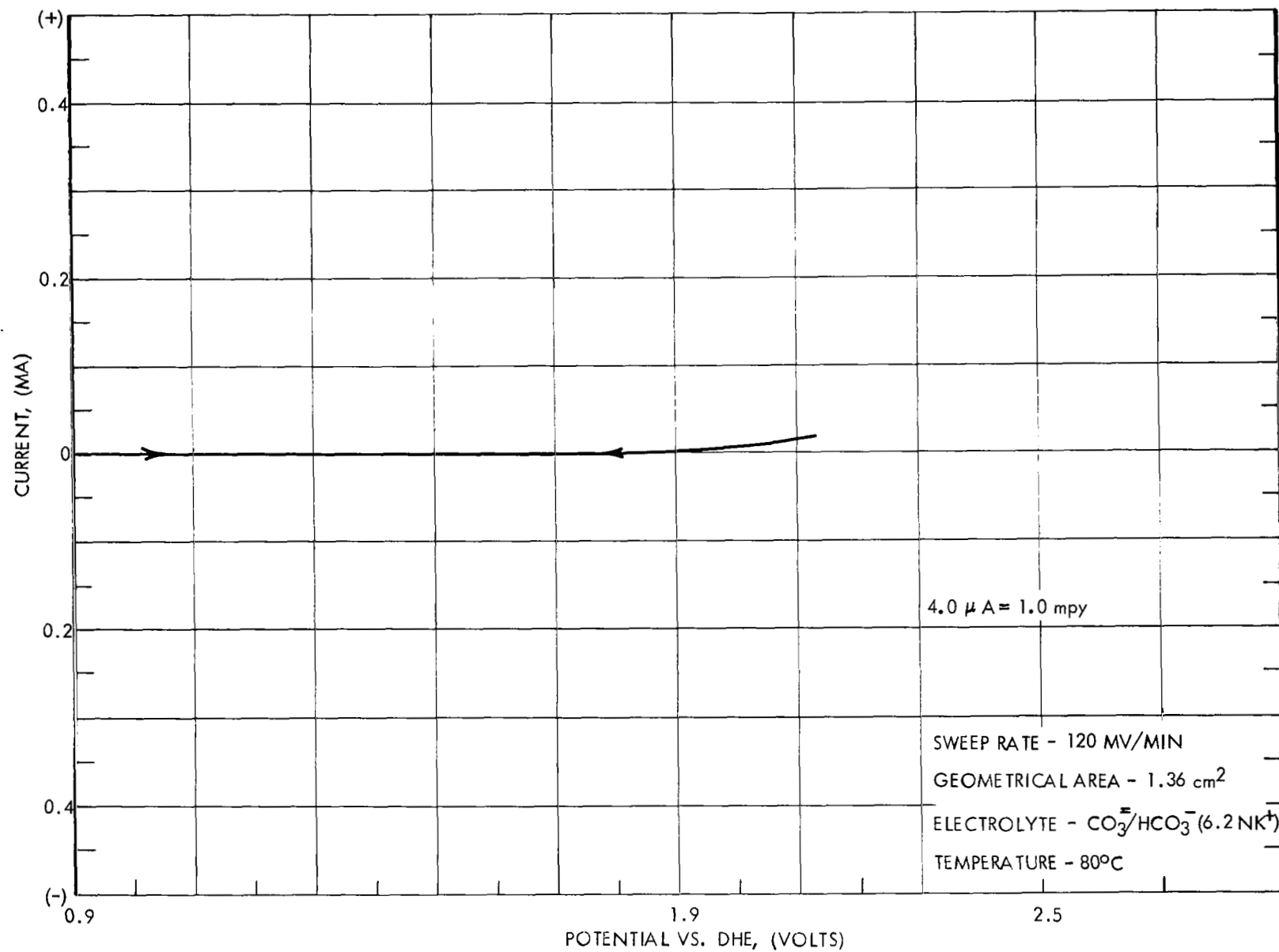
FIGURE 46 POTENTIOSTATIC SCAN FOR TITANIUM/ N_2 IN K_2CO_3
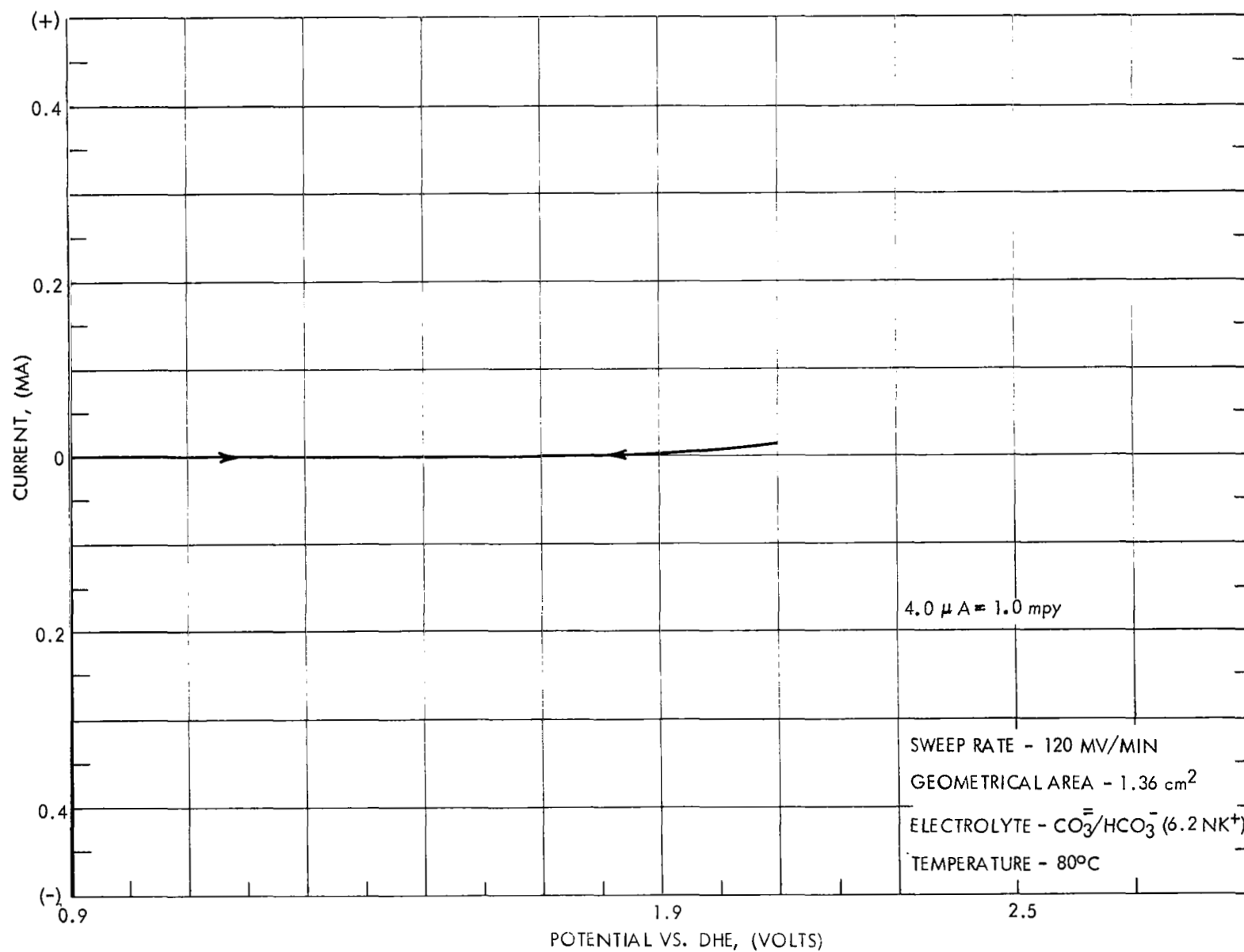
FIGURE 47 POTENTIOSTATIC SCAN FOR TITANIUM/O$_2$ IN K$_2$CO$_3$

- Y-axis: CURRENT, (MA), ranging from (+) 0.4, 0.2, 0, 0.2, 0.4 (-)
- X-axis: POTENTIAL VS. DHE, (VOLTS), with markings at 0.9, 1.9, 2.5

4.0 μA $\approx$ 1.0 mpy

SWEEP RATE - 120 MV/MIN
GEOMETRICAL AREA - 1.36 cm^2
ELECTROLYTE - CO$_3^=$/HCO$_3^-$ (6.2 NK$^+$)
TEMPERATURE - 80°C
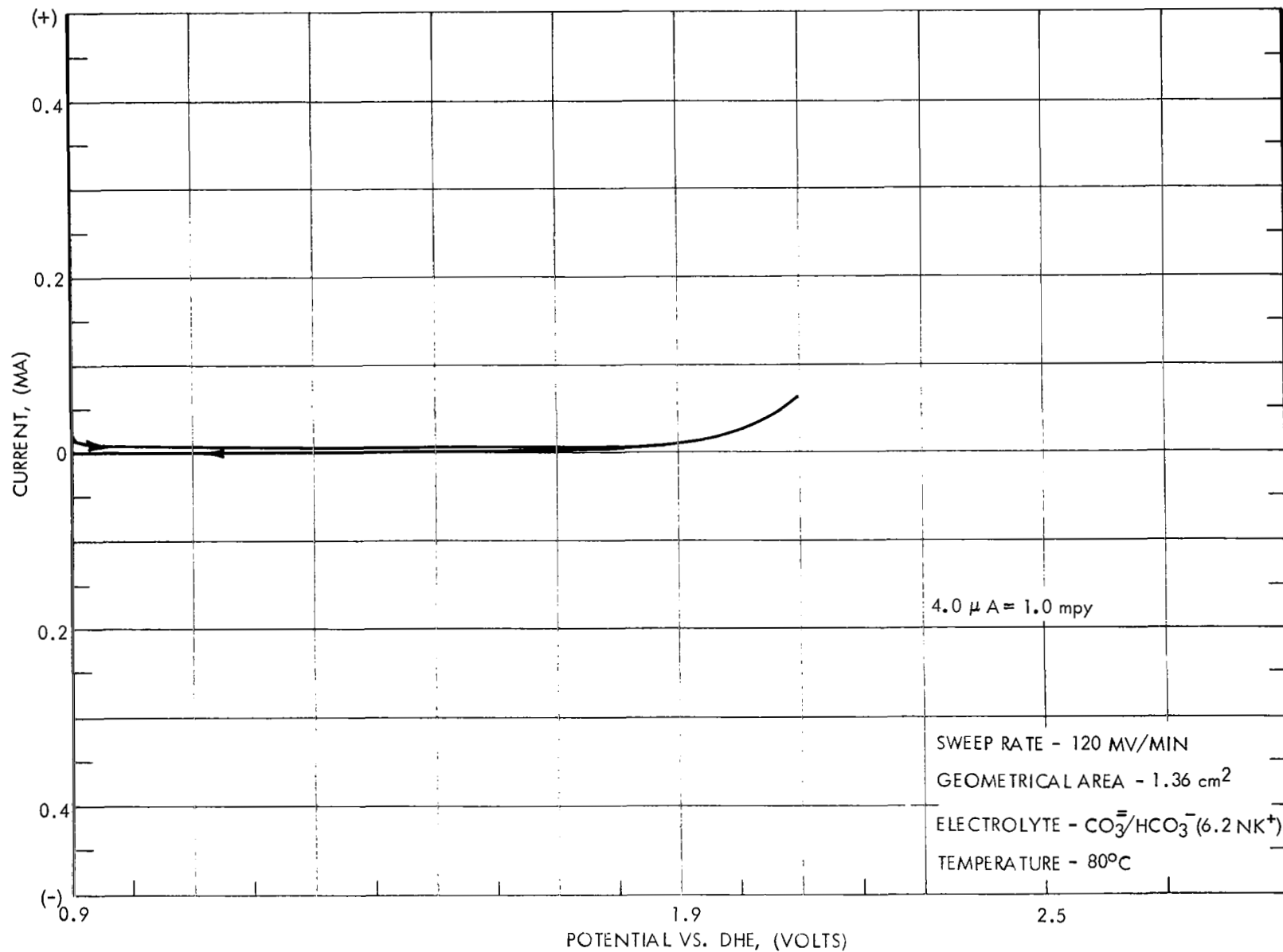
FIGURE 48 POTENTIOSTATIC SCAN FOR TITANIUM/10% CO_2 - 90% O_2
IN K_2CO_3

CURRENT, (MA)

POTENTIAL VS. DHE, (VOLTS)

4.0 μA = 1.0 mpy

SWEEP RATE - 120 MV/MIN

GEOMETRICAL AREA - 1.36 cm^2

ELECTROLYTE - $CO_3^=$/HCO_3^- (6.2 N K^+)

TEMPERATURE - 80°C
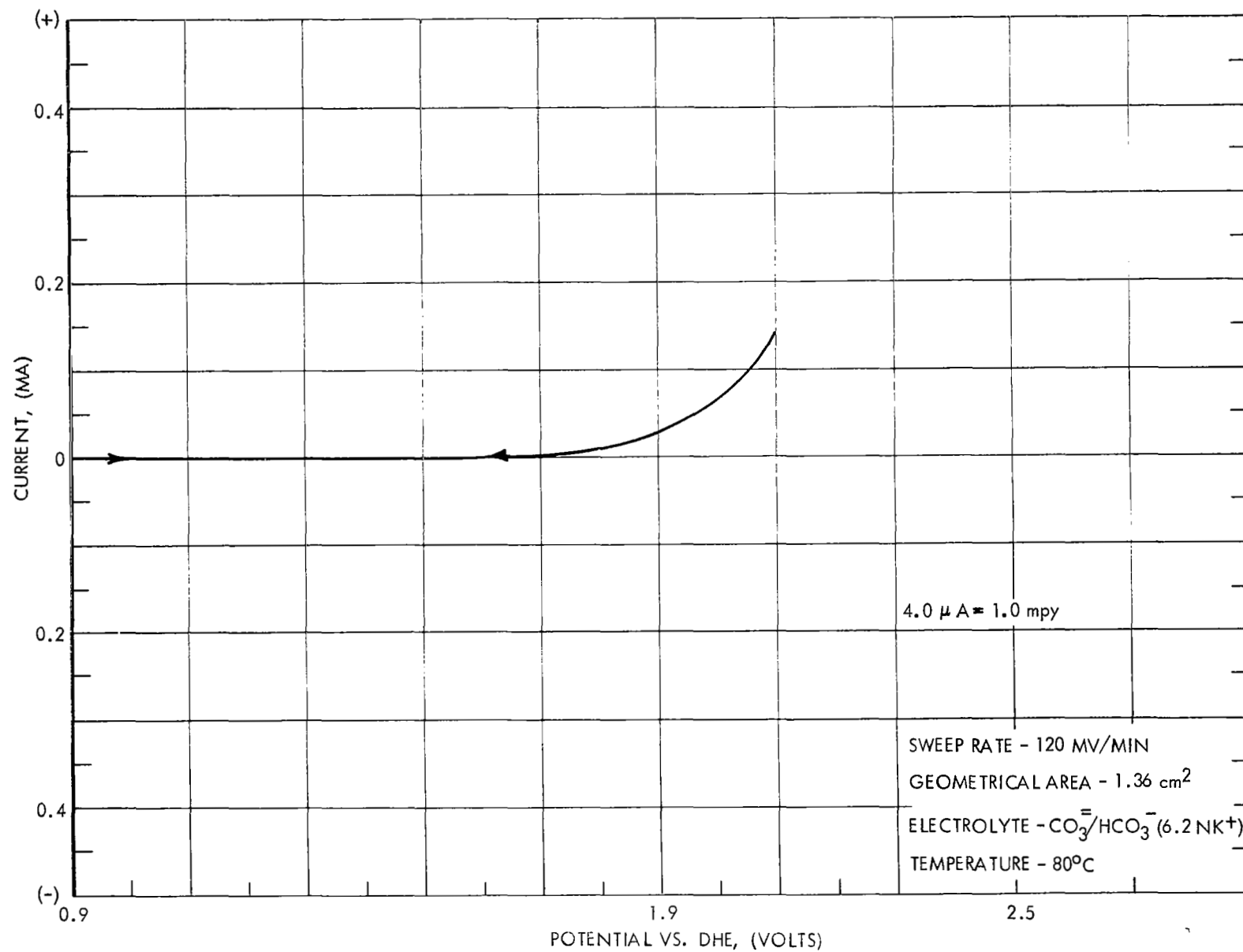
FIGURE 49 POTENTIOSTATIC SCAN FOR TITANIUM/CO$_2$ IN K$_2$CO$_3$

Graph labels:

CURRENT, (MA)

(+)
0.4
0.2
0
0.2
0.4
(−)

POTENTIAL VS. DHE, (VOLTS)

0.9   1.9   2.5

4.0 μA $\approx$ 1.0 mpy

SWEEP RATE − 120 MV/MIN

GEOMETRICAL AREA − 1.36 cm^2

ELECTROLYTE − CO$_3^=$/HCO$_3^-$ (6.2 N K$^+$)

TEMPERATURE − 80°C
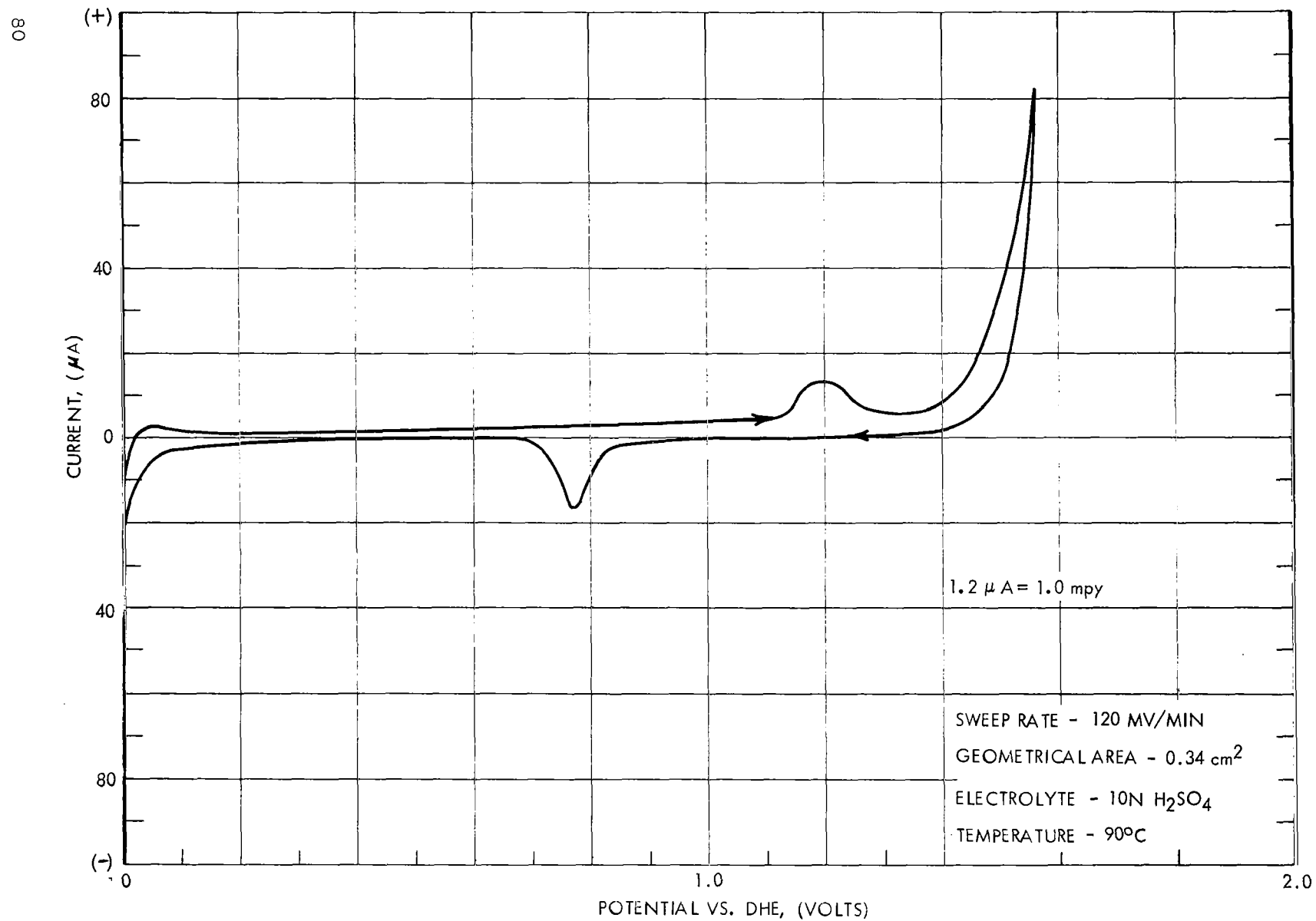
FIGURE 50 POTENTIOSTATIC SCAN FOR PLATINUM/N$_2$ IN H$_2$SO$_4$
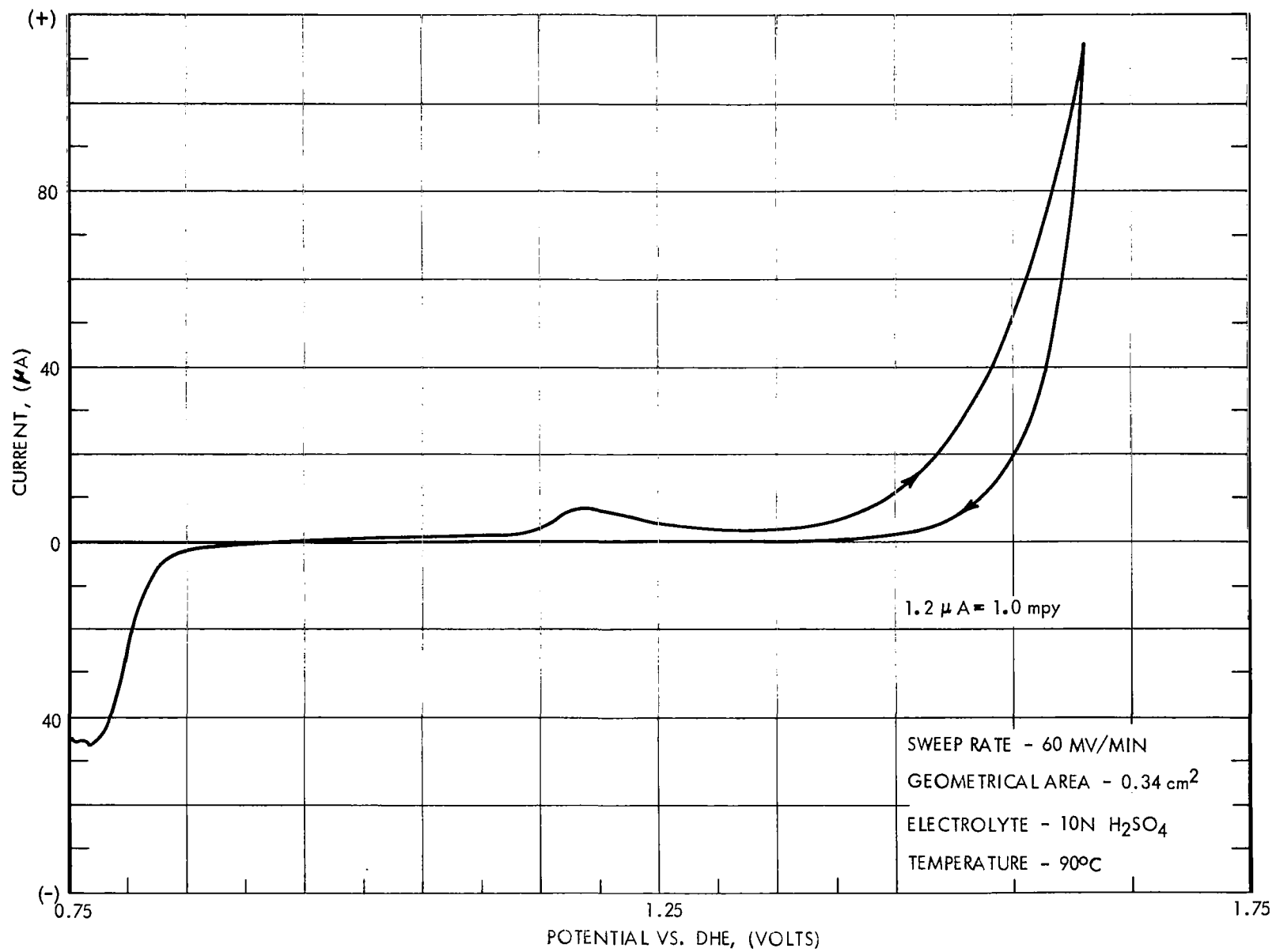
FIGURE 51 POTENTIOSTATIC SCAN FOR PLATINUM/O$_2$ IN H$_2$SO$_4$

Chart labels:
- (+)
- CURRENT, (μA)
- 80
- 40
- 0
- 40
- 40
- (-)
- POTENTIAL VS. DHE, (VOLTS)
- 0.75
- 1.25
- 1.75

1.2 μA = 1.0 mpy

SWEEP RATE - 60 MV/MIN

GEOMETRICAL AREA - 0.34 cm^2

ELECTROLYTE - 10N H$_2$SO$_4$

TEMPERATURE - 90°C
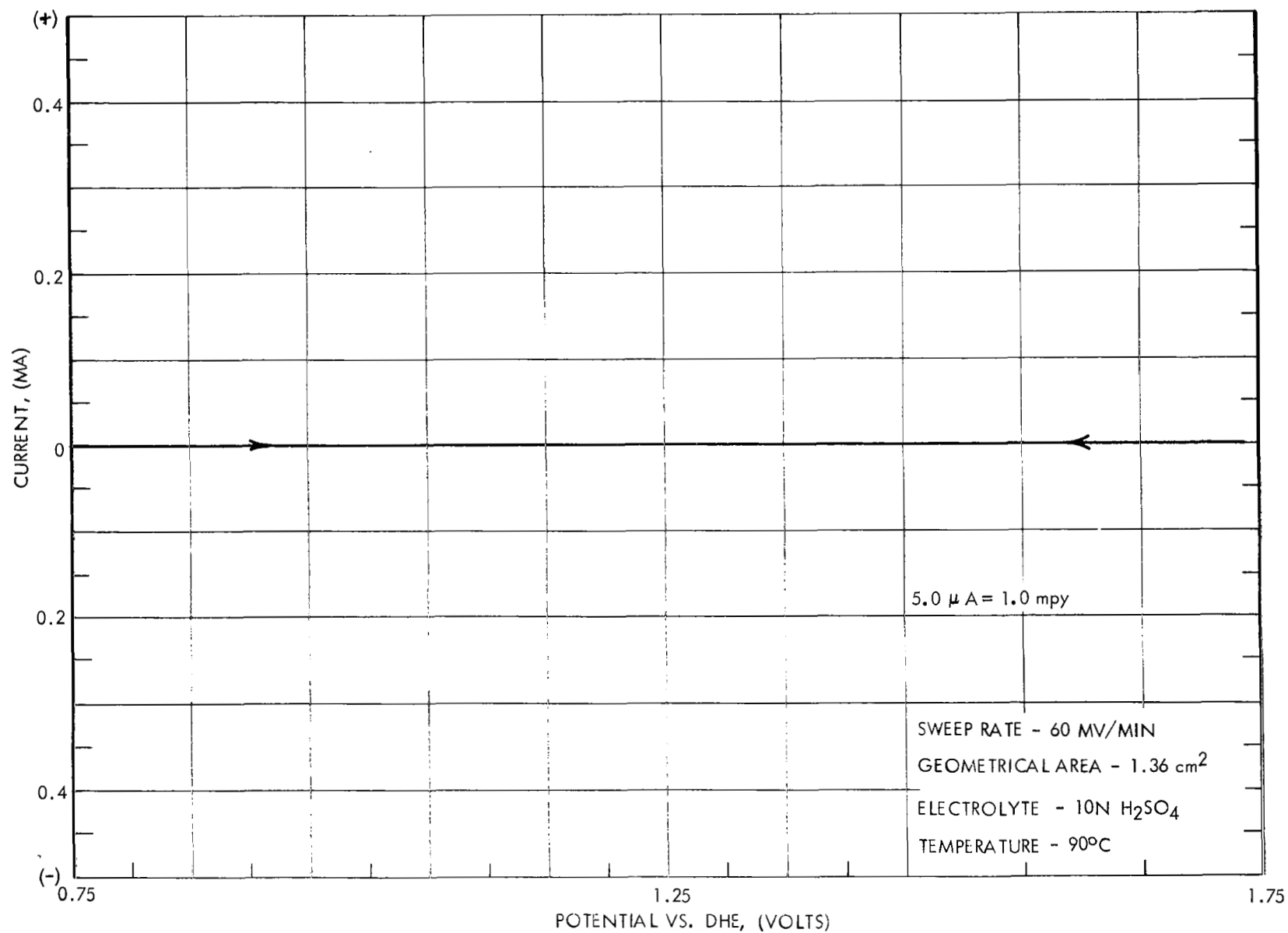
FIGURE 52 POTENTIOSTATIC SCAN FOR TANTALUM/N$_2$ IN H$_2$SO$_4$
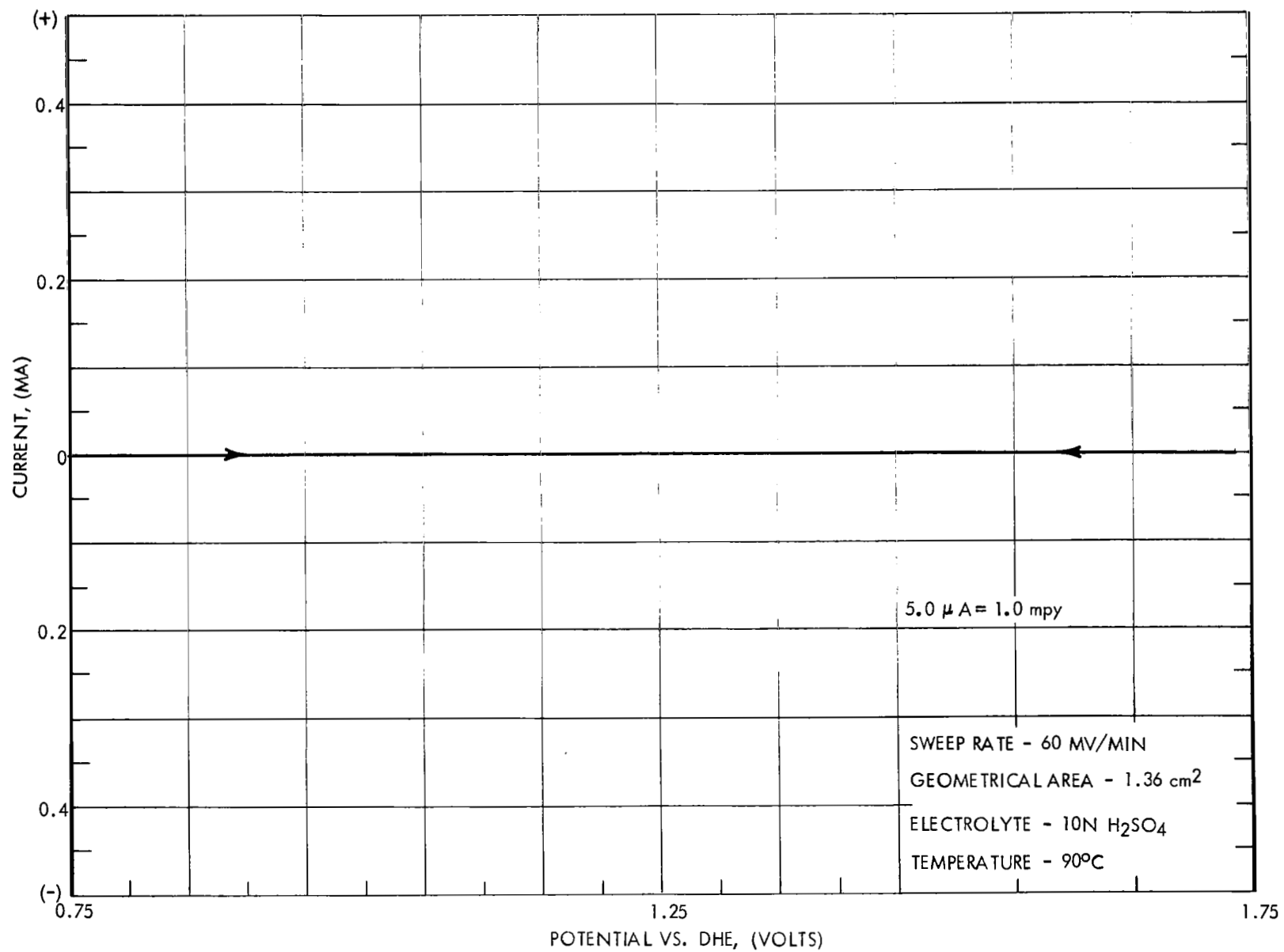
FIGURE 53 POTENTIOSTATIC SCAN FOR TANTALUM/O$_2$ IN H$_2$SO$_4$

Chart annotations:

- CURRENT, (MA) [vertical axis]
- (+) 0.4 0.2 0 0.2 0.4 (-)
- POTENTIAL VS. DHE, (VOLTS) [horizontal axis]
- 0.75 1.25 1.75

5.0 μA = 1.0 mpy

SWEEP RATE - 60 MV/MIN
GEOMETRICAL AREA - 1.36 cm^2
ELECTROLYTE - 10N H$_2$SO$_4$
TEMPERATURE - 90°C
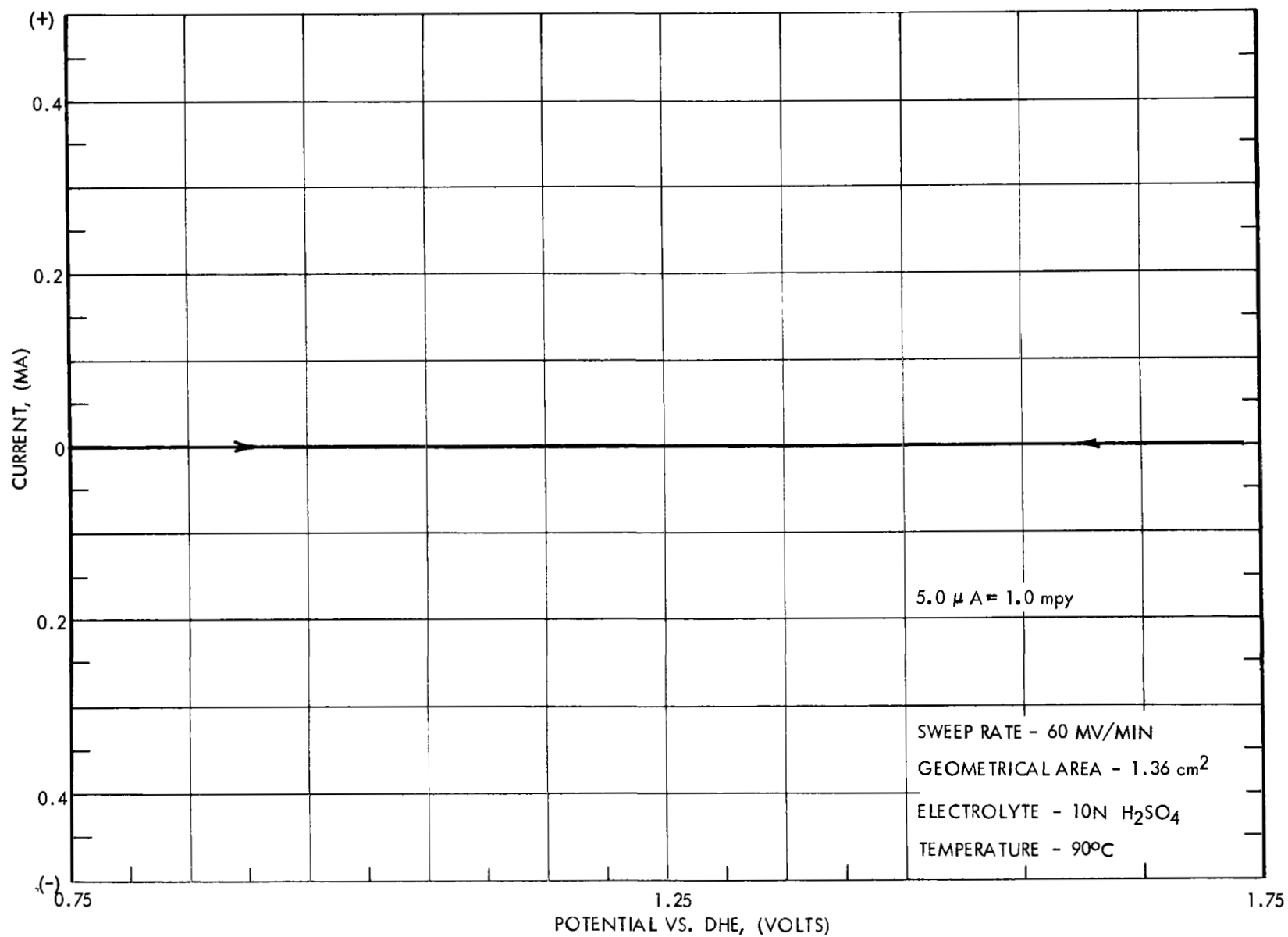
FIGURE 54 POTENTIOSTATIC SCAN FOR TANTALUM/CO_2 IN H_2SO_4

5.0 μA = 1.0 mpy

SWEEP RATE - 60 MV/MIN

GEOMETRICAL AREA - 1.36 cm^2

ELECTROLYTE - 10N H_2SO_4

TEMPERATURE - 90°C
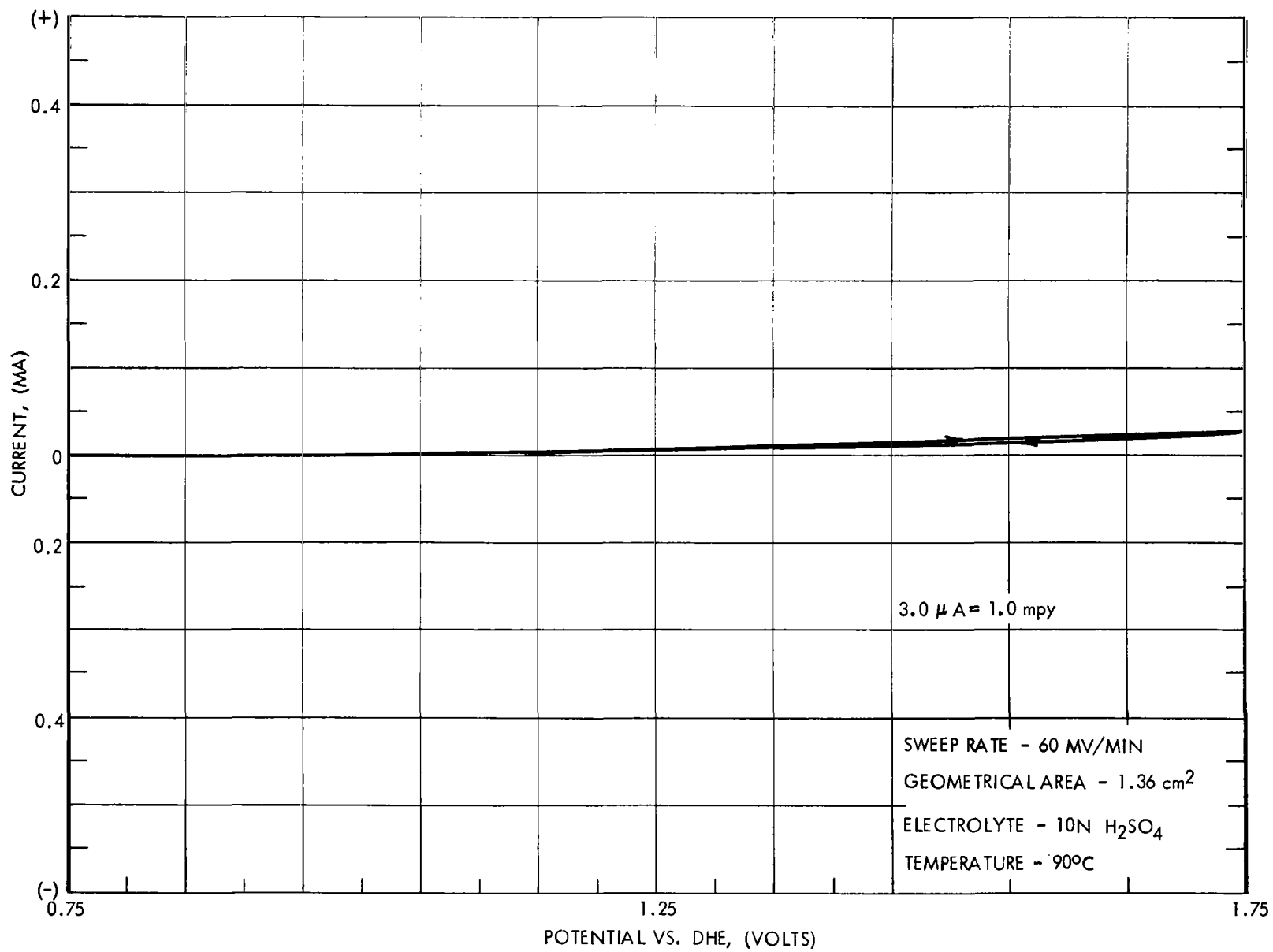
FIGURE 55 POTENTIOSTATIC SCAN FOR ZIRCONIUM/N$_2$ IN H$_2$SO$_4$
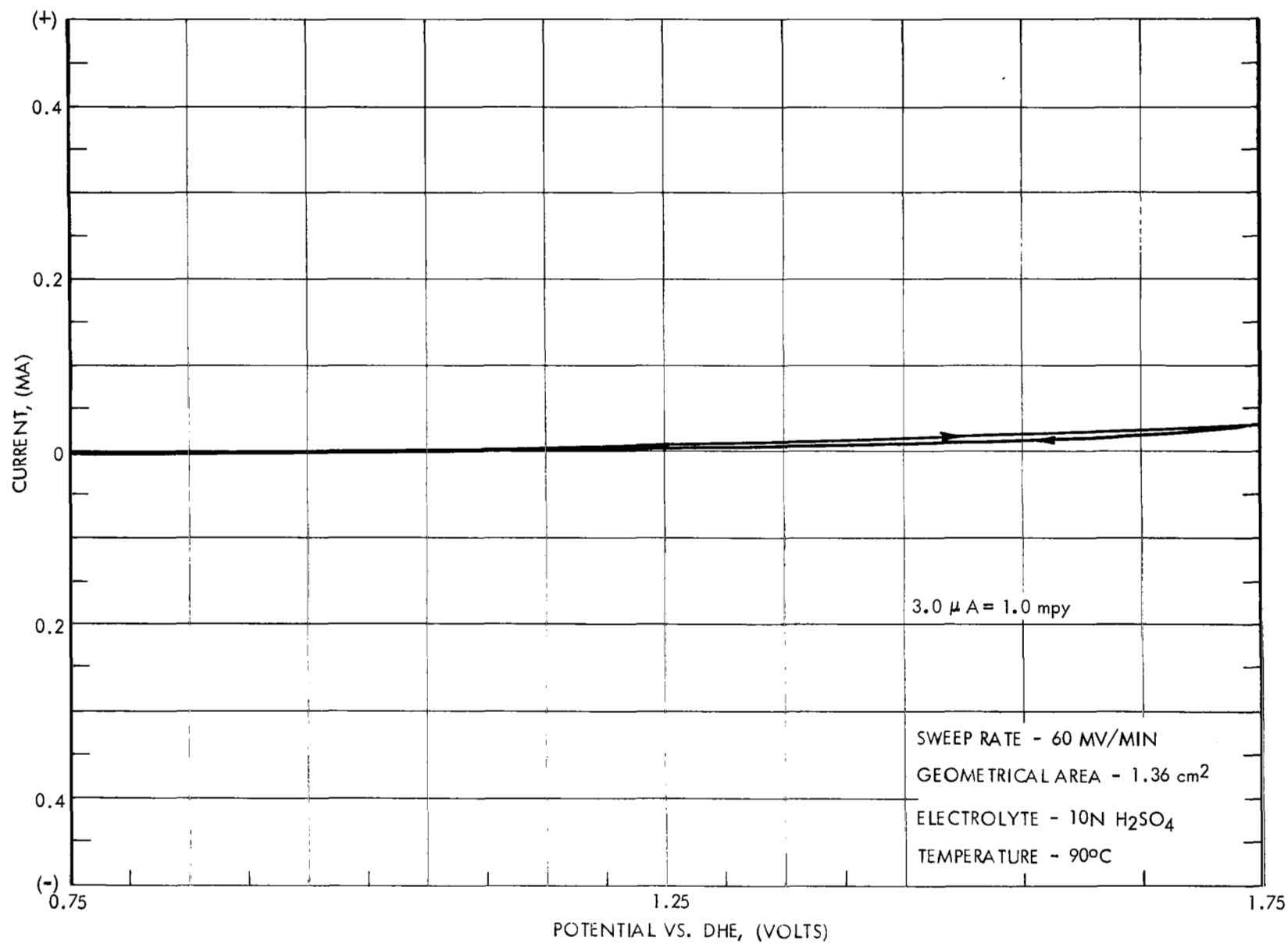
FIGURE 56 POTENTIOSTATIC SCAN FOR ZIRCONIUM/O_2 IN H_2SO_4
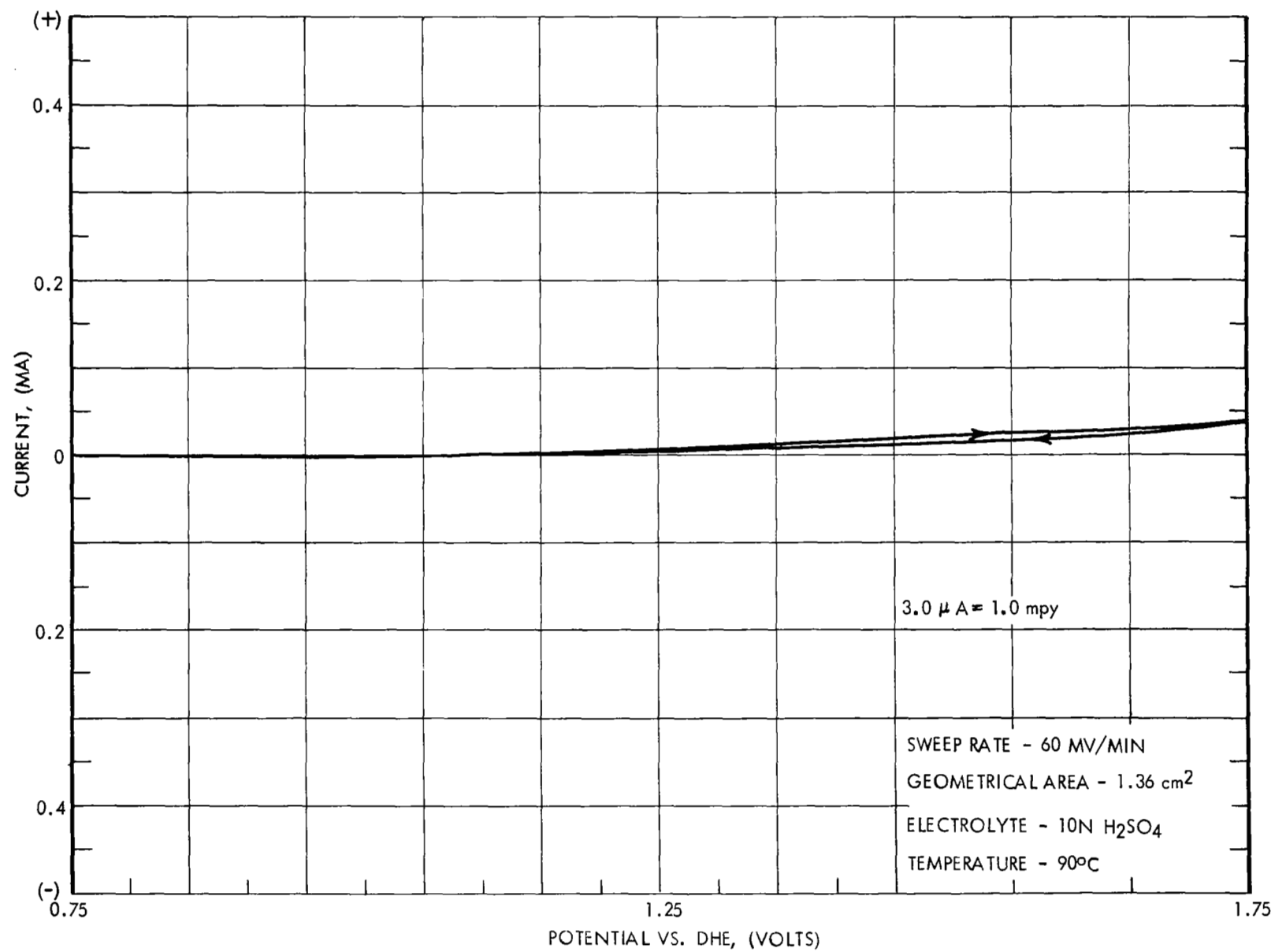
FIGURE 57 POTENTIOSTATIC SCAN FOR ZIRCONIUM/CO_2 IN H_2SO_4

Chart axes and labels:

(+) ... 0.4 ... 0.2 ... 0 ... 0.2 ... 0.4 ... (-)

CURRENT, (MA)

POTENTIAL VS. DHE, (VOLTS)

0.75 ... 1.25 ... 1.75

3.0 μA = 1.0 mpy

SWEEP RATE - 60 MV/MIN

GEOMETRICAL AREA - 1.36 cm^2

ELECTROLYTE - 10N H_2SO_4

TEMPERATURE - 90°C
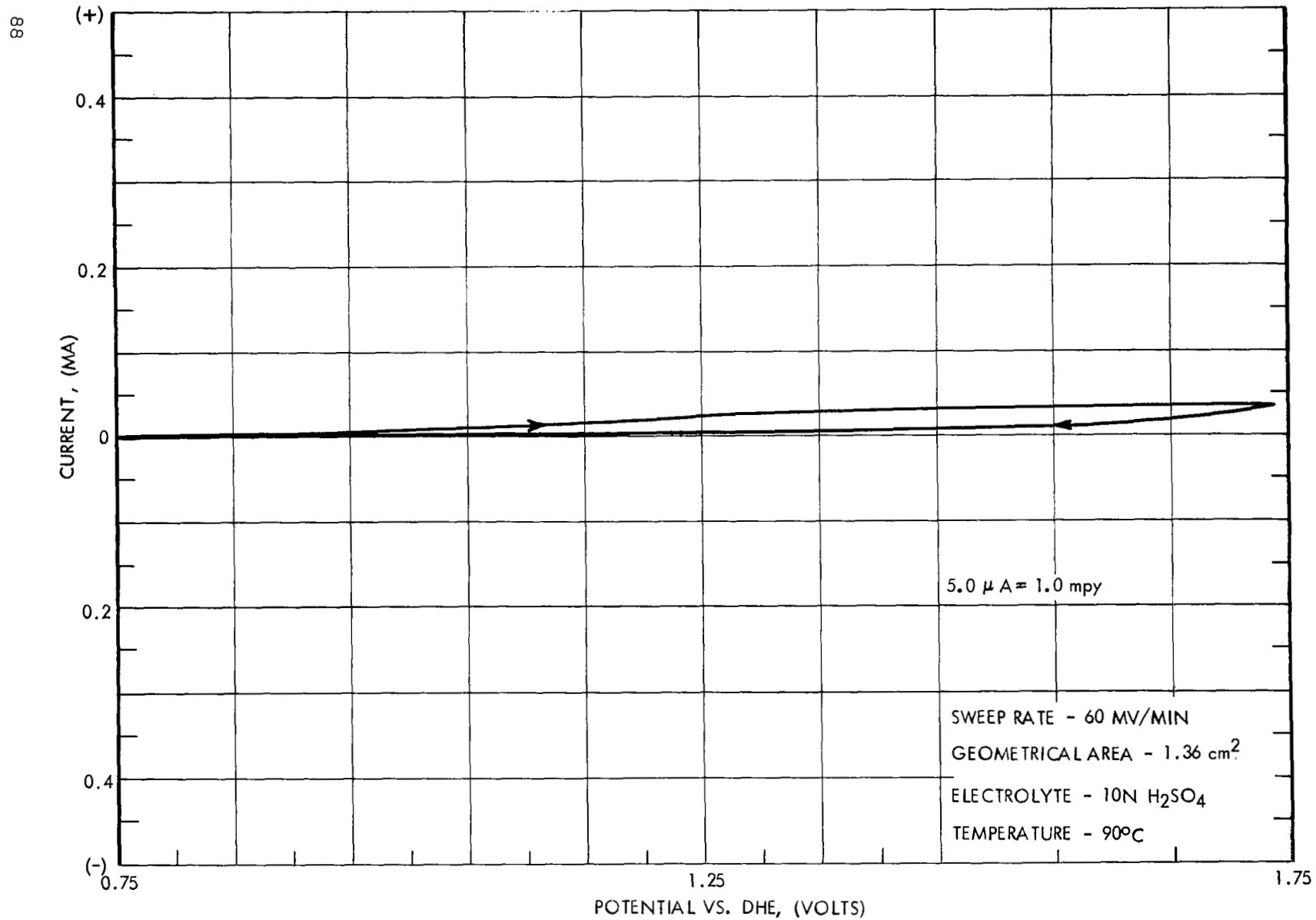
FIGURE 58 POTENTIOSTATIC SCAN FOR NIOBIUM/N$_2$ IN H$_2$SO$_4$
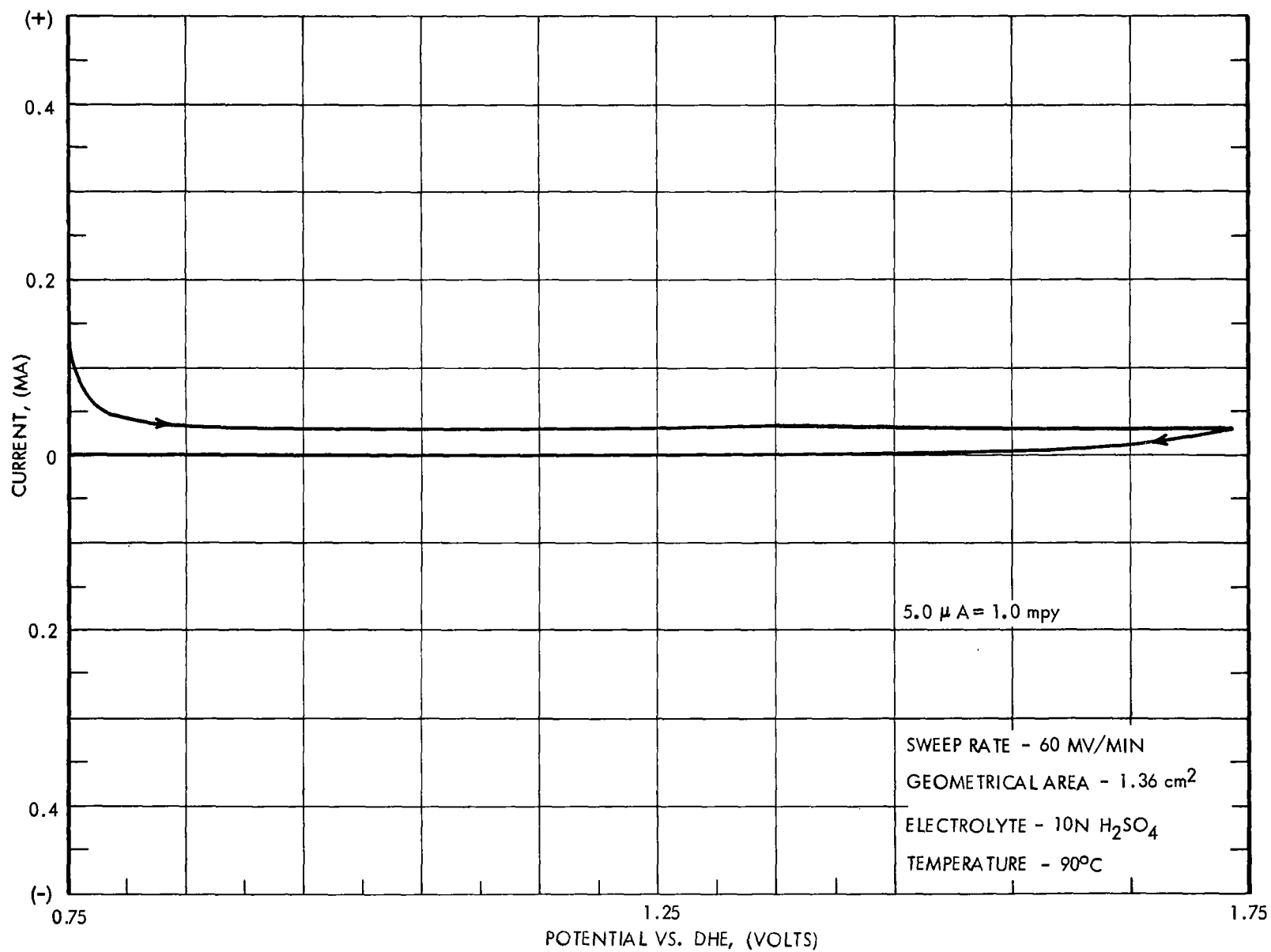
FIGURE 59 POTENTIOSTATIC SCAN FOR NIOBIUM/O$_2$ IN H$_2$SO$_4$

5.0 μA = 1.0 mpy

SWEEP RATE - 60 MV/MIN

GEOMETRICAL AREA - 1.36 cm^2

ELECTROLYTE - 10N H$_2$SO$_4$

TEMPERATURE - 90°C

CURRENT, (MA)

POTENTIAL VS. DHE, (VOLTS)
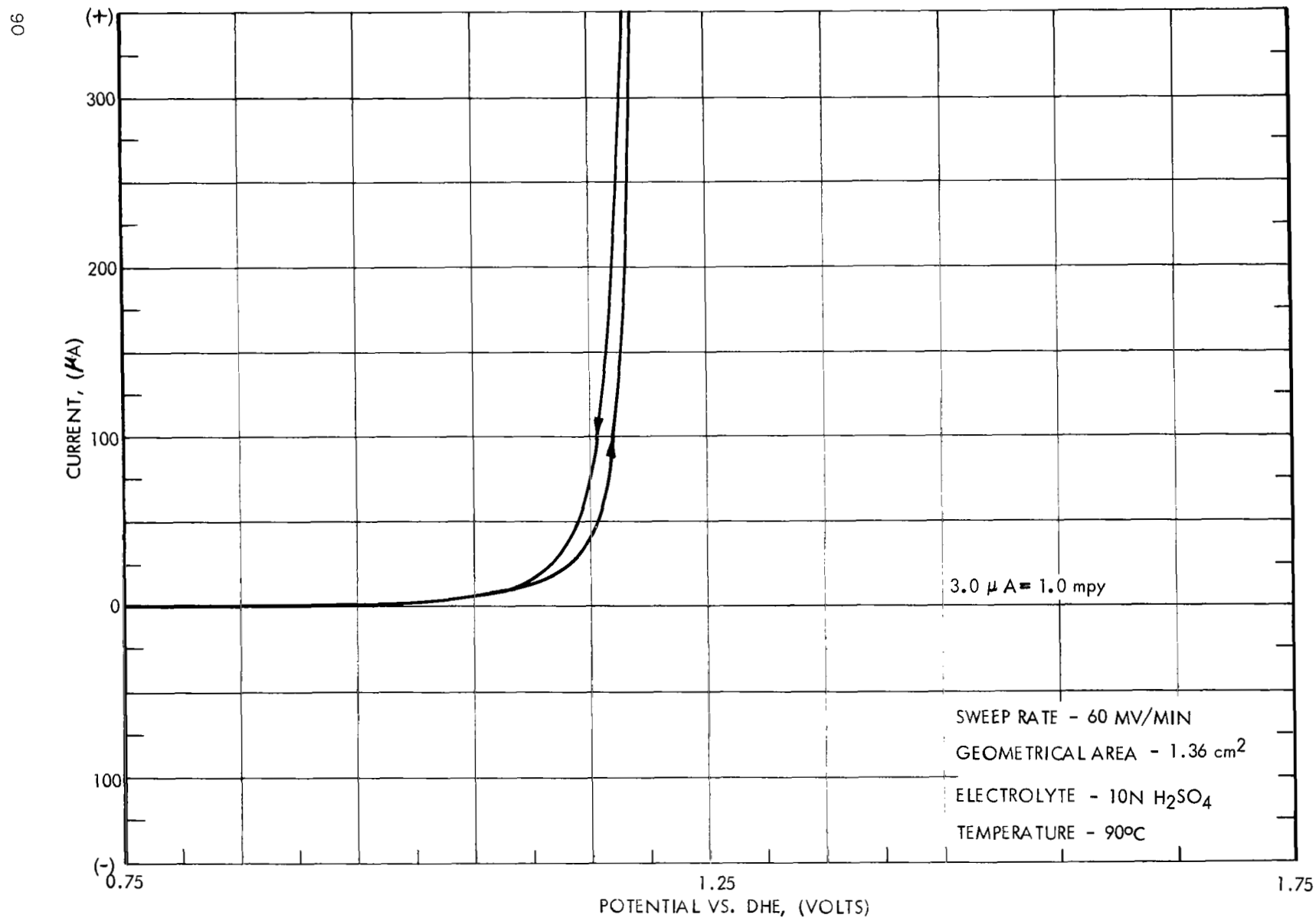
FIGURE 60 POTENTIOSTATIC SCAN FOR NIONEL (INCOLOY) 825/N_2
IN H_2SO_4
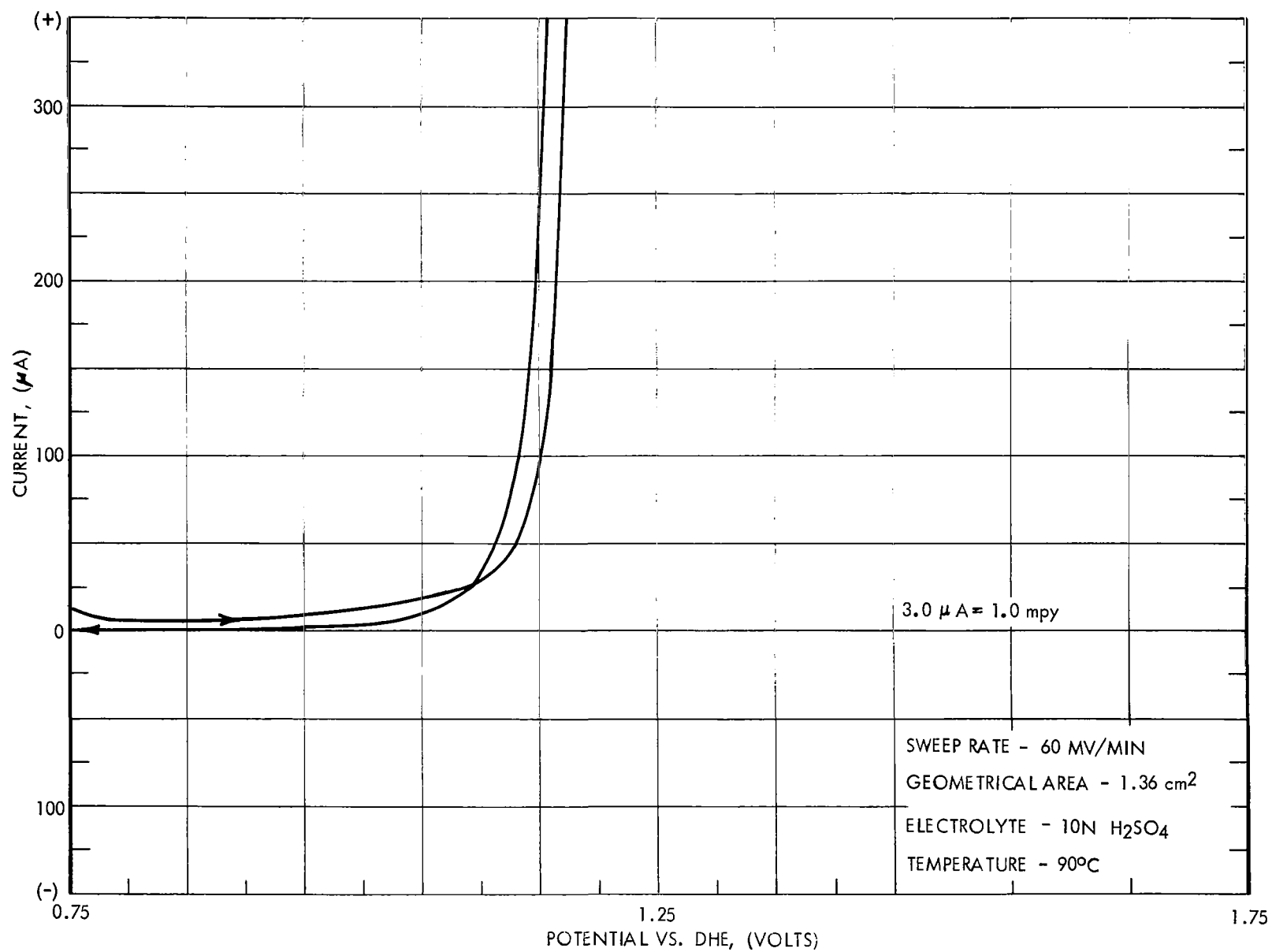
FIGURE 61 POTENTIOSTATIC SCAN FOR NIONEL (INCOLOY) 825/O_2
IN H_2SO_4

CURRENT, (μA)

(+)
300
200
100
0
100
(-)

POTENTIAL VS. DHE, (VOLTS)
0.75   1.25   1.75

3.0 μA = 1.0 mpy

SWEEP RATE – 60 MV/MIN
GEOMETRICAL AREA – 1.36 cm^2
ELECTROLYTE – 10N H_2SO_4
TEMPERATURE – 90°C

3.1.3   Chemical Immersion Testing

This testing consisted of preparing coupons (2" x 2") of the selected metallic materials, conducting pre-test and post-test examinations including measurements of weight, thickness and electrical resistance. Metallurgical examinations of the samples were conducted prior to and following the chemical immersion tests and are described in Section 3.1.4.

Two inch square coupons of the selected materials - Platinum, Zirconium, Titanium and Tantalum - were prepared for chemical immersion testing. Each sample was photographed and measured for weight, thickness, and electrical resistance. Certifications of chemical composition of the materials were provided by the manufacturers and are listed in Table 5.

The test equipment was made available from Contract No. NAS 3-7638 and provided the environmental test conditions necessary for this evaluation. Individual beakers were placed in the compartments of the test apparatus shown in Figure 62. Gas flow rates and beaker water levels were adjusted from the control panel external to the test chambers. Temperatures of the various beaker solutions were indicated by thermometers. The evaporation rates in the humidifiers were low because of the low gas flow rates (in the region of 10 to 15 cc/min) and make-up water was added as required.

Photographs of the sample materials were taken prior to and following the immersion tests. Black and white photographs did not show the fine shades of discoloration observed. This was attributed to the surface lustre of the materials themselves and lighting conditions also were found to accent certain effects. For these reasons the color changes observed are listed in Table 7-Metallic Materials Immersion Test, Data Summary.

3.1.3.1   Resistance Measurements of Metallic Test Specimens

One of several pre and post-test measurements required to describe changes in the nature of the metal as a result of long term exposure is the change in electrical conductivity. The method of measurement which was adopted was based on the following philosophy: a) the intent of the measurement is to determine changes in resistivity due to the formation of surface films as opposed to bulk resistivity measurements, b) due to inherent limitations in sample size dictated by contract, (mainly small thickness 0.004 $\longrightarrow$ 0.04 inch) the absolute value of resistivity is beyond the capability of conventional resistance bridges. As a result the measuring technique is not intended to yield absolute values of resistance but rather relative ones.

Figure 63 shows the test fixture used for resistance measurements. The fixture was constructed from a 3/8 inch thick lucite plate. An oval was removed from the geometric center of the
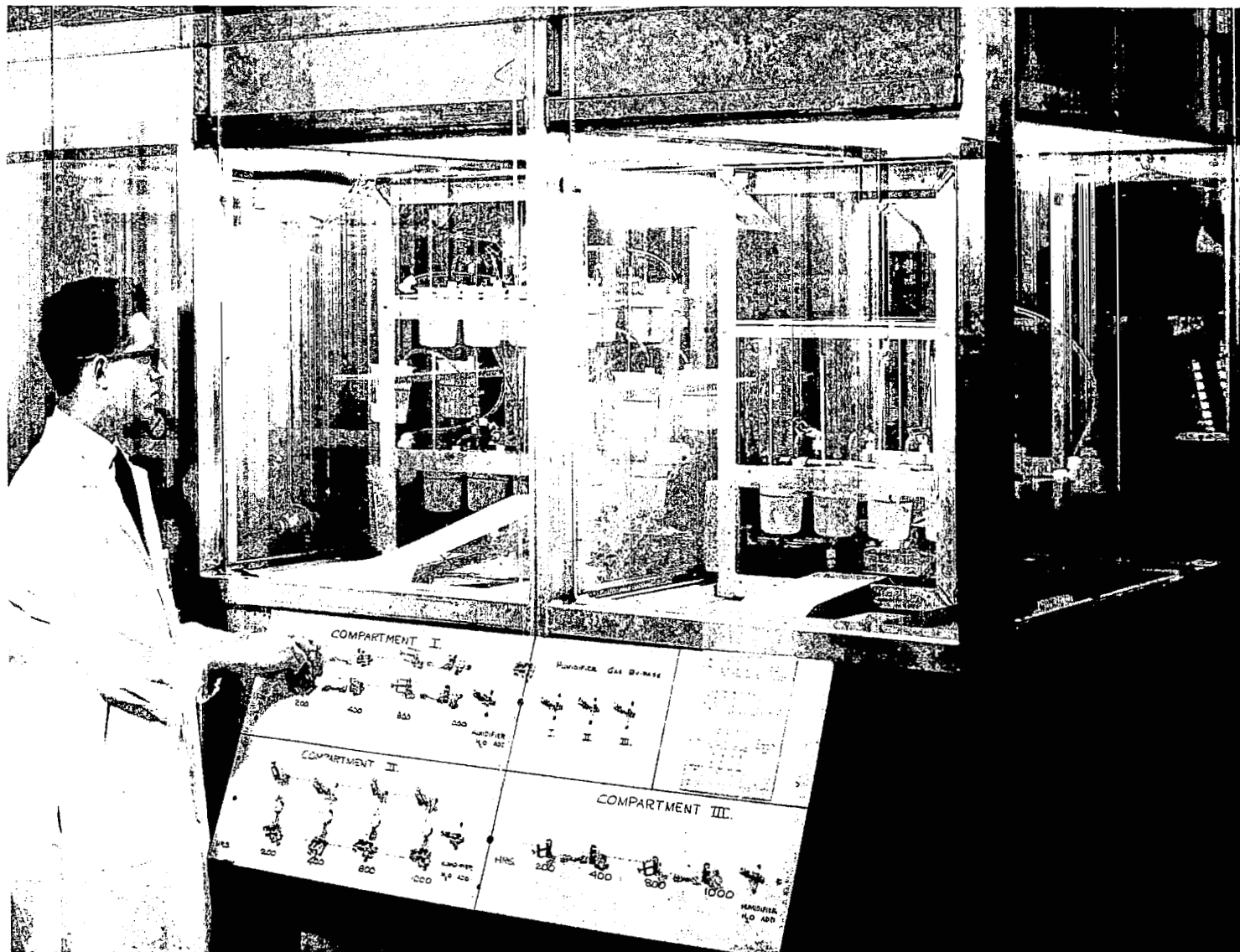
FIGURE 62 CARBONATION CELL SYSTEM, STAGES I, II AND III MATERIALS
ENVIRONMENTAL EXPOSURES TEST STAND

TABLE 7

METALLIC MATERIALS IMMERSION TEST – DATA SUMMARY

Exposure Conditions(1), Test Sample, and Exposure Time	Weight (GR)		Thickness (In.)		(3)Resistance (micro-ohm)	
	Initial	Final	Initial	Final(2)	Initial	Final(4)
(Hrs x 10²)						
I-Pt-2(5)	5.7342	5.7344	0.0043	0.0043	30	50
I-Pt-4	5.7931	5.7941	0.0043	0.0042	32	19
I-Pt-6	5.5391	5.5397	0.0040	0.0040	25	88
I-Pt-10	5.7550	5.7554	0.0041	0.0041	30	45
			0.0042*		29*	
I-Zr-2	14.2601	14.2588	0.0321	0.0319	1485	8.52x10³
I-Zr-4	14.6050	14.6046	0.0319	0.0320	1635	26.79x10³
I-Zr-6	14.5590	14.5573	0.0320	0.0319	1335	23.89x10³
I-Zr-10	14.5100	14.5091	0.0319	0.0319	1635	172.45x10³
			0.0320*		1407*	
II-Pt-2	5.6192	5.6192	0.0040	0.0041	25	45
II-Pt-4	5.7530	5.7533	0.0041	0.0042	30	33
II-Pt-6	2.7562	2.7570	0.0039	0.0038	30	28
II-Pt-10	2.8326	2.8329	0.0041	0.0041	30	55
			0.0040*		29*	
II-Zr-2	14.1848	14.1828	0.0318	0.0318	1235	27.85x10³
II-Zr-4	14.1840	14.1822	0.0321	0.0319	1485	130.45x10³
II-Zr-6	14.6050	14.6027	0.0321	0.0319	1260	179.12x10³
II-Zr-10	14.3970	14.3947	0.0321	0.0320	1185	142.79x10³
			0.0320*		1407*	
II-Ti-2	8.0150	7.8766	0.0278	0.0276	335	6.87x10³
II-Ti-4	8.1190	8.0549	0.0282	0.0277	495	0.97x10³
II-Ti-6	8.0976	8.0093	0.0282	0.0276	505	6.14x10³
II-Ti-10	8.1030	7.9264	0.0281	0.0275	455	0.65x10³
			0.0281*		473*	
III-Ta-2	24.4610	24.4597	0.0224	0.0222	2685	119.95x10³
III-Ta-4	23.9630	23.9619	0.0218	0.0218	2335	134.79x10³
III-Ta-6	24.3429	24.3420	0.0223	0.0222	2710	238.60x10³
III-Ta-10	24.4795	24.4784	0.0220	0.0223	2335	333.12x10³
			0.0221*		2541*	

(1) See Table I for exposure test conditions.
(2) Average value for five measurements.
(3) Cross Sectional area of contact element
    = 0.0156 in² (1/8 in. sq)
(4) Average values for three (3) measurements
(5) Designation for Platinum sample tested
    for 200 hours at exposure 1 conditions.

Visual Observation				Per Cent Change		Change Micro-Ohms
Metal		Solution				
Initial	Final	Initial	Final	Weight	Thickness	Resistance
Silvery bright finish	No change No change No change No change	Clear Clear Clear Clear	No change No change No change No change	0.004 0.017 0.011 0.007	-2.3 -2.0 No Change No Change	20 -13 63 15
Silver white to gray finish	Whiter cast Lt Br cast Lt Br cast Gld Br cast	Clear Clear Clear Clear	No change No change No change No change	-0.009 -0.003 -0.012 -0.006	-0.62 0.31 -0.31 No Change	7.03x10³ 25.15x10³ 225.50x10³ 170.82x10³
Silvery bright finish	No change No change No change No change	Clear Clear Clear Clear	No change No change No change No change	0.000 +0.005 +0.029 +0.011	2.5 2.4 -2.6 No Change	20 3 - 2 25
Silver white to gray finish	Whiter cast Whiter cast Lt Br cast Lt Gy cast	Clear Clear Clear Clear	No change No change No change No change	-0.014 -0.013 -0.016 -0.016	No Change -0.62 -0.62 -0.31	26.62x10³ 128.97x10³ 177.86x10³ 141.60x10³
Silver gray dull finish	Yl-Br cast Brown cast Bl Blk Gy Blk	Clear Clear Clear Clear	No change No change No change No change	-0.354 -0.790 -1.090 -0.945	-0.72 -1.8 -2.1 -2.1	6.53x10³ 0.48x10³ 5.63x10³ 0.19x10³
Metallic gray marble finish	No change No change No change No change	Clear Clear Clear Clear	No change No change No change No change	-0.005 -0.005 -0.004 -0.004	-0.89 No Change -0.45 1.4	112.27x10³ 132.45x10³ 235.88x10³ 330.78x10³

NOTE:
   *Average value for the four measurements

Bl	-	Blue	Gy	-	Gray
Blk	-	Black	Gld	-	Gold
Br	-	Brown	Lt	-	Light
Gn	-	Green	Yl	-	Yellow

plate. A 1/4 inch slot at one end of the plate (forming two jaws) allows for test sample mounting between the silver test electrodes. Variable compression was applied through the test fixture jaws to the test samples between the electrodes. The silver test electrodes (1/8 inch square) were secured to the jaw plates by set screws.

A General Electric Kelvin double bridge was employed for the test measurements. The minimum resistance capability of the instrument is 100 micro-ohms and the minimum resolution (smallest dial division) is 5 micro-ohms. The dial readout is linear so that the 5 micro-ohms resolution applies up to the maximum dial reading.

The General Electric Company bridge was checked by running a known current through a piece of 1/8 inch x 1/8 inch silver bar 22 inches long and measuring the voltage between two points 20 inches apart. A voltage drop of 10.2 millivolts was measured with a John Fluke voltmeter with 10.0 amps flowing through this silver bar. Thus, the bar had a resistance of 51 micro-ohms. This compares well with the calculated value of 41 micro/ohms for a pure silver square bar at 20°C since the test bar did not appear to be perfectly square. The bridge was then used to measure various sections of the silver bar for comparison purposes and correlations were excellent.

The silver test electrodes were butted together to determine the base line resistance of the test assembly. This was found to be 215 x 10^{-6} ohms. This resistance was a composite of the contact resistance of the silver electrode to the silver electrode and the resistance of the silver electrodes themselves.

The test metal samples were cut from 2 inch wide foil using a squaring shear. The nominal dimensions of the test samples were 2 inches square. The individual sample thickness was obtained with a micrometer and are listed in Table 7. The metals were washed in a train of organic solvents terminating in a distilled water rinse and air dried. Subsequent handling of the samples was carried out using plastic gloves. The test samples were placed in the test fixture and slightly compressed between the silver test electrodes. The resistance was then noted as a function of increasing compression.

3.1.3.2   Conclusions

Examinations conducted on the metallic material samples before and after the chemical immersion tests included measurements of weight, thickness and resistance of the metals and also visual observations of the metals and the test solutions. The prior and post test measurement data and visual observations are summarized in Table 7.

Silver Test
Electrode

Test
Sample

Silver Test
Electrode
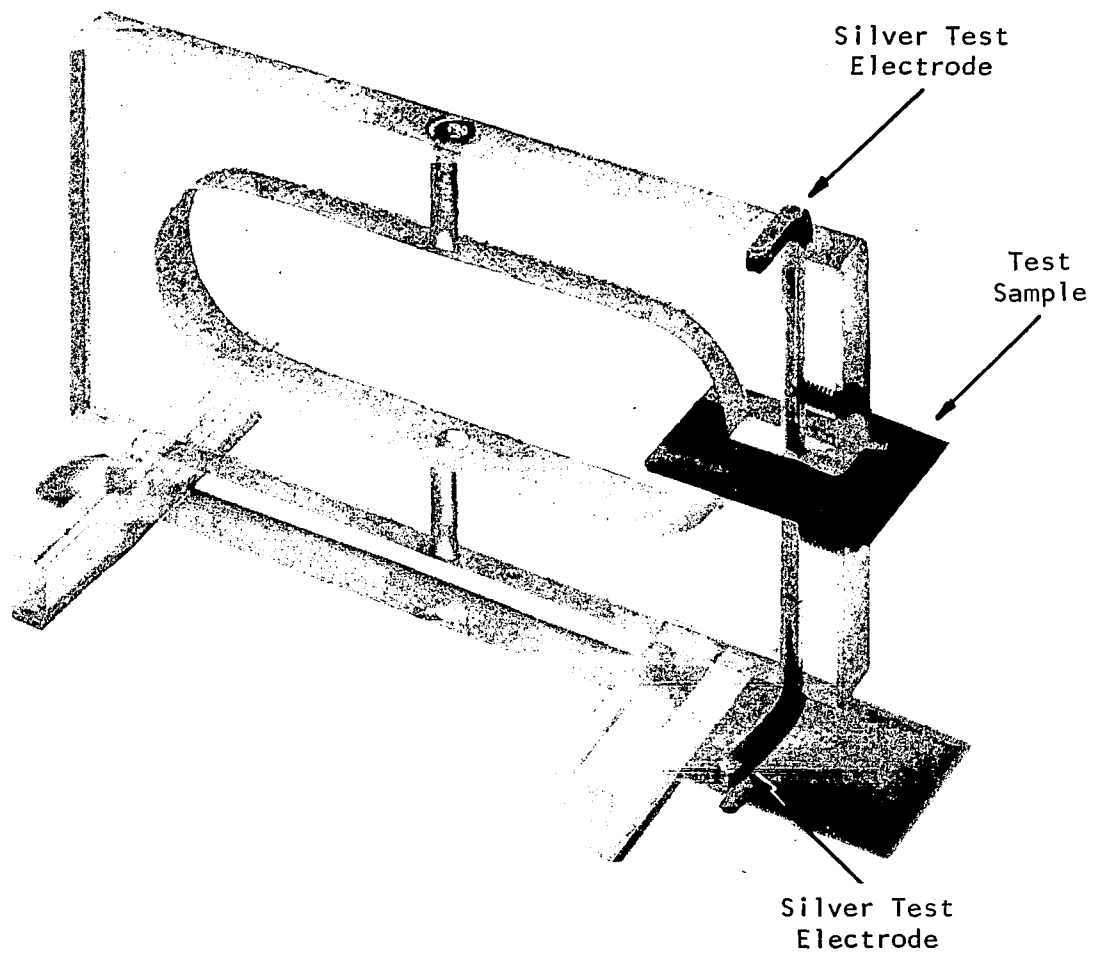
FIGURE 63 RESISTANCE MEASURING TEST FIXTURE – METALLIC MATERIALS

Weight

The net gain or loss of weight of the individual sample materials exposed to the Stage I, II and III test conditions was less than 0.03 percent except for Titanium (Exposure II) which had a loss of 1.09 percent for the 600 hour test specimen.

The Titanium 1,000 hour test sample (Exposure II) showed a 0.945 percent loss. It was observed that the maximum gain or loss for all the other samples usually occurred at the 400 or 600 hour test points. Zirconium showed the same weight loss(0.016 percent) at the 600 hour point and the 1000 hour point in the Stage II exposure. Platinum was the only material to show a weight increase, which was very slight, approximately 0.017 percent maximum and this occurred in both the Stage I and Stage II exposures.

Thickness

Thickness measurements were made to 1×10^{-4} inches. The maximum recorded change was a loss of 2.6 percent for platinum at 600 hours in Stage II exposure. The percent change of thickness in all cases was of the same order as the accuracy of the readings. Since the maximum percent change did not exceed the accuracy of the readings it is concluded that no change in thickness occurred during the 1000 hour immersion tests.

Resistance

Platinum exhibited the least change in resistance in both Stage I and Stage II alkaline exposures. The average value for this change was approximately 25 micro ohms. The other materials exhibited much larger increases varying from 2×10^3 to 300×10^3 micro ohms. Data obtained for zirconium for both Stages I and II exposures showed comparable changes for the same test durations. It should be noted that the maximum change in both the Stage I and Stage II exposures for zirconium occurred at the 600 hour test time. Titanium results were cyclic also. The 400 hour and 1000 hour values were lower than the 600 hour data.

Tantalum resistance data indicate an almost linear increase in resistance with time after the 200 hour point with a 330×10^3 mirco ohm increase in 1000 hours.

3.1.4   Metallurgical Examinations

Metallurgical examinations of the samples of platinum, titanium, zirconium and tantalum, which were subjected to the chemical immersion tests in accordance with Table 1, were conducted by the TRW Materials Laboratory. Samples in the "as received" condition (blank) were used for comparison purposes. The alkaline and acid test solutions were presented for chemical analyses in conjunction with these examinations. The findings from the various tests conducted are summarized as follows with tabulated data shown in Table 8.

3.1.4.1 X-Ray Diffraction

X-ray diffraction analyses were conducted with Ni - filtered Cu K radiation. The diffraction patterns covered the angle 2θ range from $20°$ to $60°$, which corresponds to "d" spacings of 4.44A to 1.54A. Each of the materials was examined in both the "as received" (blank) and the 1000 hour exposure conditions. The tantalum and platinum samples were unaffected by the immersion tests, but the II-Zr-10 hour sample, and all four titanium samples showed some change. The II-Zr-10 hour pattern showed a single, small peak at 2.36A which was undetectable in the specimens with less exposure. No identification could be made on the basis of this single line, though it is indicative of a surface film. The titanium series showed two additional lines; one at 1.56A and the other at 2.20A. In general, the line intensities increased with exposure time. These lines could not be identified by the standard ASTM card index, indicating that there was only an epitaxial thin film present after so short an exposure.

3.1.4.2 Emission Spectroscopy

An ARL 2-meter spectrograph was used to examine the 30% K_2CO_3 and 10N H_2SO_4 test environment solutions. The carbonate solutions showed traces of boron and silicon which were attributed to contamination from a borosilicate glass gas-bubbler. The amount of titanium in solution increased linearly with time for the titanium II exposure, Figure 64. The 10N H_2SO_4 solution used to test the tantalum showed traces of iron, which is a normal trace impurity for H_2SO_4.

3.1.4.3 Electron Microprobe Analyses

X-ray fluorescence microprobe scans were made on each of the 1000 hour test samples and their corresponding unused blanks. A one micron diameter beam was used to sweep the surface of the samples and a low intensity incident beam (5 Kev) was used so that the surface film could be better evaluated. The results of both carbon and oxygen analyses are shown in Table 8. In all samples analyzed, with the exception of the tantalum, the results show that there was more carbon on the unused blank samples than there was on the corrosion-tested samples. Similarly, with the exception of platinum, there was a significantly greater amount of oxygen present on the surface of the corrosion tested samples compared with the blank samples.

It is not possible to give a more quantitative analysis for the amounts of each element present without conducting a more extensive investigation with some equipment modification. However, the relative values observed are fairly accurate because there was little background interference at the low voltage at which these samples were examined.

TABLE 8

SUMMARY OF METALLURGICAL EXAMINATION RESULTS

Sample and Exposure	Spectrographic Soln. Anal. (ppm)	X-Ray Diffraction Results	X-Ray Fluorescence Microprobe Results (relative inten. units)	
			Carbon	Oxygen
Pt Blank	N/A	Std. Pt Pattern	71	6
I-Pt-2 I-Pt-4 I-Pt-6 I-Pt-10	Same analysis all Solutions 1-10 Silicon 1 Boron	Same as Blank	27	3
II-Pt-2 II-Pt-4 II-Pt-6 II-Pt-10	(Same as above)	Same as Blank	40	3
Zr Blank	N/A	Std. Zr Pattern	395	12
I-Zr-2 I-Zr-4 I-Zr-6 I-Zr-10	Same Analysis all Solutions 1-10 Silicon 1 Boron	Same as Blank	58	26
II-Zr-2 II-Zr-4 II-Zr-6 II-Zr-10	(Same as above)	line at d = 2.36A	94	20
Ti Blank	N/A	Std. Ti Pattern	125	6
II-Ti-2 II-Ti-4 II-Ti-6 II-Ti-10	Ti* 50 100 500 900	Line at d = 1.56A 10 36 relative 11 intensity 44	53	11
Ta Blank	N/A Fe**	Std. Ta Pattern	19	3
III-Ta-2 III-Ta-4 III-Ta-6 III-Ta-10	1 <1 <1 10-12	Same as Blank	22	7

*Detection Limit of Ti Better than 1 ppm in 30% K_2CO_3
**Detection Limit of Fe better than 1 ppm in 10N H_2SO_4

3.1.4.4 Metallographic Examination

Metallographic examinations were performed on the 1000 hour test samples and on the corresponding "as received" (blank) samples at 100X and 250X magnification. There was no real difference between the blank and the corrosion tested samples. Typical microstructures of these specimens at 250X magnification are shown in both the unetched and etched conditions in Figures 64 through 80. There are pits on some of the Tantalum and Zirconium specimens which are a result of the surface preparation and etching procedures. They can be removed by additional polishing but only at the expense of sharp edge definition.

3.1.4.5 Bend Tests

Bend tests were performed on the II-Ti-10, I-Zr-10 and the II-Zr-10 test samples and their respective blanks to determine if the exposed samples had been embrittled during corrosion testing. The tests were performed by 3-point loading, using pins of 0.125 inch radius set at a 0.6 inch span, and a probe of 0.09 inch radius. There was no visible cracking observed after a greater-than-90° bend in the titanium and virtually no difference between the blanks and the exposed samples. All the zirconium samples showed visible cracks at angles less than 30°. The differences between the exposed zirconium samples could be due to an inhomogeneous starting material rather than being attributable to the difference corrosive environments. The results are listed in Table 9.

3.1.4.6 Conclusions

The test samples of platinum, titanium, zirconium and tantalum which had been exposed for 1000 hours to the corrosive environments shown in Table 1 indicate almost negligible corrosion rates as determined by the metallurgical examinations above.

The only evidence of corrosion was the appearance of thin films on all the 1000 hour specimens (detected only by visual examination), and the presence of titanium in its test solution. Estimated film thicknesses are in the region of one micron based on the Electron microprobe tests.

TABLE 9

BEND TEST RESULTS

Sample No.	Bend Angle After Spring Back (deg.)	Peak Load Deflection (In.)	Flexural Modulus in Bending (x10^6 psi)	Flexural Strength (Ksi)
Ti Blank	96	0.157	14.92	200.5
II-Ti-10	101	0.150	14.27	200.4
Zr Blank	26	0.063	12.62	193.9
I-Zr-10	28	0.088	12.82	200.0
II-Zr-10	17	0.058	12.94	188.9

Flexural Modulus $= \dfrac{L^3}{4\,b\,d^3}\ \dfrac{P}{Y}$ psi,

Flexural Strength $= \dfrac{3PL}{2\,b\,d^2}$ psi,

Where:
L = span, in.
b = width, in.
d = thickness, in.
P = load, lb
Y = deflection, in.
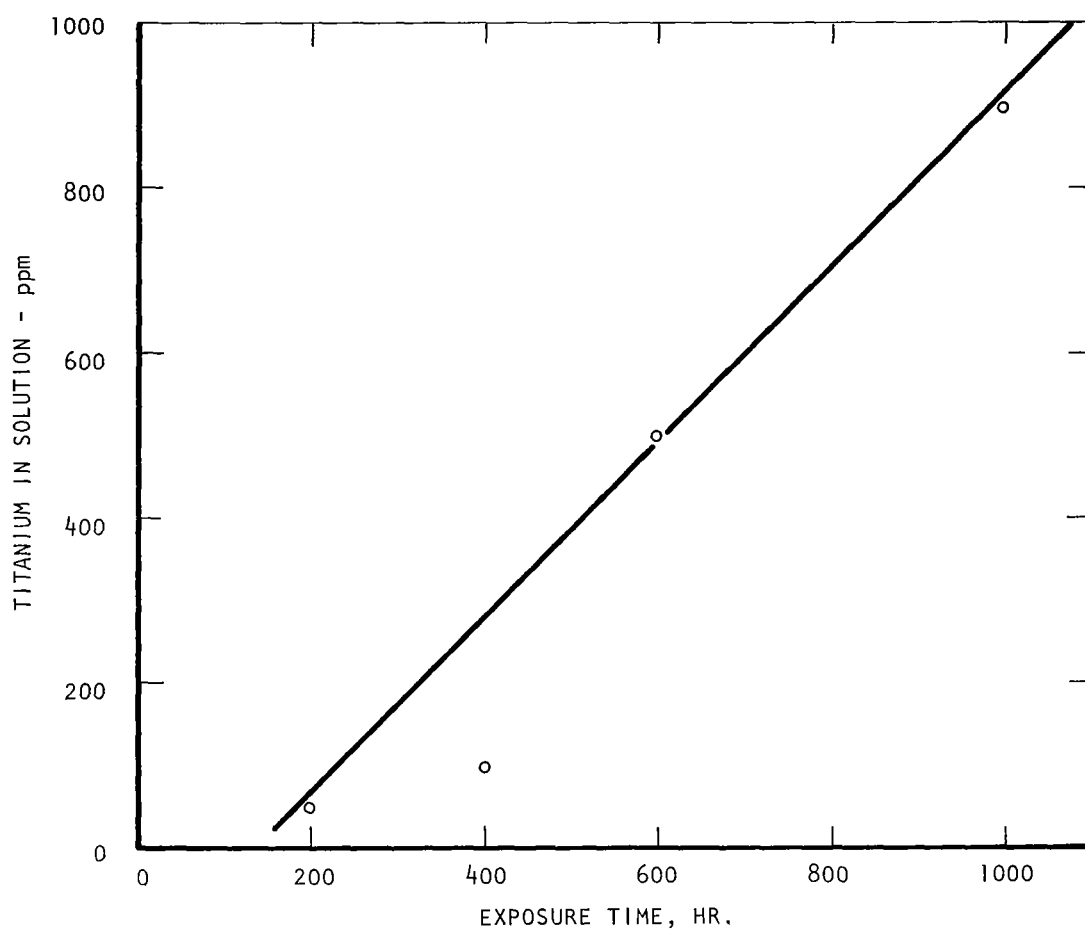
FIGURE 64 RESULTS OF SPECTROGRAPHIC ANALYSIS OF TITANIUM
IN 30% K_2CO_3 SOLUTION

Figure 65   Photomicrograph - Zirconium Blank - Unetched, 250X
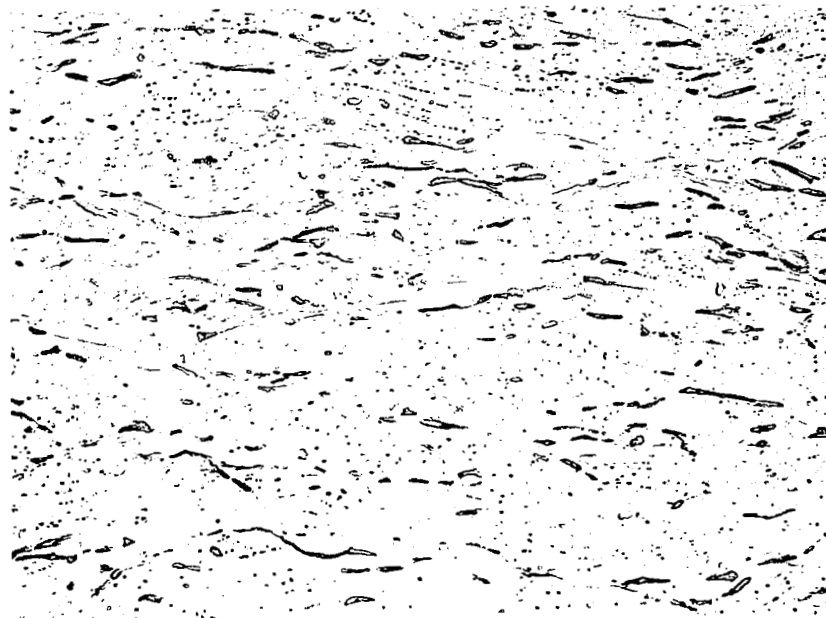
Figure 66   Photomicrograph - Zirconium Blank - 250X

104

Figure 67   Photomicrograph - Platinum Blank - 250X
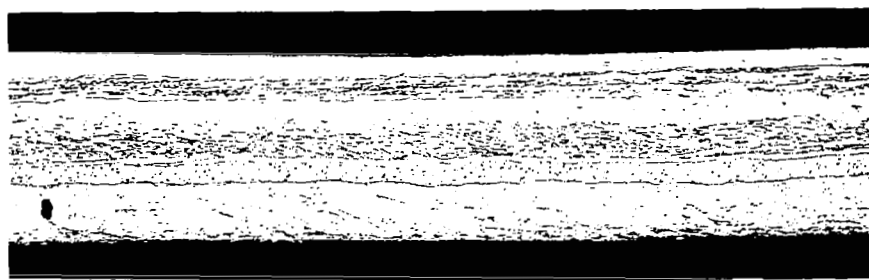
Figure 68   Photomicrograph - Platinum - (II-Pt-10), 250X

Figure 69   Photomicrograph - Zirconium - Unetched
             (I-Zr-10), 250X
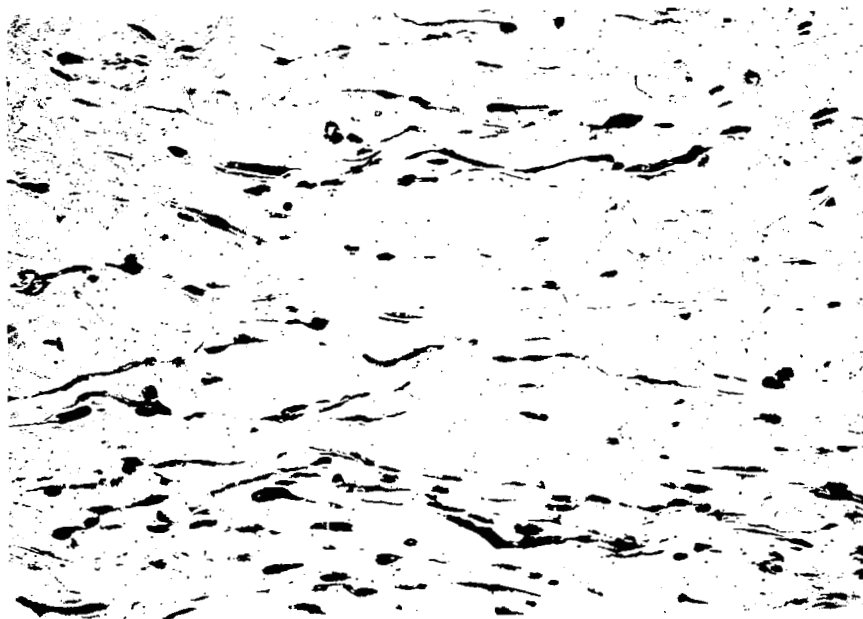
Figure 70   Photomicrograph - Zirconium - 250X

106

Figure 71   Photomicrograph - Zirconium - Unetched
(II-Zr-10), 250X
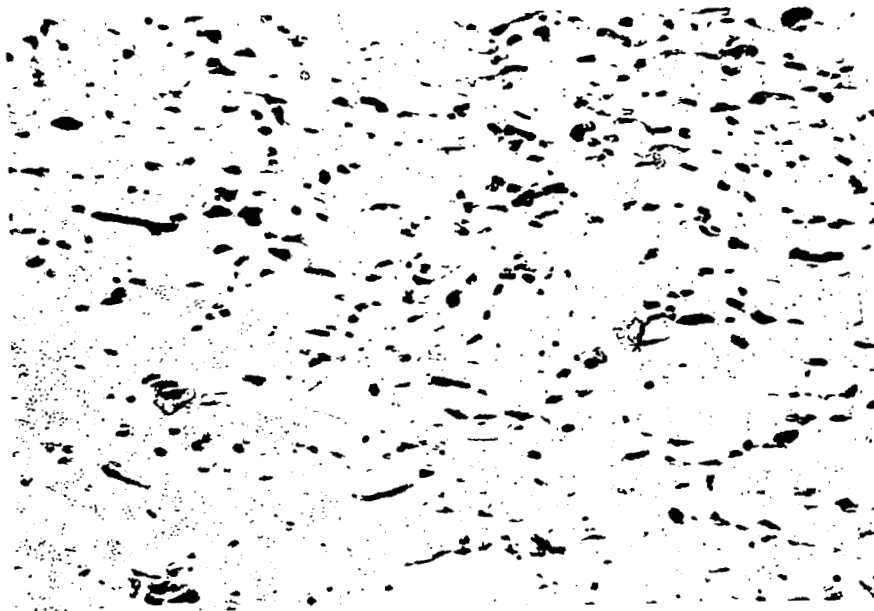
Figure 72   Photomicrograph - Zirconium (II-Zr-10), 250X

Figure 73   Photomicrograph - Titanium Blank - Unetched, 250X
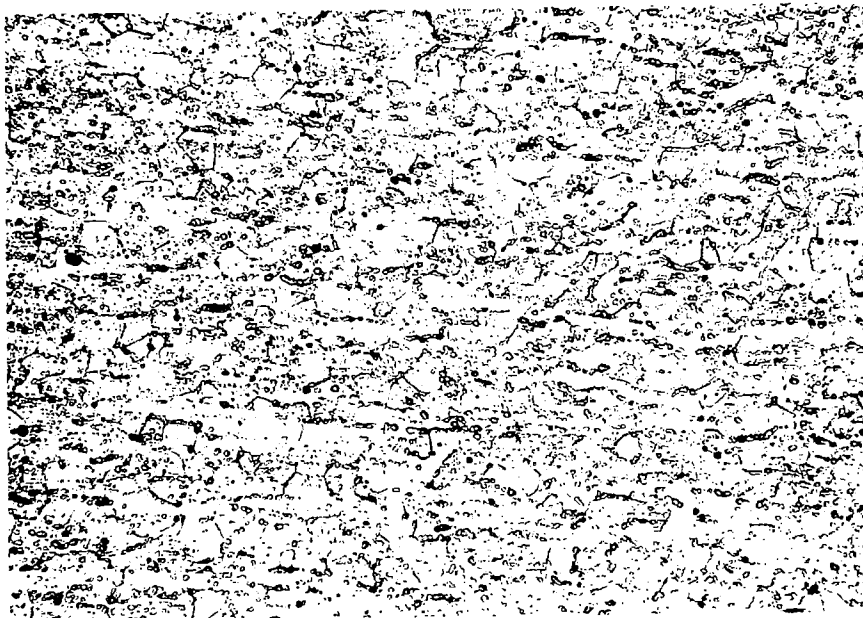
Figure 74   Photomicrograph - Titanium Blank - 250X

Figure 75   Photomicrograph - Titanium - Unetched
             (II-Ti-10), 250X
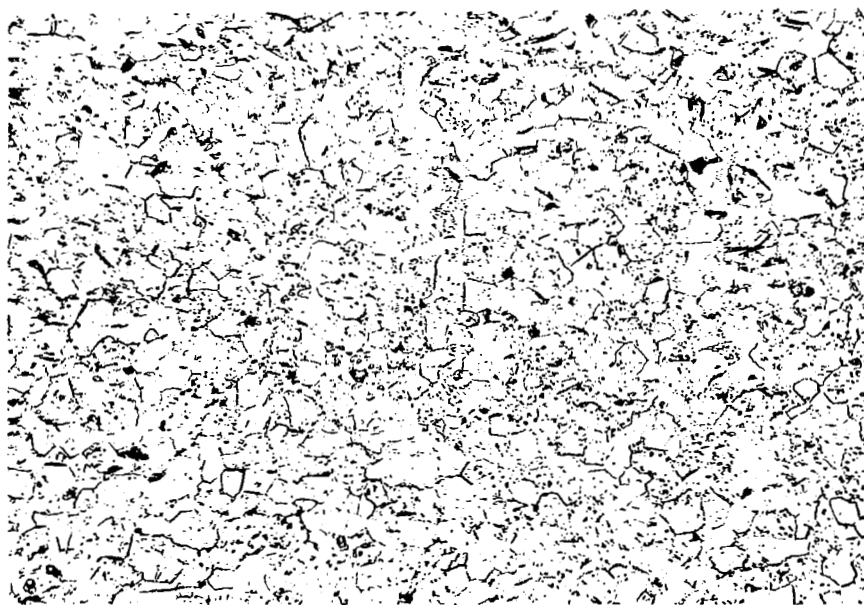
Figure 76   Photomicrograph - Titanium (II-Ti-10), 250X

Figure 77   Photomicrograph - Tantalum Blank - Unetched, 250X
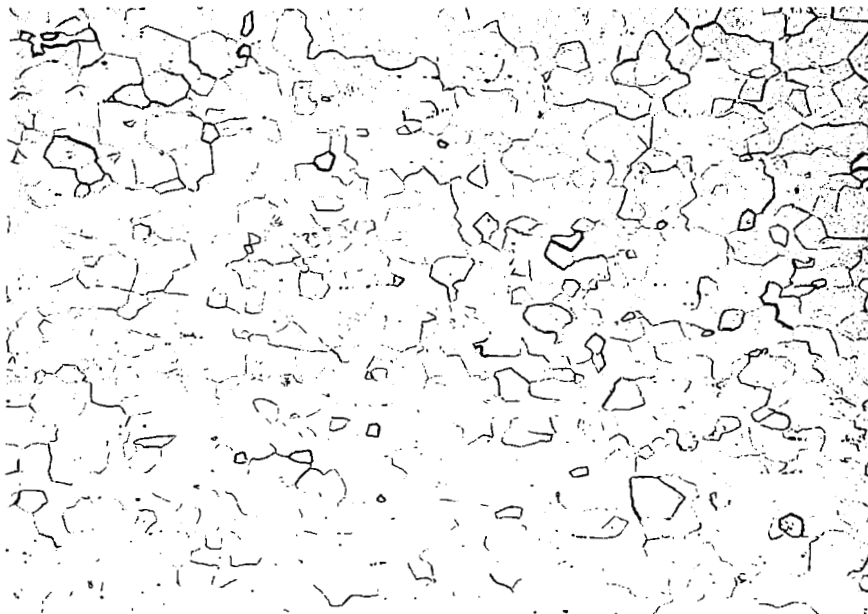
Figure 78   Photomicrograph - Tantalum Blank - 250X

110

Figure 79   Photomicrograph - Tantalum - Unetched
             (III-Ta-10), 250X
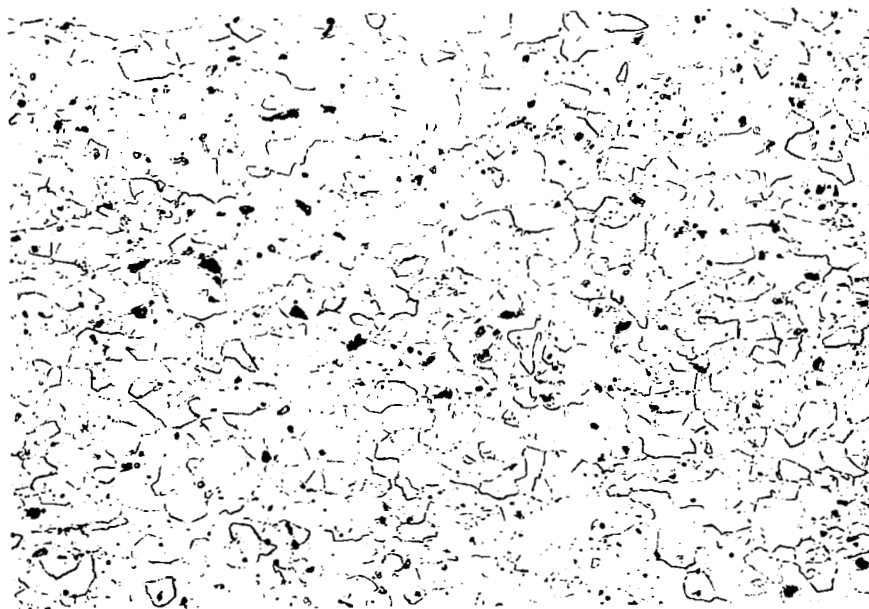
Figure 80   Photomicrograph - Tantalum (III-Ta-10), 250X

111

3.2 Acid Matrix Evaluation

This phase of the program consisted of selecting matrix materials from the variety of preparations commercially available. The program plan required the selected samples to be tested to determine the most suitable candidate material.

The matrices are required to provide long operational life, eventually in excess of 10,000 hours at 195°F in sulphuric acid of 38% weight concentration. The properties of major interest which were evaluated are:

1) Chemical compatibility with the electrolyte - this includes survival of the matrix and stability of dimensions and selected properties.

2) Void Volume

3) Bubble pressure when saturated with electrolyte at 195°F.

3.2.1 Materials Review and Preliminary Screening

A review of the trade journals and the vendors' literature yielded the following list of materials that may serve as matrices and includes filters, battery electrode separators and porous mats. A brief description of the material characteristics relating to the application follows for the materials listed below.

Material	Manufacturer
Glass Fiber Filter	Reeve Angle & Company
Refrasil-Silica fiber	HITCO
Polysep	National Lead Company
Kynar	Gelman Instrument Company
Daramic	Dewey & Almy - W. R. Grace Company
Polypropylene Felt	American Felt Company
Polypropylene Felt	Kendell Fiber Products
Microporous Teflon	General Plastic Corporation
Zitex-Microporous Teflon	Chemplast, Inc.
Microporous Teflon TA-1 Mat	American Cyanamid Company
Ace Sil	Amerace Corporation
Polymeric Gel Membrane	Amicon Company
Armalon	duPont

Glass Fiber Filter (H. Reeve Angle & Company)

This material has the wetting properties desired, but is attacked by mineral acids, leaving a fiber structure that is essentially silica.

112

Refrasil (H. I. Thompson & Company - HITCO)

Refrasil is pure silica fiber mat. It is a very loosely packed mat, but the fibers are strong and will survive compaction. The fibers are essentially wettable by sulfuric acid and are inert. It was initially believed that the fibers might undergo gradual reversion to the stable crystalline state and lose its fibrous structure while immersed in hot sulphuric acid, but this was disproved by the tests.

Polysep (National Lead Company)

This was described by the vendor as a mat of polyethelene-coated cellulose fiber with 30% porosity and 30 micron Because of the low softening temperature of the polyethylene and the reactivity of cellulose, this material was judged unsuitable.

Kynar (Gelman Instrument Company)

Kynar is described as a felt of polyvinylidine fluoride. It is chemically resistant to sulfuric acid, but is strongly hydrophobic and therefore unsuitable.

Daramic (Dewey and Almy Chemical Div W.R. Grace Company)

Daramic is a rolled sheet of microporous polyethylene. It absorbs acetone readily, but is completely hydrophobic. The specified test temperature (195°F) is above the failure temperature of Daramic.

Polypropylene Felt (American Felt Company)

This felt wetted readily, but the effect is due to a fiber coating of surfactant. The clean fibers are hydrophobic and therefore unsuitable.

Polypropylene Felt (Kendall Fiber Products Div.)

The mat is composed of 1 denier fibers, perforated by felting needles. The vendor claims good performance in sulfuric acid, but the hydrophobic quality and the felting punctures were expected to cause a low bubble pressure and were later verified in test.

Microporous Teflon (General Plastics Corporation)

This is a rolled sheet material that can be produced in a variety of thicknesses (10 to 50 mils), porosites (50, 67, 75%), and pore sizes (1, 4 or 10 microns). However, the material is inherently hydrophobic and therefore unsuitable.

113

Zitex - Microporous Teflon (Chemplast, Inc.)

Zitex Teflon is inherently non-wetting but can be rendered wetting by a surface etching treatment. Since the wetting condition of the Teflon surface is only metastable, it is therefore considered undesirable.

Microporous Teflon TA-1 (American Cyanamid Company)

The vendor describes the Ta-1 mat as composed of etched Teflon 95% and unetched Teflon 5%. It is useful in phosphoric acid electrolyte, but sulfuric acid being an oxidizing agent, causes dewetting.

Ace Sil (Amerace Corporation)

This is a porous rubber sheet, loaded with silica. It is not compatible with hot sulfuric acid.

Polymeric Gel Membrane (Amicon Company)

This material was not commercially available when the testing program began, but is now obtainable in limited quantity. It is described as a very hygroscopic gel membrane, stable in sulfuric acid at 200°F, and with excellent electrolytic conductivity.

Armalon (duPont)

This name is applied to felts and woven fabrics, the fibers of which are coated with Polytetrafluroethylene (PTFE). Since the PTFE coating is permeable, chemical resistance is essentially that of the core material. It is very hydrophobic.

From the above list of materials, four samples listed below were recommended for preliminary testing. Only the Refrasil was judged to be suitable for use, however, three other samples were selected for the preliminary evaluation.

1) Refrasil - Silica Fiber (Hitco)

2) Kynar - Polyvinylidine Fluoride Felt (Gelman Instrument Company)

3) Polypropylene Felt - (Kendall Fiber Products)

4) Microporous Teflon TA-1 Mat - (American Cyanamid Company)

3.2.2 Matrix Screening and Physical Properties Measurements

Tests of these four materials immediately revealed the unsuitability of the latter three. Non-wetting and capillary exclusion

of electrolyte from the pores of the Kynar, polypropylene felt, and microporous Teflon caused very low bubble pressures as shown in Table 10. Thus, only the Refrasil remained a candidate for performance testing. It was decided at this point to include the ACCO-TA-1 matrix in the immersion test because of its higher bubble pressure despite the expectation that it would gradually loose its hydrophylic property during contact with sulfuric acid. The tests confirmed this expected change, however, the Ta-1 mat bubble pressure was still acceptable at the end of the 1000 hour immersion.

The matrix properties to be measured are void volume, bubble pressure, and electrolytic resistance.

3.2.2.1 Void Volume

The fractional void volume is obtained from the absolute density of the solid phase and the measured geometric density of the specimen

$$\frac{\text{void volume}}{\text{total volume}} = 1 - \frac{\text{geometric density}}{\text{absolute density}}$$

An attempt was made to use the air comparison pycnometer for determination of absolute density of the specimens, but it was found that the broad range of values obtained from specimen to specimen indicated that the instrument was not sufficiently sensitive relative to the specimen sizes. It was decided to accept the published average of values of absolute density of the materials as being more reliable than the values derived from the air pycnometer.

Determination of geometrical density is uncertain because of the softness of some of the matrices. Refrasil, for example, is a very loosely packed fibrous mat, and the measured thickness of a specimen is dependent on the pressure applied by the measuring instrument. For the test measurements, a dial gage was used which was fitted with a one-half inch diameter foot and loaded only by the weight of the spindle and a light return spring. The recorded thickness of this kind of material should therefore be accepted as only one of a range of values the matrix may assume depending on the pressure applied.

In Table 10, the Refrasil specimen is described as being 0.08 inch thick. The computed geometric density of 0.096 gm/cm³, and the void volume is 95.3%. If the same specimen is compressed to 0.04 inch thickness, the geometric density becomes 0.192 gm/cm³, and the void volume is 90.6%.

Of the materials listed in Table 10, the Refrasil and the polypropylene felt are easily compressible. The metricel VF-6 is a microporous film and is practically incompressible.

The Ta-1 mat is composed entirely of Teflon and as supplied by the vendor, it is completely water impregnated. The void volume of this material was computed from the measured geometric density and the known densities of the Teflon and the water filling the voids.

Void volume measurements were to be made on the specimens, as received, and also after 200 hours, 400 hours, 600 hours and 1000 hours immersion in 38% sulfuric acid at 195°F. These measurements were completed for the specimens of Refrasil and are reported with the reservation that they are of dubious significance because of the almost arbitrary assignment of thickness.

The specimens of TA-1 matrix could not be measured for void volume after the immersion tests because the specimens became distorted and the laminates separated to form irregular pockets filled with electrolyte. There was also evidence of partial dewetting of the matrix. Photographs in Figure 81 show samples of the TA-1 matrix material in the "as received" condition (A) and after 1000 hour immersion test (B), where the "pocket effect" is evident.

3.2.2.2   Bubble Pressure

Gas sealing capabilities of the matrices were to be measured in 38% sulfuric acid at 195°F. Specimens were mounted in a holder made from polyvinyldichloride plastic as shown in Figure 82. A disk of fine mesh polypropylene screen at the bottom of the specimen cavity was used to support the specimens against the impressed gas pressure differential. The specimen was placed on the screen, and then was clamped at the periphery by the mating part of the holder so that gas passing through the specimen issued through the four bottom holes. The holder was partly submerged in the hot sulfuric acid and permitted to attain temperature. Air under gradually increasing pressure was admitted through the metal tube until escape through the bottom holes was observed.

Measured values of bubble pressure for "as-received" specimens are recorded in Table 10. Refrasil and TA-1 are the superior materials.

3.2.2.3   Electrolytic Resistance*

The resistance was measured with electrolytic current of 50 ASF passing through the specimen. The test apparatus which was made from Teflon is shown schematically in Figure 83. It provides chambers for the electrolyte and working electrodes, and

---

*J. E. Cooper, A. Fleishcer: "Characteristics of Separators for Alkaline Silver Oxide-Zinc Secondary Batteries - Screening Methods," p. 53, AD-447301 Aeropropulsion Laboratories, USAF, WPAFB Dayton, Ohio, September, 1964.
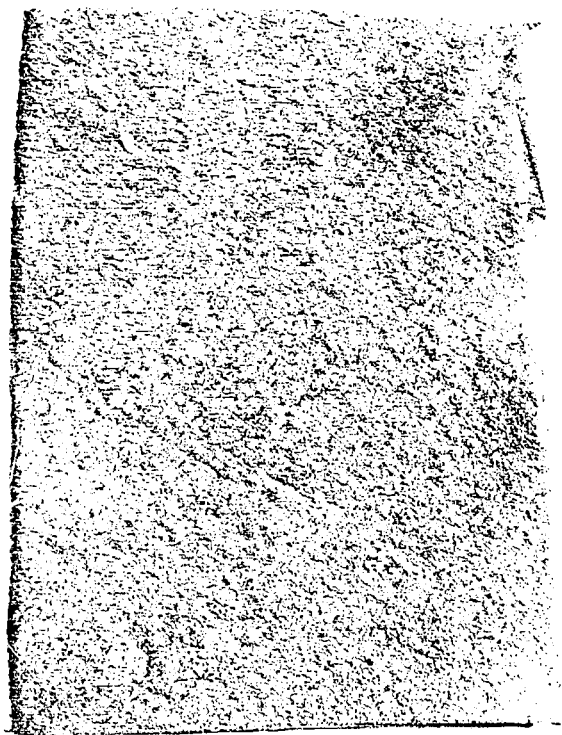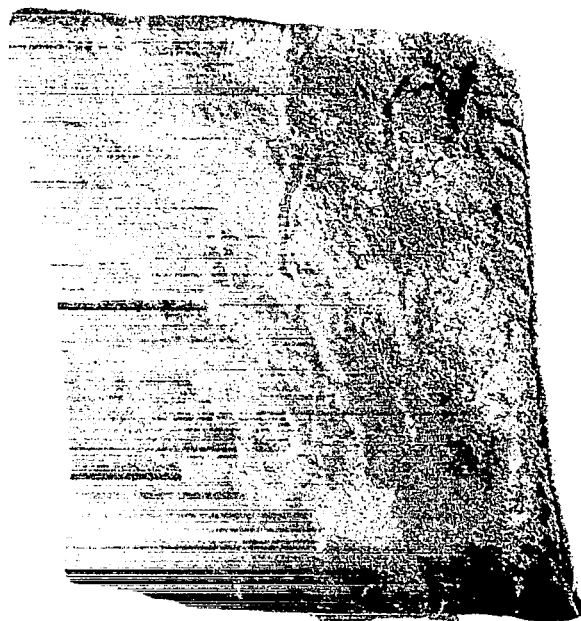
(A)   (B)

A - AS RECEIVED

B - AFTER 1000 HOURS IN 38% H_2SO_4 AT 195°F

**Figure 81   Acid Electrolyte Matrix - Microporous Teflon
TA-1 Mat (Before and after exposure to acid
electrolyte)**
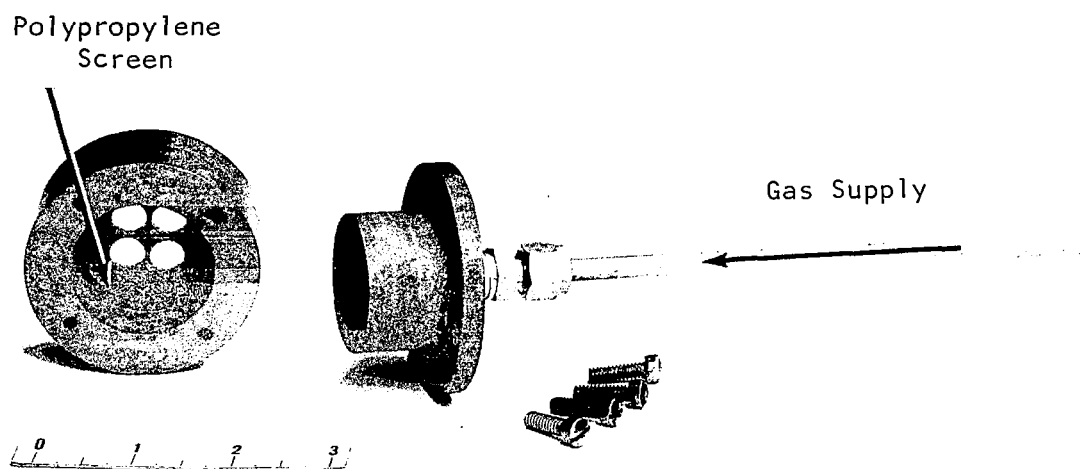
Figure 82   Bubble Pressure Test Apparatus - Matrix
            Materials

SPECIMEN

WORKING
ELECTRODE
CHAMBER

REFERENCE
ELECTRODE
WELL

0 5"DIA
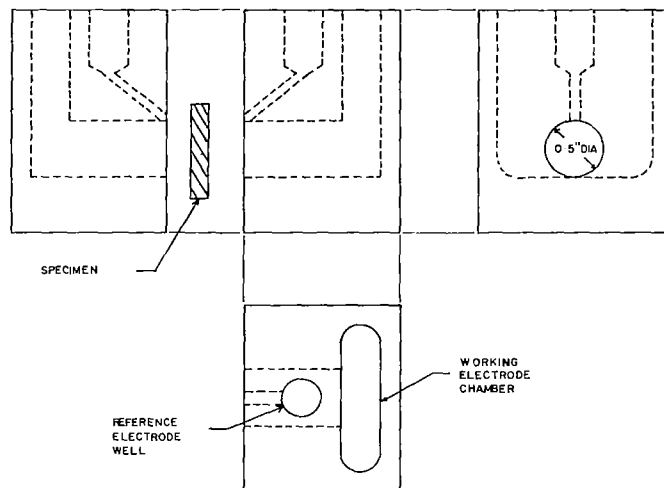
(a) Diagram of Cell used for Electrolytic
Conductivity Measurements

POTENTIOMETER

WORKING ELECTRODES

REFERENCE
HYDROGEN
ELECTRODES

SPECIMEN

POTENTIOSTAT
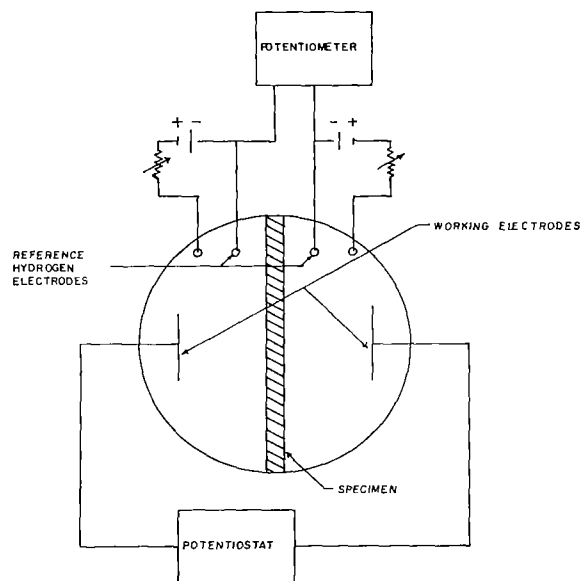
(b) Electrical Schematic of Conductivity
Measuring Apparatus

Figure 83   Electrolyte Conductivity Measurement of
Matrix Materials - Test Apparatus

119

reference electrode wells with Luggin capillary channels communicating to the specimen surface. The potential developed across the specimen is measured as the potential difference between the two reference electrodes.

The reference electrodes are dynamic hydrogen electrodes; each reference-well contains a small hydrogen and oxygen electrode, and each pair is supplied independently by a regulated direct current supply. A Teflon septum was inserted between the hydrogen-oxygen electrode pair to reduce the access of electro generated oxygen to the hydrogen electrode.

The measuring procedure is as follows: With zero-current through the specimen, the reference electrode supply currents are adjusted to produce a gentle gas evolution and also to the condition of zero-potential difference as measured by a potentiometer. Current is then passed through the specimen and the potential difference between the reference electrodes is quickly measured. These two measurements are rechecked several times to maintain constant set conditions.

Blank measurement, which is essential, is made with no specimen mounted between the cell halves. Despite the fact that the Luggin capillary orifices are virtually in face-to-face contact when there is no specimen between the cell halves, the measured potential difference generated by 50 ASF through the electrolyte is large relative to the potential measured for a specimen under test. Thus, the necessary blank correction is relatively large.

When the specimen is mounted, a test surface of one-half inch in diameter is exposed to the electrolyte. The area of the conducting specimen is 1.266 cm², assuming complete rectilinear flow lines. The values reported are the measured resistance, the net resistance of the specimen (corrected for blank), and the net resistance per unit area of specimen.

According to the original task definition, the resistance measurements were to be conducted with the specimens in 38% sulfuric acid at 195°F. It was learned that because of the design of the cell and the thermal insulating properties of Teflon, attainment and maintenance of 195°F temperature at the specimen was difficult. Also, the reference electrodes became very unreliable at higher temperatures. Consequently, the early measurements were of little quantitative value. With the concurrence of NASA personnel, measurements were performed on the specimens at room temperature. These data are reported in Table 11.

Electrolytic resistance measurements were also made on specimens after immersion in 38% sulfuric acid at 195°F. These data are recorded in Table 12. The data vary so broadly that a useful interpretation seems improbable. The Refrasil varies greatly in density of fiber packing, which fact may account for the broad

variation of measured resistances from specimen to specimen. TA-1 matrix is a thin densely packed and non-swelling material which dewets non-uniformly during the immersion treatments. The non-uniform dewetting probably accounts for the broad variations in measured resistance of tested TA-1.

3.2.2.4   Immersion Tests

The immersion tests consisted of immersing the matrix specimens in 38% sulfuric acid at 195°F for 200, 400, 600 and 1000 hours. It was required to measure changes in weight and dimensions of the specimens, and to analyze the sulfuric acid solution for constituents of the matrix materials.

Because of the loose packing of the Refrasil mat and the probability of its disintegration in the sulfuric acid, the measured specimens were enclosed between two layers of polypropylene screen cloth which were then heat-sealed at the edges. After removal from the sulfuric acid, the encapsulated specimen was rinsed free of acid by repeated immersions in water, and subsequently dried. The specimen was weighed and measured after removal from the screen envelope.

The Refrasil specimens remained virtually unchanged in the immersion tests. There were very small losses in weight (see Table 13) but these might well be attributed to simple mechanical loss of a few fibers. No appreciable changes in dimensions were detected (see Table 13) and no specimen distortion was observed. It was anticipated that the silica fibers might revert to the stable crystalline state, while remaining insoluble, however this did not occur to any detectable degree. Spectrographic analysis of the sulfuric acid after the test revealed neither silicon nor any impurity component of the silica.

The TA-1 specimens were water-saturated as received. One inch square specimens were cut and soaked in 38% sulfuric acid before the corrosion test. Upon completion of test, the specimens were rinsed free of sulfuric acid and tested for bubble pressure and resistance. The specimens were severely distorted, partially dewetted, and delaminated to form multiple convex surface pockets. Although weight change measurements could not be made because the specimens were saturated with water in the prior and post test conditions, it may be reasonably assumed that, because the TA-1 material is entirely Teflon, it is completely inert in the sulfuric acid.

3.2.3   Conclusions

From the materials commercially available (at the beginning of the study) only the Refrasil proved to be suitable for matrix service in sulfuric acid. The Refrasil is virtually inert in sulfuric acid and manifested no appreciable degree of transition from the fibrous form. The Refrasil specimen tested for 1000 hours contained no impurities leachable by sulfuric acid.

The Refrasil mat is a very loosely packed random mass of fibers. This non-uniform fiber distribution probably causes the low bubble pressure values, which seem to be the major deficiency of the Refrasil. The bubble pressure value increased by approximately 26% during the 1000 hour test period while the void volume remained essentially constant.

The TA-1 matrix is unsatisfactory primarily because it is a naturally hydrophobic material. A surface etching treatment renders the Teflon fibers hydrophilic but the condition is metastable. It was observed that dewetting occurs during the long immersion tests. The vendor also advised that dewetting would be an even greater problem in the oxidizing environment of the anode. The bubble pressure measurements seemed to indicate a slight increase, about 24%, after the initial 200 hour test, however the remaining test samples showed a gradual decrease in bubble pressure. After 1000 hours the value had decreased approximately 24% from the initial value for the material in the "as received" condition.

TABLE 10

VOID VOLUME & BUBBLE PRESSURE OF MATRIX MATERIALS (AS RECEIVED)

Specimen	Thickness (inches)	Dimensions (inches)	Weight (grams)	Geometric Density (g/cc)	Absolute Density* (g/cc)	% Void Volume	Bubble Pressure (Ins.Hg)
Refrasil (Hitco)	0.08	17.12 x 5.5	11.86	0.096	2.07	95	2.9
Polypropy-lene Felt (Kendall)	0.044	7.0 x 8.37	6.32	0.15	0.905	83	0.34
TA-1 (Am. Cyan-amid)	0.03	5.0 x 5.0	15.47	1.26	2.17	78	13.8
Metricel VF-6 (Gelman)	0.005	1.845 Dia.	0.1032	0.47	2.14	78	0.85

*Published values for the generic material.

TABLE 11

ELECTROLYTE RESISTANCE OF MATRIX MATERIALS (AS RECEIVED)

50 ASF, 38% Sulfuric Acid, Room Temperature

	TA-1 (0.030 inch thick)	Refrasil (0.080 inch thick)
ΔE Specimen 1	0.0186 volts	0.0220 volts
Specimen 2	0.0203 volts	0.0232 volts
Average	0.0194 volts	0.0226 volts
Blank (1)	0.0182 volts	
(2)	0.0176 volts	
(Av.)	0.0179 volts	
Net ΔE	0.0015 volts	0.0047 volts
Resistance of specimen (ohms)	0.021	0.067
Specific resistance ohm cm^2	0.027	0.085

TABLE 12

ELECTROLYTIC RESISTANCE OF MATRIX MATERIALS
(POST IMMERSION TESTS)

50 ASF, 38% Sulfuric Acid, Room Temperature

Specimen	Time in Test (hrs)	ΔE (volts)	ΔE Net (volts)	Resistance (ohms)	Specific Resistance ohm-cm²
Refrasil	200	(Specimen damaged)			
A-100	200	0.0259	0.0084	0.12	0.152
	400	0.0217	0.0042	0.06	0.076
	400	0.0252	0.0077	0.11	0.14
	600	0.0210	0.0035	0.07	0.09
	600	0.0273	0.0098	0.14	0.177
	1000	0.0315	0.0140	0.20	0.253
	1000	0.0322	0.0147	0.21	0.265
TA-1	200	0.0252	0.0077	0.11	0.14
	200	0.0189	0.0014	0.02	0.025
	400	0.0280	0.0105	0.15	0.19
	400	0.0686	0.0511	0.73	0.92
	600	0.0189	0.0014	0.02	0.025
	600	0.0217	0.0042	0.06	0.076
	1000	0.0350	0.0175	0.25	0.032
	1000	0.0210	0.0035	0.07	0.09
Blank		0.0175			

TABLE 13

ACID MATRIX MATERIALS - TEST RESULTS SUMMARY

Material Sample	No.	Test Time (Hours)	Weight (grams) Initial	Final	% Change	Dimensions (inches) Initial L x W x T			Final L x W x T			Void Volume %	Bubble Pressure (inches Hg)
Refrasil A-100	1	200	0.1952	0.1923	1.49	1.0	1.0	0.121	1.0	1.0	0.121	96	3.5(1)
	2	200	0.1829	0.1790	2.13	1.0	1.0	0.128	1.0	1.0	0.125	98	3.7
	3	400	0.1914	0.1902	0.63	1.0	1.0	0.133	1.0	1.0	0.132	95	3.9
	4	400	0.2016	0.2003	0.64	1.0	1.0	0.142	1.0	1.0	0.136	96	3.3
	5	600	0.1877	0.1839	2.02	1.0	1.0	0.135	1.0	1.0	0.135	96	4.9
	6	600	0.1860	0.1854	0.32	1.0	1.0	0.139	1.0	1.0	0.133	96	4.2
	7	1000	0.1844	0.1790	2.93	1.0	1.0	0.116	1.0	1.0	0.120	94	3.6
	8	1000	0.1876	0.1840	1.92	1.0	1.0	0.120	1.0	1.0	0.118	96	3.7
TA-1 Cyanamid	9	200	Not applicable			1.0	1.0	0.030	1.0	0.6	0.030	Not Measurable	17.1(2)
	10	200				1.0	1.0	0.030	1.0	0.6	0.030		16.7
	11	400(3)				1.0	1.0	0.030	0.9	0.8	(*)		15.9
	12	400(3)				1.0	1.0	0.030	0.9	0.6	(*)		13.7
	13	600(3)				1.0	1.0	0.030	0.9	0.6	(*)		15.5
	14	600(3)				1.0	1.0	0.030	0.9	0.6	(*)		15.1
	15	1000(4)				1.0	1.0	0.030	0.9	0.8	(*)		13.8
	16	1000(4)				1.0	1.0	0.030	0.9	0.8	(*)		10.5

(1) Bubble pressure for Refrasil A-100 as received = 2.9 ins. Hg.
(2) Bubble pressure for Cynamid TA-1 as received = 13.8 ins. Hg.
(3) Distorted, with gas pockets formed between layers.
(4) Distorted more severely than in (3).

(*) Surface bubbles; no reliable measurement possible.

3.3 Gasket Materials Evaluation

3.3.1   Materials Review and Selection

The selection of sample materials was initiated by consultation with various suppliers and review of manufacturers' handbooks and literature. Manufacturers also were solicited for recommendations of their products for the specified environments. Responses were received from E. I. duPont, Parker Seal and 3M Companies. It was found that data on the compatibility of materials with K_2CO_3 were not generally available and suppliers' recommendations were based on the material most compatible with water at 175°F.

Available published data reviewed were primarily concerned with fuel cell and electrolysis applications. Test data were located for H_2SO_4 and KOH environments* and Table 14 summarizes gasket materials found to be acceptable for various environments based on reports referenced in Table 15.

Teflon has demonstrated excellent chemical compatibility in acid and alkaline environments, however, it shows a tendency to flow resulting in the subsequent loss of compression when used as a gasket. It was decided therefore not to evaluate this material in this application.

Ethylene Propylene has been used successfully in fuel cells operating at temperatures of approximately 190°F with 40% KOH with demonstrated lifetime operation in excess of 3,000 hours.

Kel-F material properties are contained in 3M Handbook, Kel-F Properties and Applications. This material was selected as a candidate gasket material for evaluation in both the alkaline and acid stages because of its high chemical resistance at higher temperatures, mechanical strength and low compression set.

Viton, with somewhat similar properties as Kel F, was another candidate material selected for evaluation. "Engineering Properties of Viton" and "Industrial Report on Viton" published by E. I. duPont contain application information and characteristic properties of this material. Viton had been used successfully on the acid stage during single cell tests conducted under Contract No. NAS 3-7638. Viton is a synthetic rubber with high resistance to chemicals at elevated temperatures.

Final selection of test samples was made with the approval of the NASA Project Manager. Potential ability to withstand physical and chemical degradation, and to maintain their sealing properties for periods in excess of 1,000 hours were the major factors used in the selection of the material samples.

*Reference 3 in Table 15.

127

The materials selected for immersion testing were as follows:

Alkaline Stages (K₂CO₃)	Acid Stage (H₂SO₄)

Alkaline Stages (K_2CO_3)

1. Ethylene Propylene
2. Kel-F

Acid Stage (H_2SO_4)

1. Viton
2. Kel-F

3.3.2   Physical Properties Measurements

Three (3) samples of each approved gasket material listed on Page 129 were prepared identically in individual beakers for evaluation under the specified environmental conditions. The samples were removed from the test beakers after test times of 200, 500 and 1,000 hours. Test evaluations were made to determine changes in physical properties including (1) weight, (2) thickness, (3) compressibility and (4) permeability. The results of pre-test and post-test measurements and observations are presented in Table 16.

3.3.2.1   Permeability

The permeability of the gasket material was determined by applying Nitrogen gas pressure to one side of the specimen which was contained in a rigid fixture. The gas flow through the test sample was determined from the volume change observed in a low volume manometer with corrections for pressure and temperature changes. A sample calculation, schematic of the test apparatus and summary tables of calculations are presented in Appendix V.

Six Kel-F, three Ethylene Propylene and three Viton samples were prepared for permeability tests. All test samples were approximately 2" x 2" x 1/8". Permeability measurements were conducted on material samples in the "as received" condition and also following chemical immersion tests of 200, 500 and 1,000 hour duration.

Pre-test values obtained for the permeability of the samples to Nitrogen at room temperature in the "as received" condition were generally in close agreement with manufacturers published "typical" data listed as follows:

	Permeability to Nitrogen (cc/cm²/cm./sec/atm)
Kel-F	1.22×10^{-9}
Ethylene Propylene	0.85×10^{-9}
Viton	0.54×10^{-9}

TABLE 14

MATERIALS COMPATIBILITY RATING FOR:

	Potassium Hydroxide	Water	Oxygen	Sulfuric Acid
Accept-able	Ethylene*[2,3] Propylene	Buna N[3]	Viton[3]	Viton-A[1,3]
	Kel-F			
	Ethylene[2] Propylene Terpolymer	Ethylene[3] Propylene	Silicone[3]	Teflon[1]
				Kel-F[1]
	Teflon[2,5]	Buna S[3]		Trilok[1]
	Polyethylene[5] Propylene			Hypalon[3]
	Halon G80[5]			Fluorel
				Natural Rubber
Un-accept-able	Hypalon[2]		Ethylene[3] Propylene	Butyle[1]
	Silastic RTV[2]			Silicone[1]
			Buna N[3]	Buna N[3]
				Ethylene Propylene
				Hypalon

*Numbers refer to References in Table 15.

TABLE 15

GASKET MATERIALS REFERENCES

1. "Structural Materials for Fuel Cells," Report to Ionics, Inc., Feb. 1963. Arthur D. Little, Inc.

2. "Development of Fuel Cell Electrodes", Semi-Annual Report, Jan. 1, 1967 to June 30, 1967, Union Carbide NAS 3-9430.

3. "Seal Compound Manual", Parker Seal Co.

4. "Permeability of Chlorotrifluoroethylene Polymers", A. W. Myers, V. Tammela, V. Stannett, and M. Szwarc.

5. "Final Technical Report Water Electrolyzer Module Development", Contract DA-44-009-AMC-1021(X), Sept. 1966, Allison Division of General Motors.

Post immersion test permeability measurements are presented in Table 16. The results in general show an increase in permeability up to the 500 hour test point except for the Kel-F sample tested to exposure No. 1 which displayed a slight decrease. Samples tested for 1,000 hours showed a decrease in permeability with the exception of ethylene propylene which displayed quite a large increase. It is to be noted that the permeability change was approximately 100% for both materials listed for the 1000 hour test in the acid exposure.

3.3.2.2 Compressibility

ASTM method F36 "Standard Method of Test for Compressibility and Recovery of Gasket Materials" was used to determine the compressibility of the test samples. Each sample was compressed between a surface plate and a steel cylinder penetrator in accordance with the test standard requirements. A dial gauge was used to indicate the specimen thickness during the test.

Pre and post-test calculations are included in Appendix V - Tables 20, 21 & 22. Test data for compressibility of the materials are summarized in Table 16.

With regard to the compressibility tests which were conducted on the sample materials above it should be noted that the tests were short-time tests and as such are not evaluations of the materials for determination of "creep" or "compression set" which occurs under prolonged stress application.

TABLE 16

GASKET IMMERSION TEST - DATA SUMMAR'

Exposure Conditions(1), Test Sample, and Exposure Time (Hrs x 10²)	Weight (GR)		Thickness (in.) (3)		Compressibility (%) (2)		Permeability(7) x 10⁻⁹	
	Initial	Final	Initial	Final	Initial	Final	Initial	Final
II-K(4)-2	18.1282	18.0794	0.134	0.136	47.3	21.0	1.61	1.37
II-K-5	17.8975	17.8568	0.132	0.134	47.3	21.1	1.61	1.5
II-K-10	17.6460	17.6060	0.130	0.130	47.3	16.2	1.61	1.04
II-EP(5)-2	10.6115	10.6121	0.129	0.127	8.5	11.1	0.91	2.62
II-EP-5	11.6474	11.6403	0.140	0.140	8.5	10.3	0.91	1.04
II-EP-10	11.7438	11.7545	0.141	0.141	8.5	10.0	0.91	11.52
III-K(4)-2	17.6332	17.5827	0.132	0.133	47.3	13.5	1.61	1.95
III-K-5	17.9527	17.8955	0.133	0.134	47.3	14.9	1.61	2.71
III-K-10	17.4682	17.4073	0.131	0.132	47.3	12.6	1.61	No pos. displ. detected
III-V(6)-2	14.7707	14.8330	0.120	0.120	13.8	9.4	0.47	0.50
III-V-5	15.1447	15.2247	0.123	0.123	13.8	9.6	0.47	0.70
III-V-10	15.0963	15.2024	0.120	0.123	13.8	10.8	0.47	0.03

(1) See Table 1 for exposure test conditions
(2) From ASTM, F36-66 "Standard Method of Test for compressibility and recovery of gasket material.
(3) Given as an average value.
(4) Material KEL-F-3700, Mfg. Industrial Electric Rubber Prod.
(5) Material Ethylene Propylene (E515-8) Mfg. Parker Seal Company
(6) Material Viton (77-545), Mfg. Parker Seal Company
(7) Permeability, cc-cm/sec-cm²-ATM

Visual Observation				Per Cent Change		
Material		Solution				
Initial	Final	Initial	Final	Compressibility	Permeability	Weight
White (1) Side Yellow-White (1) Side Smooth Dull Finish	Yl-Gn-Br Shades	CLEAR	Yl-Br-Cast	-26.3	-14.9	~0.27
	Yl-Gn-Br Shades		Yellow Cast	-26.2	-0.04	~0.23
	Dark Brown Shades		Yl-Br-Color	-31.1	-35.4	~0.23
Black Uniform Dull Finish	No change (Odor given off)	CLEAR	No change	+2.6	+188.0	+0.06
	No change (Odor given off)		Bl-Gn-Cast	+1.8	+14.3	~0.06
	No change (Odor given off)		Yellow-Gn Cast	+1.5	12×10^2	+0.09
White (1) Side Yl-white (1) side - smooth dull finish	Br color on exposed sides	CLEAR	Bright Yl-Orange	-33.8	+21.1	~0.29
	Br color on exposed sides		Bright orange	-32.4	+68.3	~0.32
	Reddish-brown color		Bright orange	-34.7	-100	~0.35
Blue-Black marble shaded smooth finish	No change	CLEAR	No change	-4.4	+0.064	+0.42
	No change		No change	-4.2	+48.9	+0.53
	No change		No change	-3.0	-93.6	+0.70

NOTE: For this page only:

Bl = Blue

Br = Brown

Gn = Green

Yl = Yellow

Manufacturers listed data for "average" compression set values for the materials are as follows:

KEL-F   24% 16 hours @ 212°F

Ethylene Propylene 47% 22 hours @ 212°F

Viton   10% 24 hours @ 300°F

3.3.2.3 Weight and Dimensional Measurements

Change in Weight:

> The test samples were washed, dried and weighed. Weight measurements of the samples are listed in Table 16.

Linear Dimensions:

> Measurements were made by micrometer or dial gauge where appropriate.

3.3.3 Immersion Tests

Immersion testing consisted of immersing the gasket materials samples in 30 weight per cent K_2CO_3 at 175°F for the alkaline stages and in 38 weight per cent H_2SO_4 at 195°F for the acid stage. The various samples were immersed in the electrolytes for periods of 200, 500 and 1,000 hours. Measurements of weight, thickness, compressibility and permeability were made before and after the immersion tests as described above. The test apparatus used for the metallic materials corrosion tests was used to provide the temperature controlled environment for the gasket materials immersion tests.

3.3.4 Conclusions

From the results of the test program conducted on the gasket materials and the data presented in Table 16, the following conclusions are drawn.

For the alkaline stage, review of the data obtained for Kel-F and Ethylene Propylene indicates: (1) weight changes are less than one per cent for both materials, (2) the compressibility of ethylene propylene increases by a small percentage (approximately 2%) while the compressibility of Kel-F decreases by 25 to 30 percent, indicating a slight hardening effect, and (3) while the permeability of Kel-F decreased, it was found that the permeability of ethylene propylene increased - rather considerably after 1,000 hours. Preference is expressed, therefore, for Kel-F gaskets for the alkaline stage.

Test results for Kel-F and Viton material samples in acid show: (1) weight changes are less than one per cent for both materials (2) the compressibility decreased for both materials, being

134

greater for Kel-F, and (3) the permeability of both materials displayed almost identical patterns. From these results, Viton is preferred for the acid stage.

Discoloration of the Kel-F samples was observed in both the alkaline and acid exposures during the 1,000 hour testing. Ethylene Propylene and Viton, however, showed no discoloration while exposed to the alkaline and acid environments respectively.

ESTIMATION OF THE ELECTRODE POTENTIAL OPERATING
DOMAINS FOR STAGES I, II AND III OF THE CARBONATION CELL SYSTEM

Notes:

1) Reaction considered: $O_2 + 2H_2O + 4e \rightleftharpoons 4OH^-$ or $O_2 + 4 H^+ + 4e \rightleftharpoons 2H_2O$

2) All potentials are reported with respect to the standard hydrogen electrode.

Stage I Parameters

Temperature:	80°C	Cathode gas composition: 0.5% CO_2
		Balance Air
Electrolyte:	28% K_2CO_3	Anode gas composition: 57% CO_2
		Balance O_2
Electrodes:	American Cyanamid AB-6	

(1) The half cell potential for the Stage I oxygen reaction is calculated from the Nernst equation and is as follows:

$$E_{O_2} = 1.229 - 0.070 \text{ pH} + 0.015 \text{ LOG } P_{O_2}$$

For pH = 13

$T = 80°C \qquad E_{O_2} = 0.319$ volt

$P_{O_2} = 1$ atm

The temperature dependence of the standard oxygen potential and the oxygen partial pressure dependence of the half cell potential have been neglected (< 50 mv).

(2) The measured half cell potential for the system O_2/Pt Black/ 6N KOH at T = 25°C and P_{O_2} = 0.2 atm is 0.228 volt. (56)

The calculated potential for the above system is derived from the following: $E_{O_2} = E_{H_2-O_2} - E_{H_2} = 0.344$V where E_{H_2} is a measured value equal to 0.885 volt and $E_{H_2-O_2} = 1.229$ V, is a calculated cell potential for an ideal H_2-O_2 fuel cell. (73)

The difference in potential between the calculated and measured E_{O_2} is: 0.344 - 0.228 = 0.116 volt representing the deviation of the calculated O_2 potential from actual conditions. It will be assumed that this difference in potential is independent of temperature (25 - 90°C).

(3) The corrected calculated oxygen half cell potential is:

      0.319 - 0.116 = 0.203 volt

The above represents an approximation to a measured oxygen half cell open circuit potential for the first stage. It is the first coordinate on the half cell polarization curve.

(4) The measured oxygen half cell potentials at a current density of 75 ASF for the system O_2/Pt Black/6N KOH at T = 25°C and P_{O_2} atm are as follows: (56)

      Anode (oxygen evolution):   0.748 volt

      Cathode (oxygen reduction):   0.002 volt

(5) The polarization of the measured oxygen half cell potentials at 75 ASF from the measured open circuit potential for the above system are as follows:

      Anode: 0.748 - 0.228 = 0.52 volt

      Cathode: 0.228 - (-0.002) = 0.23 volt

(6) An approximation to the measured half cell potential at 75 ASF for the system O_2/Pt Black/28% K_2CO_3 (Stage I) is as follows:

      Anode: 0.203 + 0.520 = 0.723 volt

      Cathode: 0.203 - 0.230 = -0.027 volt

(7) An approximation to the concentration polarization at the anode (due to OH^- ion limitations) may be obtained by determining the difference in polarization between the systems H_2/Pt Black/34% KOH Pt Black/O_2 and H_2/Pt Black/34% K_2CO_3/Pt Black/O_2 at 75 ASF.

This difference is given by the following equation:

$$\Delta E_{iR\ free} = \left[E_{OH^-} + iR\ drop \right] - \left[E_{CO_3^=} + iR\ drop \right]$$

$$= 0.89 + \frac{75 \times 0.5}{1 \times 10^3} - 0.45 - \frac{75 \times 0.5 \times 2.5}{1 \times 10^3}$$

$$= 0.39\ volt$$

(8) Adding the concentration polarization component to the approximated anode (Stage I) half cell potential gives:

      0.723 + 0.39 = 1.113 volts

Summary   1.113 ⌐ Potential 75 ASF oxygen evolution (anode)

         0.203 ⊣ Open circuit-half cell potential Stage I

            0 ⊣ SHE

      -0.027 ⌐ Potential 75 ASF oxygen reduction (cathode)

Stage II Parameters

Temperature: 80°C   Cathode gas composition 57% CO_2
                                              Balance O_2

Electrolyte: 31 %wt K_2CO_3 Anode gas composition 79% CO_2
                                              Balance O_2

Electrode: American Cyanamid AB-6

(1)   The half cell potential for the Stage II oxygen reaction is calculated from the Nernst equation and is as follows:

$$E_{0_2} = 1.229 - 0.070 \text{ pH} + 0.015 \text{ LOG } P_{0_2}$$

For pH = 10.5

       T = 80°C

     P_{0_2} = 1 atm E_{0_2} = 0.494 volt

(2)   See (2), Stage I derivation.

(3)   The corrected calculated oxygen half cell potential is

      0.494 - 0.116 = 0.378 volt

(4)   See (4), Stage I derivation.

(5)   See (5), Stage I derivation.

(6)   An approximation to the measured half cell potential at 75 ASF for the system $O_2/Pt/31$ % wt K_2CO_3 (Stage II) is as follows:

      Anode: 0.378 + 0.520 = 0.898 volt

      Cathode: 0.378 - 0.230 = 0.148 volt

(7)   See (7), Stage I derivation.

(8) Addition of the concentration polarization component to the approximated anode half cell potential gives:

$$0.898 + 0.39 = 1.288 \text{ volts}$$

Summary

1.288 ⌐ Potential 75 ASF-oxygen evolution (anode)

0.378 ⊣ Open circuit-half cell potential Stage II

0.148 ⊣ Potential 75 ASF-oxygen reduction (cathode)

0 ⌐ SHE

Stage III Parameters

Temperature: 90°C   Cathode gas composition = 79% CO_2
                                            Balance O_2
Electrolyte: 38% H_2SO_4 Anode gas composition = 100% oxygen

Electrodes: American Cyanamid AA-1

pH < 0

The measured oxygen reduction potential for the system Pt/O_2/30% wt H_2SO_4 at 60 ASF, T = 65°C is 0.75 with respect to a hydrogen* electrode in the same solution and at the same temperature (76). It is expected that the actual potential will be more anodic due to the higher operating temperature and electrolyte concentration.

The measured cell potential for the system O_2 (PO_2 = 0.2 atm)/ Pt Black/38% H_2SO_4/Pt Black/O_2 (PO_2 = 1 atm) at 60 ASF, T = 90°C is = 1.075 volts (61, 75). This cell potential is a measure of the potential difference between the oxygen reduction and evolution process.

Addition of the oxygen reduction half cell potential to the oxygen concentration cell potential gives the oxygen evolution half cell potential at 60 ASF equal to 1.825 volts (0.75 + 1.075) with respect to a hydrogen electrode in the same solution and at the same temperature.

Summary   1.825 ⌐ Potential oxygen evolution (anode) 60 ASF

0.75 ⊣ Potential oxygen reduction (cathode), 60 ASF

0.0 ⌐ H_2 electrode in same solution and temperature

*This electrode is assumed to be equal in potential to the SHE.

APPENDIX II

ESTIMATION OF HYDROGEN ION CONCENTRATION (pH) of STAGES I, II, AND III OF THE CARBONATION CELL SYSTEM

The hydrogen ion concentration (pH) of an aqueous solution of potassium carbonate is a function of the partial pressure of the carbon dioxide in contact with the solution at constant temperature and concentration of potassium ions. Therefore, the pH of Stages I and II may be obtained from an expression describing the concentration of H^+ (or OH^-) as a function of carbon dioxide partial pressure.

The non electrochemical reactions which occur in the carbonation stages are as follows:

(1) $CO_2 + CO_3^- + H_2O \rightleftharpoons 2H\ CO_3^-$

(2) $CO_3^- + H_2O \rightleftharpoons HCO_3^- + OH^-$
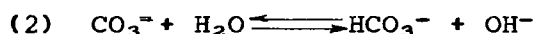
The concentration of the individual species at equilibrium is determined by the ionization constants for the above reactions, which are

(3) $K_1 = \dfrac{\left[HCO_3^-\right]^2}{\left[CO_2\right]\left[CO_3^=\right]}$ (4) $K_2 = \dfrac{\left[HCO_3^-\right]\left[OH^-\right]}{\left[CO_3^=\right]}$

The solution concentration of carbon dioxide CO_2 may be expressed as a function of the gas phase partial pressure of carbon dioxide (Henry's Law) as follows:

$$\left[CO_2\right] = k\ P_{CO_2}$$

The expression for K_1 and K_2 may now be rearranged as follows:

$$\dfrac{\left[H\ CO_3^-\right]}{\left[CO_3^=\right]} = \dfrac{K_1\ k\ P_{CO_2}}{\left[H\ CO_3^-\right]} \quad ; \quad \left[OH^-\right] = \dfrac{K_2\ \left[CO_3^=\right]}{\left[H\ CO_3^-\right]}$$

Substituting Equation (3) into (4) gives:

(5) $\left[OH^-\right] = \dfrac{\left[H\ CO_3^-\right]}{k\ P_{CO_2}}\ \dfrac{K_2}{K_1}$

The product of the concentration of hydroxyl (OH^-) and hydrogen ions in an aqueous solution at a given temperature is a constant and is expressed by the following equation:

(6) $Kw = \left[H^+\right]\left[OH^-\right]$ = ion-product constant.

Rearrangement of (6) and substitution of (5) gives:

$$(7) \quad \left[H^+\right] = \frac{K_w k \; P_{CO_2}}{\left[H\, CO_3^-\right]} \frac{K_1}{K_2} \quad \text{where pH} = -LOG\left[H^+\right]$$

The parameters K_w, k, K_1 K_2 are constant at any given temperature. The concentration of $H\, CO_3^-$ may be expressed as a function of P_{CO_2}.

The validity of the above derived pH = F (PCO_2) relationship was checked by computing the pH of reaction (1) for a given set of parameters and comparing it to a measured value.(57)

The derivation is as follows:

Parameter	Value	Reference
P_{CO_2}	1 atm	
T	80°C	
C	2.5 moles/liter	(57)
K_1	1.37×10^3	
k	0.00915	(extrapolated; from Handbook of Chemistry & Physics)
$K_2 = \dfrac{K_w^{\,*}}{K_{H\, CO_3}}$	1.79×10^{-4}	(from Handbook of Chemistry & Physics)
K_w	2.95×10^{-13}	(from International Critical Tables Vol 6, p 152 Table of Best Values)

The $\left[H\, CO_3^-\right]$ is derived from Equation (3) as follows:

$$K_1 = \frac{\left[H\, CO_3^-\right]^2}{\left[CO_3^=\right]\left[CO_2\right]}$$

Let x = concentration of reacted $\left[CO_3^=\right]$

C = initial concentration of $\left[CO_3^=\right]$ Moles/Liter

2X = equilibrium concentration of $\left[H\, CO_3^-\right]$

C-X = equilibrium concentration of $\left[CO_3^=\right]$

*Used ionization value at 25°C assumed the ratio to be independent of temperature.

141

Rearrangement of (3) and substitution of the given values gives:

$$\frac{4\ x^2}{(C-X)\ (0.0092\ P_{CO_2})} = 1.37 \times 10^3$$

Therefore,

$$X = 1.6$$

$$\left[H\ CO_3^-\right] = 2 \times 3.2\ \text{Moles/Liter}$$

Derive $\left[H^+\right]$ from Equation (7)

$$\left[H^+\right] = \frac{K_w\ K_1}{K_2}\ \frac{k\ P_{CO_2}}{\left[H\ CO_3^-\right]}$$

$$\left[H^+\right] = \frac{2.95 \times 10^{-13} \times 1.37 \times 10^3}{1.79 \times 10^{-4}} \times \frac{0.0092 \times 1}{3.2}$$

$$\left[H^+\right] = 6.5 \times 10^{-9}$$

Derive pH: $pH = -LOG\ (H^+)$

$$= -\left[LOG\ 6.5 + LOG\ 10^{-9}\right]$$

$$= 9 - 0.8$$

$$pH = 8.2$$

The measured pH for the same system conditions is reported as 8.85. (57)

The following table is a summary of the estimated pH of Stages I and II under the specified conditions of temperature, carbon dioxide pressure and electrolyte concentration.

	Anode	Cathode
Stage I	8.7	10
Stage II	8.3	8.4
Stage III*	<0	<0

*"Strong" electrolyte independent of gas phase composition.

APPENDIX III*

POURBAIX DIAGRAMS
CONSTRUCTION METHOD, INTERPRETATION & LIMITATIONS

The purpose of a Pourbaix diagram is to distinguish conditions for which a given corrosion reaction is or is not possible. Essentially Pourbaix diagrams are a composite formulation of the equilibria of all the reactions possible in a given system as a function of two independent variables. The other possible variables are considered as parameters. These two independent variables are chosen in such a way that the equilibrium formulae are linear or practically linear. The independent variables are the equilibrium electrode potential and the pH of the solution in the case of electrochemical systems involving an aqueous solution. By this method the equilibrium conditions of all the reactions possible in a given system are represented on a plane diagram by families of straight lines.

For each element considered the equilibrium conditions (both where there is a possibility of exchanging electrical work with the exterior and where there is not) are characterized for systems whose constituent species are: the element in question, its ions in aqueous solution, water and its constituents (hydrogen ions, and hydroxol ions, gaseous hydrogen and oxygen) and the products of the reactions of the element with these species (oxides and hydroxides, hydrides, etc.). In this manner, the equilibrium conditions of electrochemical reactions can be represented by a relation between the equilibrium potential and a linear combination of logarithms of activities or concentrations. In a particular case of non-electrochemical reactions, the equil-ibrium conditions assume a simple form as no equilibrium potential is involved. These conditions are then expressed by a relation between an equilibrium constant and a linear combination of logarithms of activities or concentrations.

The linear combination of the logarithms of the species' activities different from hydrogen ions is given a nature of a parameter which is variable from one curve to another in each family of equilibrium curves. For electrochemical reactions which do not involve hydrogen ions, the locus of points representing equilibrium conditions will be straight lines parallel to the pH axis. For purely chemical reactions involving hydrogen ions they will be straight lines parallel to the potential axis. When there is only one species of variable thermodynamic level, the parameter which is then proportional to

---

the logarithm of the activity of this species characterizes the conditions of "practical existence of this species in the medium", as for example, the domain of conditions under which the equilibrium can be realized in the presence of appreciable concentrations of the species. Figure 84 depicts the general nature of the Pourbaix diagrams for some of the reactions of the system iron/water at 25°C.

The general nature and construction of a Pourbaix diagram is outlined and developed with the assistance of this diagram as follows. The reversible hydrogen electrode potential varies linearly with pH at constant temperature and pressure. The reversible oxygen electrode potential varies in the same way with pH and is readily derived from the Nernst equation. The data for these two electrode processes acting reversibly at 25°C are plotted on a potential/pH diagram shown in Figure 84, in which the field represented by the graph becomes divided into three areas. Within the central area bounded by the sloping lines, water is thermodynamically stable and cannot be decomposed electrolytically into hydrogen and oxygen. The remaining areas are those in which it is possible to decompose water. Thus, water can be electrolyzed only when the cathode potential is below the lower line (Reversible H_2 Reaction) and the corresponding anode potential is above the upper line (Reversible O_2 Reaction). It is essential to realize that the diagram indicates only the possibility that water can be electrolyzed. In actual practice, even when the appropriate potential conditions are satisfied the rate of electrolysis may be so small that at some chosen potential the possibility of water decomposition can be ignored.

Similarly, other reactions such as the iron/water system can be superimposed on Figure 84, to yield the domains of corrosion immunity and passivation for iron, for example, the electrode reactions which occur among iron metal, ferrous and ferric ions and numerous other oxidation products of iron such as magnetite and haematite. The reversible electrode potential of iron in equilibrium with ferrous ions is derived from the Nernst equation and is seen to be independent of pH. On the potential/pH diagram (Pourbaix), the iron/ferrous ion equilibrium is therefore expressed by a series of horizontal lines each corresponding to a particular activity of ferrous ions. These horizontal lines are shown on Figure 84 for ferrous ion activities of 10^0, 10^{-2}, 10^{-4}, and 10^{-6} gram-ions per liter. It is to be noted that the lines end abruptly at pH values varying from 6.6 to 9.6. This occurs since the equilibrium cannot exist between iron and ferrous ions at an activity of much more than 10^{-6} gram-ions per liter in a solution whose pH is greater than 9.6, because ferrous hydroxide is precipitated. In a similar manner the reversible equilibrium between ferrous ions and ferric hydroxide are plotted in Figure 84, for four activities of ferrous ions. The four lines pass from the top left hand corner of the figure to positions near the center corresponding to zero electrode potential and stop at pH
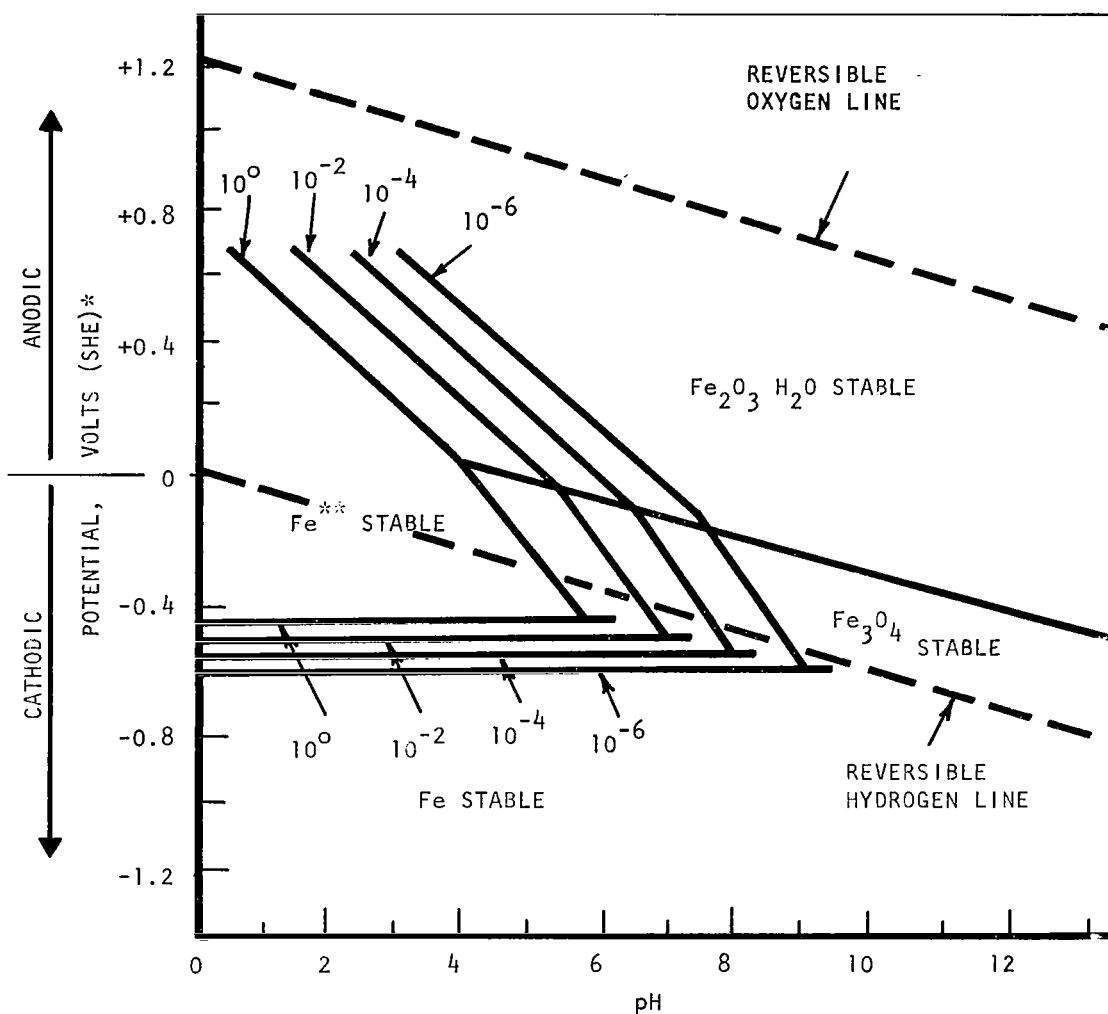
Figure 84   Potential pH Relations for Some Reactions
of Iron at 25°C

values from 4.0 to 7.0 because of the reduction of ferric hydroxide. The continuation of these lines as shown represents the equilibrium between ferrous ions and magnetite.

The interpretation of the various areas of this potential pH diagram is as follows. Assume that a pure specimen of iron metal is maintained at a potential of -0.44 volts in a de-oxygenated aqueous solution of pH equal to zero. The diagram indicates that iron will dissolve until a ferrous ion activity of unity is reached. At the same time hydrogen may be evolved at the iron since the conditions are maintained below the reversible hydrogen line. It should be noted that these indications of possible reactions have been derived from arguments based on reversible equilibrium conditions only. If Figure 84 is completed with the remaining potential pH relations for the electrode reactions of iron and its oxidation product and by taking into account the fact that some of the iron oxides are known to form a protective film on the metal following their formation, domains of corrosion, immunity and passivation can be sketched. This is shown in Figure 85.

The following definitions of the terms corrosion, immunity and passivation should be noted.

Corrosion is the reaction of a metal with its non-metallic environment that results in a continuing dissolution of the metal. In the case of the Pourbaix diagrams the lower limit of corrosion of a metal is arbitrarily set at potential which forms 10^{-6} gram-ions per liter.

Passivation is the process leading to a more or less perfect passivity of the material. Passivity is defined as the state of a metal in which corrosion in a particular environment is prevented by modifications of its surface, for instance, by the formation of a thin protective layer of oxide. The reaction product involved in passivity may vary widely in the degree of protection it provides.

Immunity is that state of a metal in which corrosion is thermodynamically impossible in a particular environment. The limitations in the application of Pourbaix diagrams to real systems may be briefly summarized as follows. Real corrosion situations often involve significant departures from equilibrium. The diagram refers to the pure metal, not alloys, and to pure water, free of substances capable of either forming soluble complexes or insoluble compounds. The pH value indicated in the diagram is that of the solution in direct contact with the metal and is not necessarily that of the solution as a whole. Information on the rate of corrosion is not given directly by the diagram.

PASSIVATION IF THE OXIDE
STABLE IN THIS AREA IS
PROTECTIVE

CORROSION:
IRON IONS STABLE
IN THIS AREA

CORROSION: IRON
FORMS AN ANION

IMMUNITY: METAL IS CATHODIC

ANODIC

CATHODIC

POTENTIAL, VOLTS (SHE)*

pH

*STANDARD HYDROGEN ELECTRODE
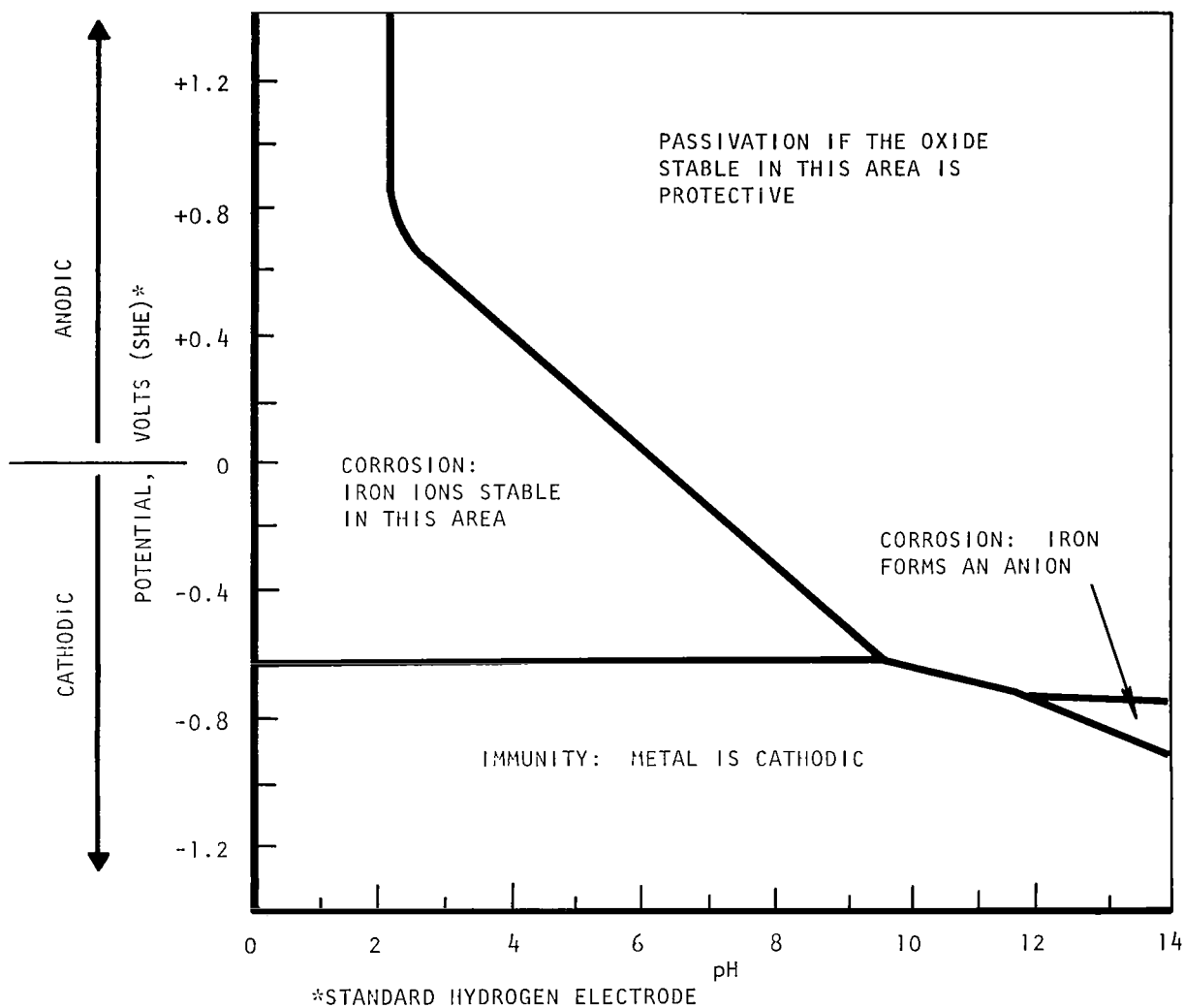
Figure 85   Domains of Corrosion, Immunity and Passivation
for Iron in Aqueous Solution at 25°C

147

APPENDIX IV

CONSTANT POTENTIAL CORROSION TEST

Reduction of spectrographic analyses of electrolyte solutions to average corrosion rates in mils per year.

1. Test Conditions

Metal	Potential w.r.t. DHE*	Temperature °C	Purge Gas	Electrolyte
Platinum	2.1	80	N_2	30% K_2CO_3
Zirconium	2.1	80	N_2	30% K_2CO_3
Titanium	2.1	80	N_2	30% K_2CO_3

*DHE - Dynamic H_2 Electrode

2. Data Summary

Test Cell	Vs	i_{mpy}	c_m	t (secs)	MW	e	i_c	mpy	d_f	As
$Pt/N_2/K_2CO_3$	0.200	3.44	<1.0	3.2×10^5	195.09	0.505×10^{-3}	<1.58	<0.5	1.268	1.00
$Zr/N_2/K_2CO_3$	0.600	2.90	<1.0	1.6×10^5	91.22	0.236×10^{-3}	20.4	<7.0	1.282	1.374
$Ti/N_2/K_2CO_3$	0.600	4.01	<1.0	3.35×10^5	47.90	0.124×10^{-3}	18.2	<4.5	1.259	1.374
$Pt/N_2/H_2SO_4$	0.415	1.17	1.0	4.0×10^5	195.09	0.505×10^{-3}	2.83	2.4	1.375	0.34

Vs   -   Final test solution volume, Liters (25°C)

i_{mpy} -   Corrosion current equivalent to 1.0 mil per year in micro amperes.

c_m -   Concentration of metal in solution at end of test, ppm by weight.

t   -   Test duration at constant potential, seconds.

MW   -   Gram molecular weight of metal.

e   -   Electrochemical equivalent of metal, grams/ampere-second.

i_c -   Average corrosion current, microamperes.

mpy   -   Average corrosion current expressed in mils per year.

d_f -   Electrolyte solution density at end of test, grams/cc (25°C).

As   -   Surface area of test electrode, cm².

ΔV_m -   Volume of metal in a 0.001 inch layer at surface of sample,

$$= As \times 0.00254 \ (cm^3)$$

$$i_c = \frac{c_m \times d_f \times V_s \times 10^3}{e \times t^*} \quad \text{microamperes}$$

$$i_{mpy} = \frac{d_m \times \Delta V_m \times 10^{-1}}{e \times 3.154^*} \quad \text{microamperes}$$

*t = seconds in one year = 3.154×10^7

148

APPENDIX V

PERMEABILITY AND COMPRESSIBILITY CALCULATIONS
FOR GASKET MATERIALS

Gas volume change - pressure and temperature corrections. See Figure 86. From the standard gas equation,

$$P_i \ V_i = n_i \ R \ T_i$$

where "i" represents initial conditions.

Therefore,

$$n_i = \frac{P_i \ V_i}{T_1 R}$$

and

$$n_F = \frac{P_F \ V_F}{T_F R}$$

where "F" represents the final conditions.

The final volume of the gas is given by

$$V_F = V_i \pm \triangle V$$

The change in the number of gram moles is, therefore

$$n_F - n_i = \frac{P_F \ V_F}{T_F R} - \frac{P_i \ V_i}{T_1 R}$$

or

$$\triangle n = \left[\frac{P_F \ (V_i \pm \triangle V)}{T_F} - \frac{P_i \ V_i}{T_1} \right] \ 1/R \qquad (1)$$

The sample calculation is shown for the pre-exposure permeability test for the Kel-F sample in Table 17. The following are the values for the terms in equation (1):

V_1 = FIXTURE GAS VOLUME, cm^3

V_2 = TUBE GAS VOLUME (INITIAL), cm^3

V_i = INITIAL GAS VOLUME ($V_1 + V_2$), cm^3

V_F = FINAL GAS VOLUME = $V_i \pm \Delta V$

h = HEIGHT OF LIQUID COLUMN, cm

LOW VAPOR PRESSURE MANOMETER FLUID (sp.gr.1.04)
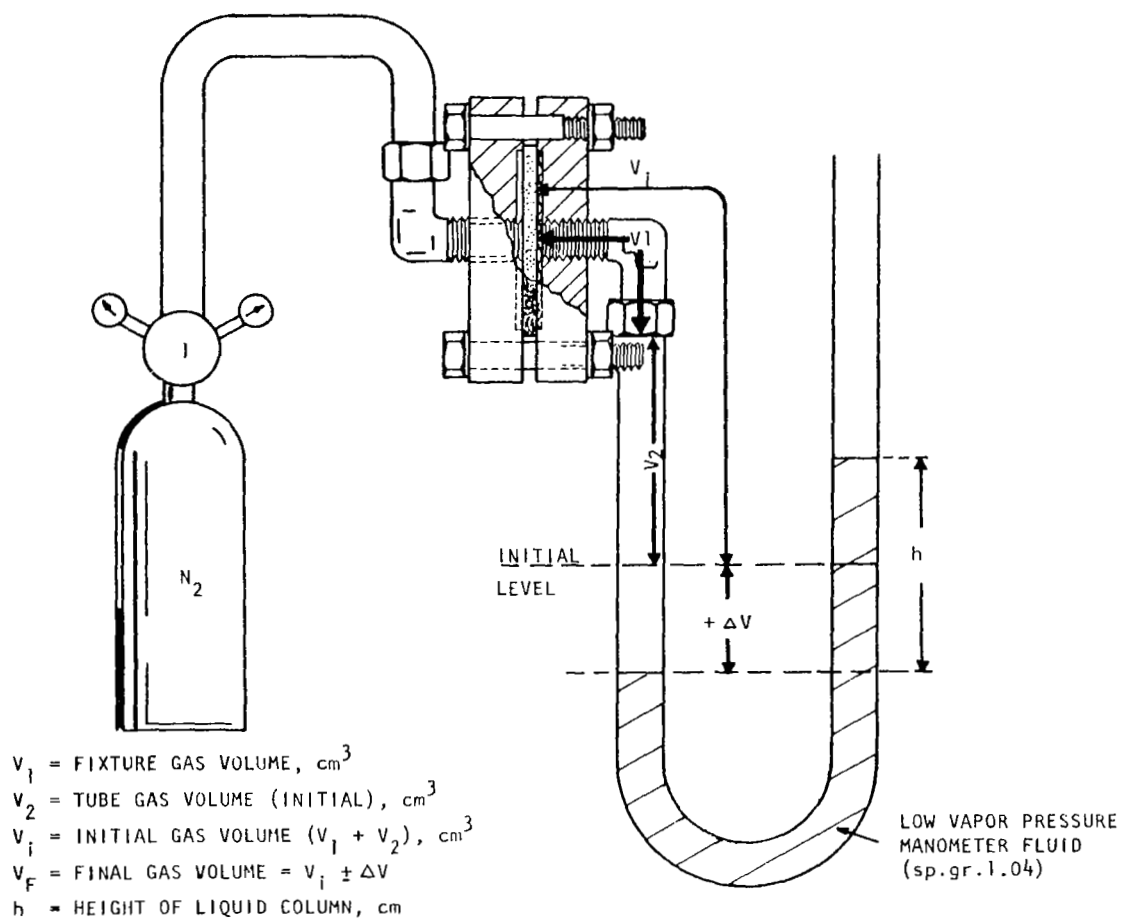
Figure 86   Permeability Test Apparatus

$$P_F = 741.2 \text{ mm Hg} + 0.8 \text{ (cm } H_2O) \times 0.583 \text{ mm Hg} = 741.78 \text{ mm Hg}$$

$$P_i = 744.5 \text{ mm Hg}$$

$$V_i = 4.008 \text{ cc}$$

$$T_F = 23.9°C + 273.2 = 297.1°K$$

$$T_i = 25.6°C + 273.2 = 298.8°K$$

$$\Delta V = 0.4 \ (0.1345) = 0.0538 \text{ cc}$$

(0.1345 cc/cm of U-tube is average value for gravimetric and volumetric measurements: see below under Test Apparatus.)

n = number of gram-moles

R = gas constant = 62,360 cc-mm Hg/mole °K

Substituting these values into equation (1) gives

$$n = \left(\frac{741.78 \times 4.0618}{297.1} - \frac{744.5 \times 4.008}{298.8} \right) \times \frac{10^{-4}}{6.236}$$

$$= 0.0248 \times 10^{-4} \text{ moles}$$

$$= 0.0248 \times 10^{-4} \times 22.4 \times 10^3 = 0.555 \times 10^{-1} \text{ cc at STP.}$$

Calculations for the test specimens are made by substituting the measured values into the following formula defining (P) permeability of the materials.

$$P = \frac{\text{cc (STP)} \times \text{cm (thickness)}}{\text{Time (sec)} \times \text{Area A(cm}^2) \times \Delta P \text{ (atm)}}$$

$$\text{Area A} = \frac{3.14}{4} \times (1.75)^2 \times (2.54)^2$$

$$= 15.281 \text{ cm}^2$$

$$\Delta P = 1 \text{ Atm.}$$

The calculations of the permeability (P) of the materials are listed in Tables 18 and 19 and are summarized with the general gasket immersion data in Table 16.

Test Apparatus - Calibration and Measurements for Initial Gas Volume Determination

Fixture No.	Fixture Vol. V_1 (cc)	Tube Length L (cm)	Tube Vol.(1) V_2 (cc)	Total Gas Vol. (2) $V_1+V_2 = V_i$
1	2.10	14.191	1.908	4.008
2	2.05	14.127	1.900	3.950
3	2.125	14.396	1.936	4.061

(1)　Calculation of volume of tube per cm length of U-tube

　　(a) Gravimetric

　　Initial measurement　　　　7.6 cm

　　Final Measurement　　　　　6.5 cm

　　　　　　　　　　　　　　　1.1 cm length of fluid removed
　　　　　　　　　　　　　　　　　(one side)

Fluid density = 1.04 gm/cc
Fluid weight　= 0.310 gm
Fluid volume = 0.298 cc

$$\text{Volume per cm length} = \frac{0.298}{2.2} = 0.1354 \text{ cc/cm.}$$

　　(b) Volumetric

Volume of liquid per cm. of U-tube as determined using pipette = 0.1336 cc/cm.

Use average value of gravimetric and volumetric measurements, i.e.,

$$\frac{0.1354 + 0.1336}{2} = \frac{0.2690}{2} = 0.1345 \text{ cc/cm.}$$

(2)　This computed volume (V_i) is the calibrated initial volume for the three test fixtures and is used in the general equation (1) and page 153. See also Table 17.

TABLE 17

PERMEABILITY TESTING
DATA POINTS FOR PRE IMMERSION TESTS

Material Sample	KEL-F	Viton	Ethylene Propylene
Test Time (Hr:Min)	0:00	0:00	0:00
	216:06	216:06	216:06
Manometer Reading (cm)	7.55	7.05	6.83
	7.95	6.85	6.75
V_i (cc)	4.008	4.061	3.950
Temp (^{O}F)	78	78	78
	75	75	75
Patm. (mm Hg)	744.5	744.5	744.5
	741.2	741.2	741.2

TABLE 18

SUMMARY OF PERMEABILITY CALCULATIONS FOR GASKET MATERIALS

Sample Data	Measured Volume (cm³ stp)	Time (sec) x 10⁵	Thickness (cm)	cc-cm x 10⁻³	Sec-cm² x 10⁶	P* x 10⁻⁹
KEL-F P.T.**	0.0555	7.776	0.3429	19.048	11.883	1.61
E.P.P.T.	0.3202	7.766	0.3353	10.737	11.883	0.905
Viton P.T.	0.0173	7.776	0.3226	5.585	11.883	0.47
II-K-2a	0.0449	7.506	0.3409	15.695	11.470	1.37
II-EP-2a	0.1823	1.494	0.3277	5.976	2.283	2.62
III-K-2a	0.0540	6.066	0.3343	18.083	9.269	1.95
III-V-2a	0.0189	7.506	0.3043	5.776	11.470	0.504
II=K-5a	0.0485	6.912	0.3358	16.296	10.562	1.543
II-EP-5a	0.3126	6.912	0.3351	11.102	10.562	1.042
III-K-5a	0.0532	4.38	0.3404	18.126	6.693	2.708
III-V-5a	0.0235	6.912	0.3119	7.332	10.562	0.695
II-K-10a	0.0255	5.29	0.3302	8.433	8.084	1.043
II-EP-10a	0.2601	5.29	0.3581	93.142	8.084	11.522
III=K-10a	No positive displacement detected in=379 hours					
III-V-10a	0.0008	5.29	0.3048	0.2438	8.084	0.03

$$* \quad \frac{cc\text{-}cm}{Sec\text{-}cm^2\text{-}\Delta P \text{ (ATM)}}$$

** Pre-Test

TABLE 19

PERMEABILITY TESTING DATA POINTS FOR POST IMMERSION TESTS

Sample & Exposure Time (1)	200 Hr Samples			500 Hr Samples				1000 Hr Samples				
	II-K-2	III-V-2	II-EP-2	III-K-2	II-K-5	III-V-5	II-EP-5	III-K-5	II-K-10	III-V-10	II-EP-10	III-K-10
Test Time(2)	0:00	0:00	0:00	0:00	0:00	0:00	0:00	0:00	0:00	0:00	0:00	0:00
(Hrs: Min.)	208:38	208:38	41:38	168:40	192:00	192:00	192:00	121:40	146:48	146:48	146:48	379:14
Manometer Reading (cm)	7.75	6.85	6.75	6.75	7.60	6.80	6.67	6.80	7.7	7.0	7.14	8.0
	7.85	6.10	8.26	6.59	7.60	6.80	6.75	7.00	8.0	7.1	9.13	7.6
V_i (cm³)	4.008	4.061	3.950	3.950	4.008	4.061	3.950	4.061	4.008	4.061	3.950	4.008
Temperature °F	76	76	76	74	74	74	74	76	77	77	77	78
	74	74	74	74	78	78	78	80	79	79	79	75
Patm. (mm Hg)	741.2	741.2	741.2	736.7	740.7	740.7	740.7	758.8	745.0	745.0	745.0	747.4
	745.0	745.0	736.7	745.0	754.2	754.2	754.2	749.5	748.8	748.8	748.8	751.8

(1) Key for sample designation.
       II....... Exposure to K_2CO_3 solution - see Table 1 for gas composition
       III...... Exposure to H_2SO_4 solution - see Table 1 for gas composition
       K........ KEL-F
       V........ Viton
       EP....... Ethylene Propylene
       2, 5 & 10 represent 200, 500 & 1000 hour exposure test durations
       Example: II-K-2; KEL-F sample subjected to Exposure II conditions for 200 hours.

(2) Duration of permeability observation test.

TABLE 20

PRE TEST COMPRESSIBILITY MEASUREMENTS & CALCULATIONS

FOR GASKET MATERIAL SAMPLES

Sample No. (Electrolyte)	P	P-M	$\frac{P-M}{P}$ x 100	Average
Kel-F	0.1301	0.0580	44.6	
	0.1375	0.0620	45.1	47.3
	0.1344	0.0700	52.1	
Viton	0.1298	0.0199	15.3	
	0.1273	0.0159	12.5	13.8
	0.1258	0.0172	13.7	
Ethylene Propylene	0.1404	0.0129	9.2	
	0.1386	0.0117	8.4	8.5
	0.1273	0.0100	7.9	

P   =   thickness under pre load in inches.

P-M   =   difference in thickness between pre load and total load in inches.

$\frac{P-M}{P}$ x 100   =   compressibility, per cent

TABLE 21

POST TEST COMPRESSIBILITY MEASUREMENTS & CALCULATIONS
FOR GASKET MATERIAL SAMPLES

Test Time (Hrs)	Viton in H_2SO_4					KEL-F in H_2SO_4				
	Sample No.	P	P-M	$\frac{P-M}{P}$ x 100	Average	Sample No.	P	P-M	$\frac{P-M}{P}$ x 100	Average
200	III-V-2-a	0.1190	0.0095	8.0		III-K-2-a	0.1321	0.0178	13.5	
200	III-V-2-b	0.1221	0.0122	10.0	9.4	III-K-2-b	0.1373	0.0190	13.8	13.5
200	III-V-2-c	0.1300	0.0132	10.2		III-K-2-c	0.1345	0.0178	13.2	
500	III-V-5-a	0.1228	0.0110	9.0		III-K-5-a	0.1343	0.0238	17.7	
500	III-V-5-b	0.1275	0.0122	9.6	9.6	III-K-5-b	0.1329	0.0170	12.8	14.9
500	III-V-5-c	0.1200	0.0121	10.1		III-K-5-c	0.1339	0.0190	14.2	
1000	III-V-10-a	0.1211	0.0117	9.7		III-K-10-a	0.1293	0.0147	11.4	
1000	III-V-10-b	0.1240	0.0121	9.8	10.8	III-K-10-b	0.1325	0.0175	13.2	12.6
1000	III-V-10-c	0.1265	0.0163	12.9		III-K-10-c	0.1373	0.0181	13.2	

TABLE 22

POST TEST COMPRESSIBILITY MEASUREMENTS & CALCULATIONS
FOR GASKET MATERIAL SAMPLES

	KEL-F- in K_2CO_3 Electrolyte					Ethylene Propylene in K_2CO_3				
Test Time (Hrs)	Sample No.	P	P-M	$\frac{P-M}{P}$ x 100	Average	Sample No.	P	P-M	$\frac{P-M}{P}$ x 100	Average
200	II-K-2-a	0.1346	0.0348	25.9		II-EP-2-a	0.1257	0.0106	8.4	
200	II-K-2-b	0.1312	0.0220	16.8	21	II-EP-2-b	0.1410	0.0182	12.9	11.1
200	II-K-2-c	0.1349	0.0273	20.2		II-EP-2-c	0.1300	0.0160	11.9	
500	II-K-5-a	0.1343	0.0292	21.7		II-EP-5-a	0.1397	0.0105	7.5	
500	II-K-5-b	0.1382	0.0271	19.6	21.1	II-EP-5-b	0.1420	0.0161	11.3	10.3
500	II-K-5-c	0.1283	0.0280	21.8		II-EP-5-c	0.1348	0.0162	12.0	
1000	II-K-10-a	0.1281	0.0178	13.9		II-EP-10-a	0.1405	0.0124	8.8	
1000	II-K-10-b	0.1339	0.0201	15.0	16.2	II-EP-10-b	0.1253	0.0138	11.0	10.0
1000	II-K-10-c	0.1360	0.0268	19.7		II-EP-10-c	0.1282	0.0132	10.3	

LIST OF REFERENCES

1. G. Bianchi, "Basic Researches in Metal Corrosion – Electro-chemical Behaviour of Oxygen and Hydrogen Peroxide," Technical Final Report, Contract No. AF 61(052)-260, March 30, 1962.

2. S. B. Brummer and J. Giner, "Electrochemical Oxidation of Saturated Hydrocarbons," Fourth Interim Technical Report, Contract No. DA 44-009 AMC 410(T), October 21, 1965.

3. H. A. Christopher, "Electrodes for Low Temperature Acid Systems," 20th Annual Proceedings Power Sources Conference, May 24-26, 1966.

4. W. J. Conner, B. M. Greenough, and G. M. Cook, "Design and Development of a Water Vapor Electrolysis Unit," NASA CR-607, Contract No. NAS 2-2630, September 1966.

5. General Electric, "Hydrocarbon – Air Fuel Cells," SemiAnnual Technical Summary Report No. 5, ARPA Order: Number 247, Contracts DA44-009-ENG-4909 and DA44-009-ENG-479(T), June 30, 1964.

6. P. J. Rappaport, "The Effect of Carbonated Electrolyte on The Performance of Sintered Plate Nickel-Cadmium Cells," Technical Report ECOM-2559, DA Task 1CO 14501 A 34A-00, AD 614 104, February, 1965.

7. A. Riga, R. Greef, and E. Yeager, "The Electrochemical and Dissolution Properties of Nickel Oxide," Technical Report No. 2, Contract No. Nonr 1439(09), AD 646, 456, December 1, 1966.

8. S. R. Schulze, Thesis, Massachusetts Institute of Techno-logy, August 1966.

9. Tyco Laboratories, Inc., "Development of Cathodic Electro-catalysts for Use in Low Temperature H_2/O_2 Fuel Cells with an Alkaline Electrolyte," Report for Period January 1-31, 1966, Contract NASW-1233, N66-23837, January 31, 1966.

10. J. Giner, Journal of The Electrochemical Society, Vol. III, No. 3, (1964).

11. N. D. Greene, Corrosion, Vol. 15 (1959).

12. N. D. Greene, W. D. France, Jr., and B. E. Wilde, Corrosion, Vol. 21, (1965).

13. M. Stern and A. C. Makrides, Journal of The Electrochemical Society, Vol. 107 (1960).

14. R. Littlewood, Corrosion Science, Vol. 3, Pergamon Press Ltd. (1963).

15. J. E. Reinoehl, F. H. Beck and M. G. Fontana, Corrosion, Vol. 21, No. 12 (1965).

16. A. G. Guy and F. N. Rhines, Metal Treatment and Drop Forging, (February 1962).

17. M. Pourbaix and F. Vandervelden, Corrosion Science, Vol. 5, Pergamon Press Ltd. (1965).

18. M. Pourbaix, Corrosion Science, Vol. 5, Pergamon Press Ltd. (1965).

19. P. V. Popat and A. Kuchar, "Materials of Construction for Hydrocarbon-Air Fuel Cells with Hot Concentrated Phosphoric Acid Electrolyte," Interim Report Number 1, Contract No. DA 44009-AMC-479(T), ARP Order: 247, April 1, 1964.

20. G. Trabanelli, F. Zucchi and L. Felloni, Corrosion Science, Vol. 5, Pergamon Press Ltd. (1965).

21. J. R. Myers, F. H. Beck, and M. G. Fontana, Corrosion, Vol. 21, (1965).

22. G. Economy, Journal of The Electrochemical Society, Vol. 108 (1961).

23. O. Radovici, S. Ciolac and C. Vass, Corrosion Science, Vol. 7, Pergamon Press Ltd. (1967).

24. I. G. Murgulescu, O. Radovici, and M. Borda, Corrosion Science, Vol. 5, Pergamon Press Ltd. (1965).

25. Tyco Laboratories, Inc., "Development of Cathodic Electrocatalysts for Use in Low Temperature H_2/O_2 Fuel Cells with an Alkaline Electrolyte," Second Quarterly Report, Contract No. NASW-1233, N66-24550, December 31, 1965.

26. G. Bianchi, F. Mazza, and T. Mussini, "Oxygen and Hydrogen Peroxide Electrochemical Behaviour on Chromium, Nickel, Cobalt and Stainless Steel Electrodes," TN 8, Contract No. AF 61(052)-260, AD 278 690, February 1962.

27. B. Bianchi, F. Mazza, and T. Mussini, "Electrochemical Processes of Oxygen and Hydrogen Peroxide in Metal Corrosion and Protection," 2nd International Congress on Metallic Corrosion, AD 645 807, (1966).

28. General Electric, "Hydrocarbon - Air Fuel Cells," SemiAnnual Technical Summary Report No. 9, ARPA Order: Number 247, Contract DA44-009-AMC-479(T), June 30, 1966. (AD 640 521)

160

29. Esso Research & Engineering Company, "Hydrocarbon - Air Fuel Cell," Report No. 8, Contract DA 36-039 AMC-0374(E), ARPA Order: 247, December 31, 1965. (AD 634 078)

30. General Electric, "Hydrocarbon - Air Fuel Cells," SemiAnnual Technical Summary Report No. 6, ARPA Order: 247, Contracts DA44-009-ENG-4909 and DA44-009-AMC-479(T), AD 612 766, December 1964.

31. V. Corso, Jr., et al, "Hydrocarbon Fuel Cell Electrodes," Progress Report No. 2, Contract No. DA-44-009-AMC-897(T), AD 632 531, April 22, 1966.

32. General Electric, "Hydrocarbon - Air Fuel Cells," SemiAnnual Technical Summary Report No. 10, ARPA Order: 247, Contract DA44-089-AMC-479(T), AD 649 895, December 31, 1966.

33. D. E. Davies and W. Barker, Corrosion, Vol. 20 (1964).

34. M. Prazak, Corrosion, Vol. 19, No. 3 (1963).

35. R. 9. Steigerwald and N. D. Greene, Journal of The Electrochemical Society, Vol. 109, (1962).

36. C. C. Seastrom, Corrosion, Vol. 20, No. 6 (1964).

37. R. E. Eberts, Corrosion, Vol. 21, (1965).

38. D. A. Jones and N. D. Greene, Corrosion, Vol. 22, (1966).

39. P. Neufeld, Corrosion Science, Vol. 4, Pergamon Press Ltd. (1964).

40. A. Piotrowski and R. Lebet, Corrosion Science, Vol. 4, Pergamon Press Ltd., (1967).

41. Product Engineering, P 18, July 17, 1967.

42. J. Giner, Electrochimica Acta, Vol. 8, Pergamon Press Ltd. (1963).

43. R. J. Piersma, T. B. Warner, and S. Schuldiner, Journal of the Electrochemical Society, Vol. 113, No. 8, (1966).

44. J. E. Harrar, I. Shain, Analytical Chemistry, Vol. 38 (1966).

45. F. I. Nobel, B. D. Ostrow, and D. W. Thomson, Plating, October (1965).

46. Chem. Eng. News, P. 47, July 19, 1965.

47. N. D. Tomashov, Corrosion, Vol. 20 (1964).

48. R. A. Legault and M. S. Walker, Corrosion, Vol. 19 (1963).

49. W. J. James, M. E. Straumanis, and J. W. Johnson, Corrosion, P 15-23, (January 1967).

50. P. F. King, Journal of the Electrochemical Society, Vol. 113, No. 6 (1966).

51. R. S. Perkins, R. C. Linvingston, T. N. Andersen, and H. Eyring, Journal of Physical Chemistry, Vol. 69, No. 10, (1965).

52. D. L. DeRespiris, "Test Data Electrolytic Concentration of Carbon Dioxide," TRW EN-2620, September 30, 1964.

53. G. Gruneberg, et al, "Process for Operating Fuel Cells," 3,082,282, Patented March 19, 1963.

54. H. N. McCoy, American Chemical Journal (1903).

55. D. L. DeRespiris, "Equilibrium Study on the H_2CO_3/K H CO_3/ CO_2 System," TRW EN-2630, November 11, 1964.

56. American Cyanamid Memorandum dated May 24, 1967.

57. L. A. Matusevich and V. S. Bagotskiy, "Study of Equilibrium Carbonate - Bicarbonate Electrolyte in the Presence of Potassium Formate," JPRS-38687, TT-66-35111, Joint Publ. Research Service, Nov. 17, 1966, pp. 8-14.

58. A. N. Campbell, E. M. Kartzmark, D. Bisset, and M. E. Bednas, Canadian Journal of Chemistry, Vol. 31, No. 4, (1953).

59. A. A. Lang and A. J. Kukava, Canadian Journal of Chemistry, Vol. 36, (1958).

60. B. E. Conway and E. Gileadi, Canadian Journal of Chemistry, Vol. 40 (1962).

61. S. H. Langer and R. G. Haldeman, The Journal of Physical Chemistry, Vol. 68, No. 4, (1964).

62. R. Thacker and J. P. Hoare, Journal of the Electrochemical Society, Vol. 113, No. 8, (1966).

63. R. Thacker, Nature, Vol. 207, August 1965.

64. M. Levy, Corrosion, (Aug. 1967) pp 236 - 244.

65. Pourbaix Atlas of Electrochemical Equilibrium

66. E. D. Verink, Jr, Simplified Procedure for Constructing Pourbaix Diagrams, Corrosion (Dec. 1967)

67. Potter, Electrochemistry, Cleaver-Hume Press Ltd, 1961.

68. Huntington Alloy Products Division, Technical Bulletin T-5, 1965, International Nickel Company.

69. Delahay, New Instrumental Methods in Electrochemisty, Interscience Publishing Inc., 1954.

70. Greene, Corrosion, Vol. 18, No. 4, April 1962.

71. Beckman Instruments, Bulletin 7076A.

72. Janz, Reference Electrode, Academic Press, 1961.

73. Latimer, Oxidation Potentials, Prentice Hall, 2nd Ed, 1961.

74. R. G. Haldeman, W. A. Barber, and W. P. Colman, Research and Development of High-Performance Light-Weight Fuel Cell Electrodes, American Cyanamid Co., NASA CR-54084, June 29, 1964.

75. TRW Final Report, NASA CR72086 (1966).

76. TRW, March Technical Progress Letter, Fuel Cell Power System Study (NPRD-23) 1966.